Harvesting Vibration Energy by Employing Piezoelectricity and Electromagnetism

By
Ranjith Embuldeniya

A Thesis Submitted to Saint Mary's University, Halifax, Nova Scotia
in Partial Fulfillment of the Requirements for
the Degree of Master of Science in Applied Science.

April 11, 2023, Halifax, Nova Scotia

Approved: Dr. Adel Merabet
Supervisor
Division of Engineering
Saint Mary's University

Approved: Dr. Ehab Elsharkawi
Committee Member
Division of Engineering
Saint Mary's University

Approved: Dr. Bashir Khan
Committee Member
Department of Mathematics and Computer Science
Saint Mary's University

Approved: Dr. Jason Gu
External Examiner
Department of Electrical and Computer Engineering
Dalhousie University, Halifax, NS

Date: April 11, 2023

Acknowledgment

No journey in the academic field is achieved without guidance and mentorship and companionship. I embarked on my journey with courage and confidence but however the first few steps always need steadying in the world of research, especially for a new researcher. It was my supervisor Prof. Adel Merabet, who never let me walk it alone in those early fledgling days. No choice of words would be sufficient enough to thank him for his enormous support and mentoring throughout my undertaking. Dr. Bashir Khan and Dr. Ehab Elsharkawi, too, deserve my gratitude as members of the supervisory committee who have been witnesses to my progress and who together with Dr. Adel Merabet were partners at all important milestones of deliberation.

Special thanks goes out to my course co-ordinator, Dr. Samuel Verrs for his advice and guidance during the tenure of the whole course, which was influential enough to help me to take the right decision always, and Dr. Keith Bain for the 'tying up' all ends of administrative detail.

I also thank Dr. Adam Sarty and Dr. Coleen Barber, who although from the sidelines, did everything necessary and all they could to keep us on track so that we were properly guided whether it be academic or other administrative concerns, especially during the COVID period.

A great thanks goes out to all my friends and colleagues in the Engineering division, who were always approachable at times of need and were sources of inspiration. I am grateful for their all-around cooperation. I thank the academic support staff for their constant readiness to extend the required logistical support whenever needed.

The staff of Saint Mary's University cannot be overlooked as I take note of them as being one of the most efficient such staff I have ever encountered.

Last but not least, I thank the entire Saint Mary's University as a whole and the Faculty of Graduate Studies in particular for providing me with a seat to achieve academic excellence by pursuing this Master's Degree and providing me with such an excellent opportunity to explore into and wade through the engineering arena of the modern world.

Harvesting Vibration Energy by Employing Piezoelectricity and Electromagnetism

by Ranjith Embuldeniya

Abstract

Many energy technologies have their environmental footprint. However, energy from renewable sources does not. Venturing into green ways of producing energy is the order of the day. This project aims at generating energy from vibrations created in pedestrian movement through the joint application of piezoelectricity and electro-magnetism. Harvesting vibration energy through these two methods would be to harness what would otherwise be a largely unharnessed energy source. Piezoelectricity offers an advantage over other generation schemes by generating electricity “intrinsically,” obviating the need for moving parts and mechanical complexity. Electro-magnetism, on the other hand, does involve moving parts but is much less complex compared to other renewable energy technologies. This project dwells deeply into weighing the pros and cons of employing these two technologies and assessing whether, together, they would be a good contender to other existing renewable energy sources in the context of being a feasible micro-power generator.

11th Apr 2023

Table of Contents

List of Tables

List of figures

List of abbreviations/ composite units/symbols/subscripts/superscripts/acronyms

Abbreviations

emf – electromotive force

min - minute

rpm - revolutions per minute

rms - root mean square

DoD - depth of discharge

PE - piezoelectric

PF - power factor

EM - electro-magnetic

OP-AMP - operational amplifier

Standard SI Units

Standard SI units with their standard prefixes (powers of ten) could be used

Composite units (Other SI derivatives could be used)

C/N - piezoelectric charge constant in Coulombs per Newton

g/cm^3 - density in grams per cubic centimeter

W/m^2 - power density in Watt per square meter

Greek Symbols

$d\psi/dt$ - time differential of magnetic flux

ε - Dielectric constant

ϕ,Θ - angle

Δ - Delta (to denote an infinitesimally small change)

ψ - magnetic flux

η - efficiency

π = Mathematical constant PI

Σ - Sum

ϖ - Angular frequency

Ω - Ohm

∇- Del operator

Subscripts (unless defined otherwise)

m, n	Integer values that denote a particular mode of induced field or applied strain
1,2,3	Linear action *x, y* and *z*-axis directions (respectively) unless otherwise defined
4,5,6	Shear action *x, y* and *z*-axis directions (respectively) unless otherwise defined
i, j, k, p, q	Vector directions
x, X, y, Y, z, Z	Denote *x, y,* and *z*-axis directions respectively

Superscripts (unless defined otherwise)

E	a zero or constant electric filed
T	a zero or constant stress field
t	transpose of a matrix
D	compliance is measured in open circuit

Symbols

˚C - degree Celsius

A - Ampere

A_r - area

B_r – remnant magnetic field

C_q - amount of charge (q = x, y)

C - capacitor, capacitance

D - electric displacement or charge density

d - piezoelectric charge constant

E - electric field strength

F_a - applied force (a = x, y)

F - Farads

f -frequency

f_r - resonance frequency

H - Henry

Hz – (frequency in) Hertz

I - electrical current

k - electro-mechanical coupling factor

KWh - Kilowatt hour

R - resistance

B - magnetic field

J - Joule

L - inductance

N - Newton

N_t - number of turns

P_L- polarization

P - power

P_r - remnant polarization

Q,q - charge in Coulombs

Q_m - mechanical quality factor

s - compliance

S - strain

T - stress

t - time

v - velocity

V - Volt

V_{rms} - root mean square voltage

W - Watt

Wb - Weber

Y - Young's modulus

Acronyms

BCC - body centered cubic

BJT - bipolar junction transistor

CMOS - complementary metal oxide semiconductor

DBTT - ductile-brittle transition temperature

DC - direct current

DSP - digital signal processor

DTMOS - dynamic threshold voltage MOSFET

FCC - face centered cubic

FEP - Fluoroethylenepropylene

FEP - Fluoroethylenepropylene

HCP - hexagonal close packed

IPCC - intergovernmental panel on climate change

LED - light emitting diode

MEMS - micro electromechanical systems

MOSFET - metal oxide semiconductor field effect transistor

PCE - power conversion efficiency

PEH - piezoelectric energy harvester

PETP - Polyethyleneterephthalate

PMN - PT - Lead Magnesium Niobate – Lead Titanate

PP - Polypropylene

PVDF - Polyvinylidene fluoride

PWM - pulse width modulation

PZN-PT - Lead Zinc Niobate – Lead Titanate

PZT - Lead Zirconate Titanate

SEF - sustainable energy floor

SSHI - synchronous switch harvesting on inductor

THD - total harmonic distortion

VDBA - voltage differencing buffered amplifier

β PVDF - β phase PVDF

1. INTRODUCTION

1.1 Background

Many energy technologies have their environmental footprint. Energy from renewable sources though, has zero effect on environmental pollution, and hence its contribution towards climate change is non-existent, as no combustion takes place during their energy-generating process. Harvesting vibration energy is to tap into what would otherwise be a largely unharnessed energy source. Attempting to do this through piezoelectricity is a very green way of producing energy. It offers the definite advantage of being lightweight, reliable, and wear-proof.

This research project's purpose is to fathom if piezoelectric-based technology offers the potential to be a good supplement to other existing or emerging renewable energy sources in the context of being a micro-power generator within a Canadian setting, especially Nova Scotia. It will focus on harnessing energy from public areas where random, ambient, sporadic, or predicted routine activity is experienced, especially pedestrian movement and traffic movement. The report reviews modalities adopted in recent projects that have been successful in some of the world's Capitals.

The core area of the project is to do with the employment of a piezoelectric sub-assembly constituting multiple piezoelectric elements (discs) coupled with an electro-magnetic induction sub-assembly. This would be referred to as a 'Composite harvesting unit.' At the onset, thorough consideration is given in selecting the best material to be made use of in the piezoelectric sub-assembly.

Then the most appropriate physical design for the application will be discussed. Once the optimum material has been decided upon and one physical design out of many has been selected,

the construction of the ‘Composite harvesting unit’ is carried out. The energies produced by these two distinct working principles would be coupled to generate one single output.

Delving into optimum electronic circuitry, focusing mainly on power conditioning circuits will be undertaken in this project, as there are three different circuit configurations considered and each will have to have its best suited power conditioner so that optimum power is delivered to the load. Energy storage is another area that would receive special attention.

It’s also pertinent to say that installations and assemblies practically launched hitherto have been mostly in hot and humid environments or indoors. Our weather here in Nova Scotia is a distant contrast to these tropical or dry conditions. Therefore special consideration must be given to making installations sufficiently rugged and capable of withstanding harsh weather.

This report will

(1) Consider literature available on the subject of energy harvesting by employing piezoelectricity

(2) Discuss the technical details from a molecular structural perspective and a mathematical perspective in trying to explain the natural occurrence of piezoelectricity

(3) Draw inferences in terms of design and budget constraints from existing projects in other parts of the world where piezoelectricity is being harnessed at a commercial scale

(4) Make adjustments to (3) above as applicable to Nova Scotia

(5) Suggest the most appropriate workable model to amalgamate the energy produced by two distinct methodologies, namely piezoelectricity and electro-magnetism.

(6) Make recommendations on how to make the product sustain extreme weather conditions prevalent in most parts of Nova Scotia.

1.2 Why piezoelectricity as an alternate energy source?

(1) Fossil fuels are running out

(2) Fossil fuels are environmentally damaging

(3) Piezoelectricity is sustainable or renewable

(4) Piezoelectricity is a predictable outcome as long as the traffic patterns are known

(5) It's a clean energy source

(6) Its output doesn't depend on weather conditions as in solar power

(7) Energy produced could be stored locally and be made available for dynamic demand, offsetting some amount of grid power.

1.3 What is piezoelectricity in simple terms

Piezoelectricity is the phenomenon of an electric charge being generated in certain materials when they are subjected to mechanical stress. The opposite also becomes true in that when a piezoelectric material is subject to an electric field, it changes dimensions.

1.4 Possible situations and surroundings where generation of piezoelectricity could be practically implemented

(1) Airport Terminals

(2) Bus terminals

(3) Railway terminals

(4) Sidewalks

(5) Shopping malls

(6) Dance floors

(7) High Traffic streets

(8) Railway lines

(9) Entry points to busy workplaces

(10) Public libraries

(11) School hallways

(12) Hospitals

(13) Places of Worship

(14) Airport landing strips

(15) Artificial trees (Faux Plants)

(16) Human limbs (Bio nano generators)

1.5 Real-life examples of employment of piezoelectricity

(1) Small-scale applications

(a) In cigarette lighters

(b) Push start barbeques

(c) Piezoelectric microphones on acoustic guitars

(d) Energy harvesting from shoes and soldiers' boots

(e) Piezoelectric tires

(f) Medical applications

(2) Commercial scale applications

(a) Harvesting kinetic energy from walking traffic at an airport passenger terminal by East Japan Railway Company

(b) Piezoelectric lighting from dance floors in Club4climate project London U.K. and Club Watt in Rotterdam, Holland

(c) Piezoelectric energy harnessed from busy highways and train tracks, launched by Innowatchtech Inc. Israel

1.6 Aim of this research

(1) To highlight the carbon footprint left by energy sources that are not renewable.
(2) To emphasize and evaluate the scale of success of piezoelectric projects employed in real-world applications.
(3) To lay out a comprehensive technical understanding of the functionality of piezoelectricity and electro-magnetism from an energy harvesting point of view.
(4) To draw up and make concrete suggestions for employing the joint technologies mentioned in (3) above to harvest vibration energy of foot passengers and motor traffic in the Halifax Downtown area
(5) To make recommendations on how to make the product sustain the extreme weather conditions prevalent in most parts of Nova Scotia.
(6) To conclude whether the final product is a viable subsidiary energy source to supplement the main grid.

2. LITERATURE REVIEW

2.1 Background

This literature review aims at focusing on the work done by previous researchers and scholars to harvest ambient vibration energy through the employment of Piezoelectricity. Firstly, therefore, the advantages of energy harvesting are discussed, as per their findings. Thereafter the capability of different piezoelectric materials in harvesting vibration energy is compared. Results of recently carried out work, methodology, and viability of piezoelectric-based energy-harvesting systems employed to tap the ambient vibration energy generated in pedestrian movement and traffic movement are described. It is followed by some of the examples which are implemented in real life, and then those which are still in contemplation are explained. Focus will be directed on how the environment affects electrical installations. The fundamental prognosis of this project itself is ‘to tap energy that can be used but is wasted if it isn’t and to lay special emphasis on how

to expand hitherto known technologies adapted to accommodate variations in climate and withstand extreme weather.

Energy harvesting is the generic process of capturing small amounts of readily available energy in the environment and then converting it into another form of usable energy [55].

Solar panels are the most common example of such a harvester which converts light energy into electrical energy. Other harvesters take various kinds of energy present in the environment, i.e., mechanical, EM radiation, or heat, and convert them to usable forms of energy, generally electrical [11]. Figure 1 shows the hierarchy of the main energy harvesting technologies based on working principle and figure 2 shows energy harvesting technologies according to scale.

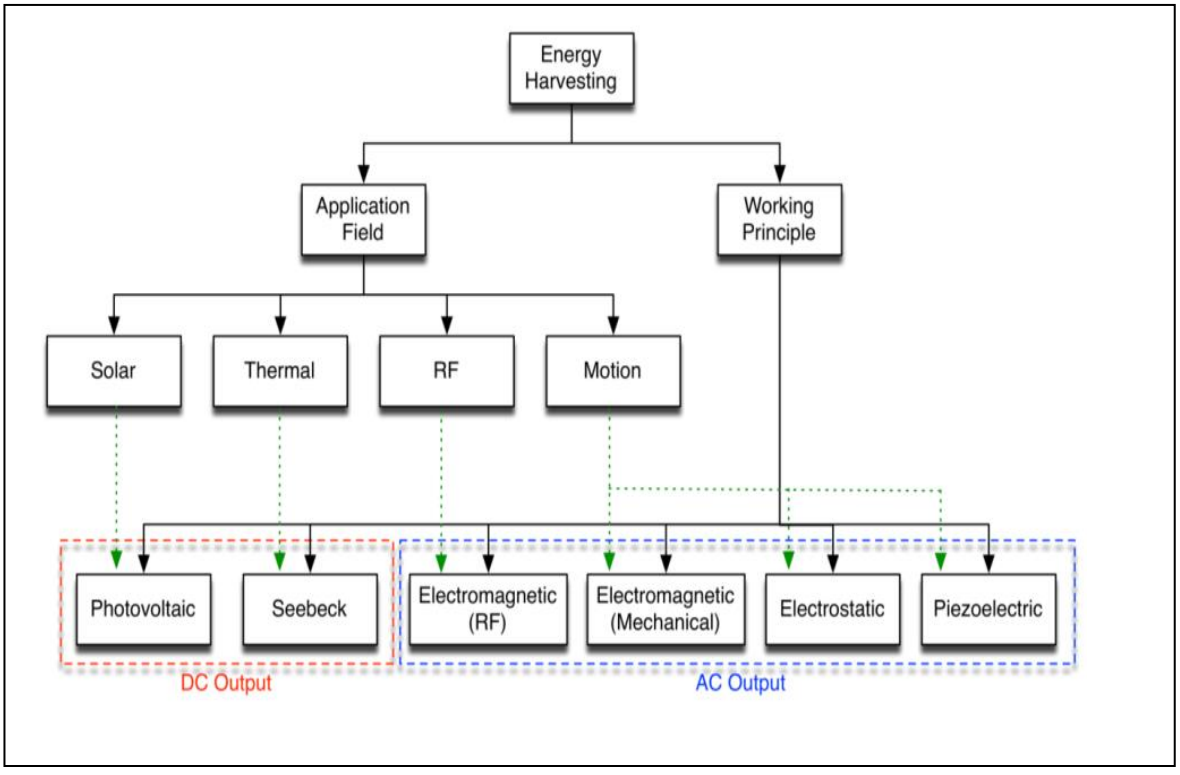

Figure 1. - Tree diagram of main energy harvesting technologies according to working principle [11].

The word piezoelectricity is made of two Greek words: ‘piezein’, which has the meaning ‘squeeze’ or ‘press’ and ‘elektron’. The ever-expanding vista of piezoelectricity was made possible by the discovery of this phenomenon by two French physicists Jacques and Pierre Curie in 1880 [24] but it was only in the ‘50s that it was used in industrial applications [16], [17].

Today Piezoelectricity is thought of as a viable means of harvesting energy from random or predictable vibrations that are created by foot or vehicle traffic in public places.

Most energy harvester systems have a common structure which constitutes of a hosting structure connected to the transducer that collects inputs through its frame, and then at the end of the system chain, a power conditioning circuit that manipulates the electrical signal to make it suitable to be fed to the load [11].

The generic layout of an energy harvesting process is shown in figure 3.

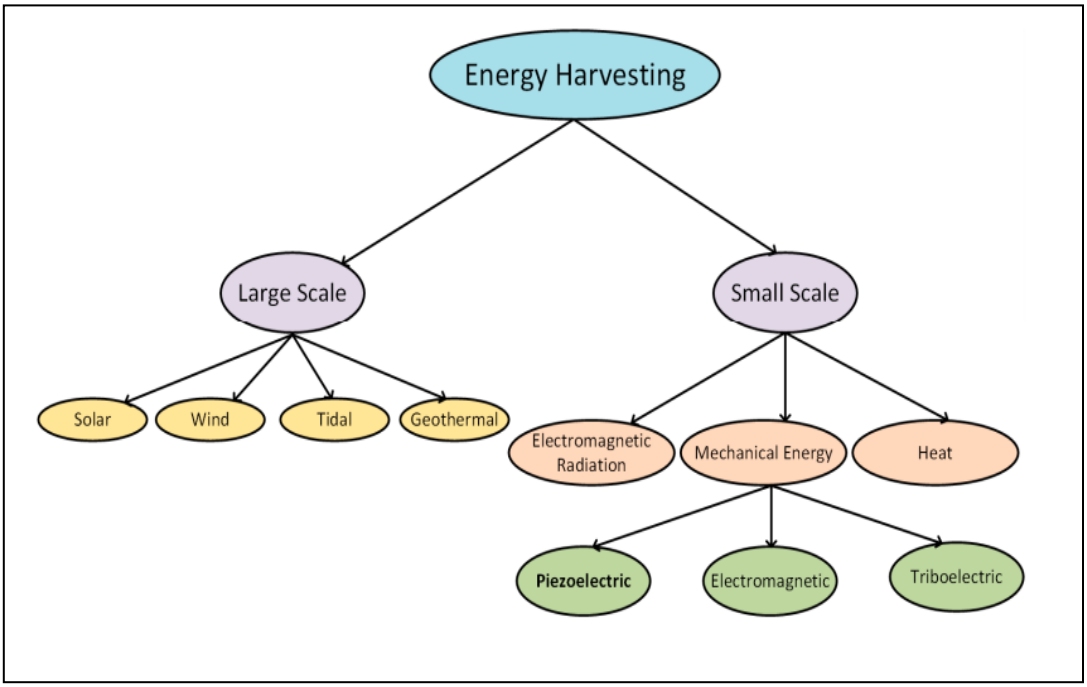

Figure 2. - Energy harvesting technologies classified according to scale [14].

This project specifically focuses on harvesting vibration energy by employing piezoelectricity. Piezoelectricity is a property possessed by certain materials which are able to produce electricity when subjected to pressure and vice versa [1], [16], [17].

From a 'thinking green' point of view, tackling the energy issue is a three-pronged approach. The first would be to have cleaner forms of energy. The second is to develop more energy-efficient appliances, and the last but not the least would be to ensure minimal losses during distribution and transformation.

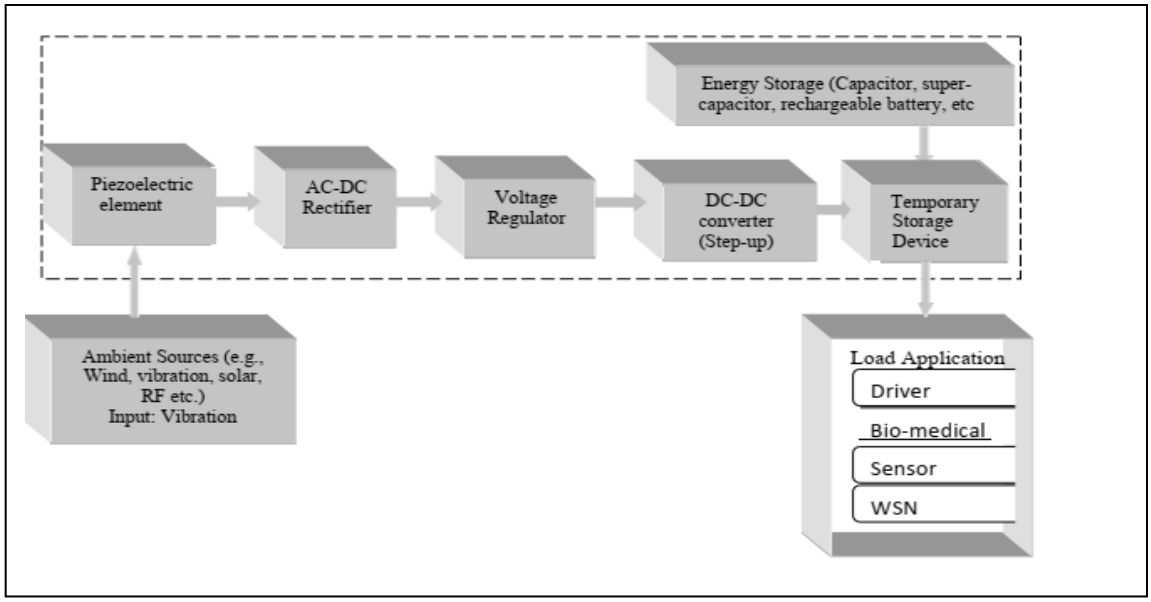

Figure 3. - The generic layout of energy harvesting modules (Experimental sub-blocks) [93].

2.2 Practical reality

Figure 4 depicts the 'power density' versus 'voltage' for different energy harvesting technologies. Among all energy harvesting techniques, piezoelectricity emerges as the most promising technology because of the simple structures it involves, which in turn make its application easy [13].

There are two quantifiers that determine the amount of energy harvested by piezoelectric applications: power and energy. Power being the unit of energy dissipated per second, is measured in Watts (W). The other metric is energy. This is defined in either Joules or KWh. Power and energy could also be re-derived as power density and energy density. They are the amounts of power or energy which could be made available within an unit area or volume. For example, a standard solar panel measures approximately 60 cm × 90 cm, or 0.54 square meters (0.54 m^2). If the solar panel generates 200 Watts then its power density would be 200/0.54 = 370 W/m^2).

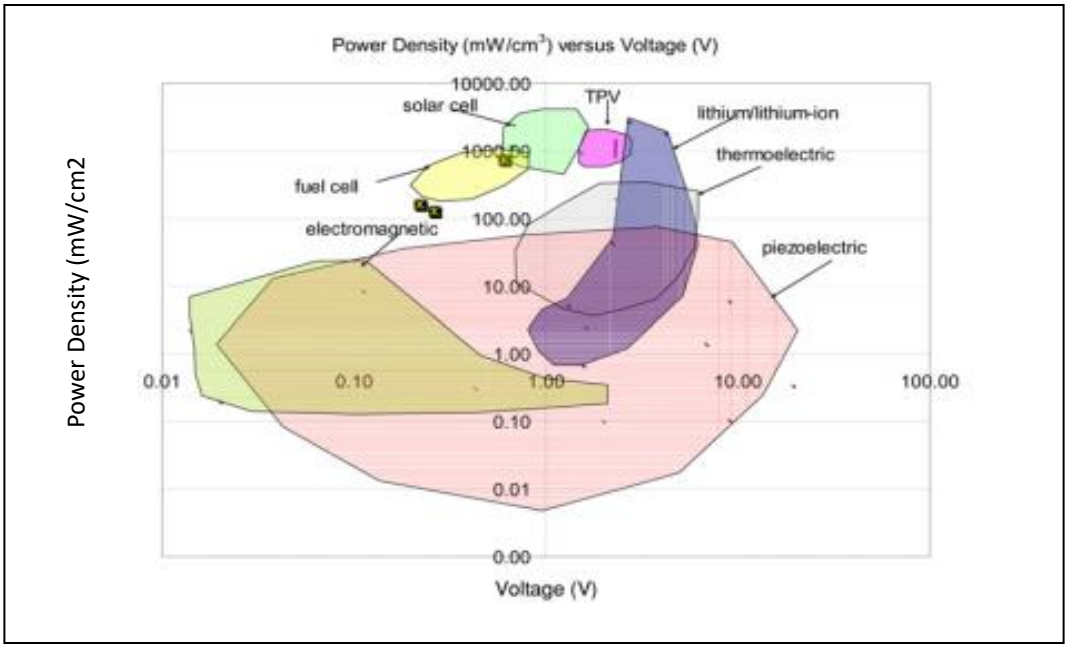

Figure 4. - Power density against voltage for different energy harvesting technologies [13].

Table 3.1 below illustrates the frequencies of various vibrations caused by domestic appliances and average human activity, which could be probable energy sources if harnessed. In this study, sources that would generate a comparatively larger output would be looked at. Some of such practical applications considered here are walkways with medium/high pedestrian traffic and roadways with medium/high traffic.

Table 3.1. - Frequency of vibration of a few common sources [59], [62].

Source of Vibration	Frequency (Hz)
Compartmet housing car engine	200
Car instrument panel	13
Casing of kitchen blender	121
Clothes dryer	121
Door frame just after closing	125
HVAC vents in office buidling	60
Small Microwave oven	121
Window panels next to busy road	100
Refrigertor	240
Human walking	1-2

There are other applications, such as harnessing energy from football stadiums, dance floors, and railway lines, worthy of mention, but to make a reach out to them would be out of the scope of this research undertaking.

2.3 Commercial projects underway internationally

Currently, there are various projects underway making use of the piezoelectric phenomenon. Tapping of vibration energy using assemblies ranging from simple embedded discs to cantilevers to special plates in public places such as sidewalks, highways, rail tracks, dance floors, and libraries is taking place [47]. In the city of Rotterdam, at the Feyenoord football club's 'De Kuip' stadium premises, Sustainable Energy Floor (SEF) tiles are placed in the entranceway at the ground level of the seating stands. This would harness energy from as many football fans as possible as they enter the stadium, as in figure 5 [34]

Figure 5. - Feyenoord football club's 'De Kuip' stadium in Rotterdam [34].

At club Watt, once again in Rotterdam in the Netherlands, a spring-loaded flooring system employs piezoelectric tiles which independently move, generating electricity from dancers moving on the floor [80]. It's nicknamed 'The sustainable dance floor.' Since 2008 piezoelectric crystals are used to create electricity from this dance floor where power is harnessed from people's dance steps and is used to meet a portion of the power demand of the nightclub. Energy Floors' colorful LED-lit floor tiles are shown in figure 6. By this process of converting kinetic energy into tangible use in terms of usable electricity, the 'Sustainable Dance Floor' has drawn

(a) (b)

Figure 6. - Electricity created from dance floors.
(a) Electricity created from dance floors by employment of piezo tiles [33].
(b) Dance floor installed with piezoelectric tiles in Club Watt Rotterdam, Netherlands [80].

increased global awareness. An identical project was launched in London by the Club4climate project, where electricity is produced from dancers' movements, which in turn charges batteries. 60% of the club's energy needs are met this way [23].

Innowattech and the Israel National Rail Company have concluded their pilot projects, which have resulted in generating 120 KWh/h from 1 Kilometer of rail. This was achieved by two piezoelectric generators inserted in every sleeper and an average load movement of 300 wagons every hour. (Israel National Roads Company Ltd, The highway to innovation 2010). See Figure 7 [20].

Figure 7. - Installing piezoelectric pads by Innowattech Inc. on Israeli railways.

Innowattech has also been involved in another Piezoelectric Electricity Generator project that was carried out in Israel to harness energy from motor traffic on highways. The construction is done with a first layer of fine gravel and sand content. Next, a layer of asphalt is laid to act as a strong base for the piezo generators, which are placed in quick-drying concrete. As per the design, they are 6 cm under road level, and 30 cm apart. Solidification takes place in 30 mins.

Then all the generators are connected in series to produce the final output. Bitumen in sheet form is used to cover all the generators, helping the concrete and asphalt adhesion. The thick layer of asphalt is what is exposed to the outside world.

Figure 8. - Innowattech project of harnessing energy from road traffic in Israel
Source: Israel National Roads Company Ltd, The highway to innovation, 2010 [26].

From practical testing, the observations are that a truck weighing approximately 5 tons generates 2000 V, and generators laid along a Kilometer stretch of dual carriageway (assuming 600 vehicles pass through in an hour), can generate about 200 KWh energy, enough to power 600-800 households [26], [80].

Near Zhaotong City, Yunnan Province, China, piezoelectric tiles are installed on the Ma-Zhao two-direction six-lane highway as shown in figure 9. Fabricated piezoelectric tiles were embedded to a total length of about 50 m. A SUV weighing 1600 Kg was used in the test as the load on the piezoelectric tiles at a wheel speed of 20 Km/hr, 40 Km/hr, 60 Km/hr, and 80 Km/hr, respectively. The measuring equipment used to monitor the open circuit voltage of the PE tile recorded an average of 350 V open circuit voltage. In a demonstration conducted by the East Japan Railway Company (JR East) in 2008, at Yaesu North Gate, Tokyo Station, as shown in

figure 10 [22], a new power-generating floor was installed at the ticket gate area, which generated electricity from the footsteps of passengers passing through the ticket gates. This power-generating floor consists of embedded piezoelectric elements, which are disc-shaped and 35 millimeters in diameter. 600 of these elements are used per square meter.

Figure 9. - The installation process of PE tiles on Ma-Zhao highway Zhaotong City, Yunnan Province, China [115].

Figure 10. - Power generating floor in Tokyo railway station [80].

The floor coverings were made of rubber or stone tiles which proved to be a good mechanism in improving energy generation. A total amount of 25 square meters of floor space is what they were aiming for, which was expected to produce over 1,400 KW per day [80].

The world's most efficient energy-converting process is found in these pedestrian floor systems known as 'Sustainable Energy Floors.' Human footsteps generate energy to meet certain requirements of illumination in the space around them. Powering local systems such as street lights and signage systems are some examples. In India, in an experiment was conducted by getting people who weighed from 40 Kg to 75 Kg to walk on piezoelectric tiles to test the voltage-generating capacity of these piezo tiles [25]. A maximum weight/force related to a maximum generated voltage. A sizeable voltage of 40 V was generated by each tile when a weight of 75 Kg was applied on them as shown in figure 11.

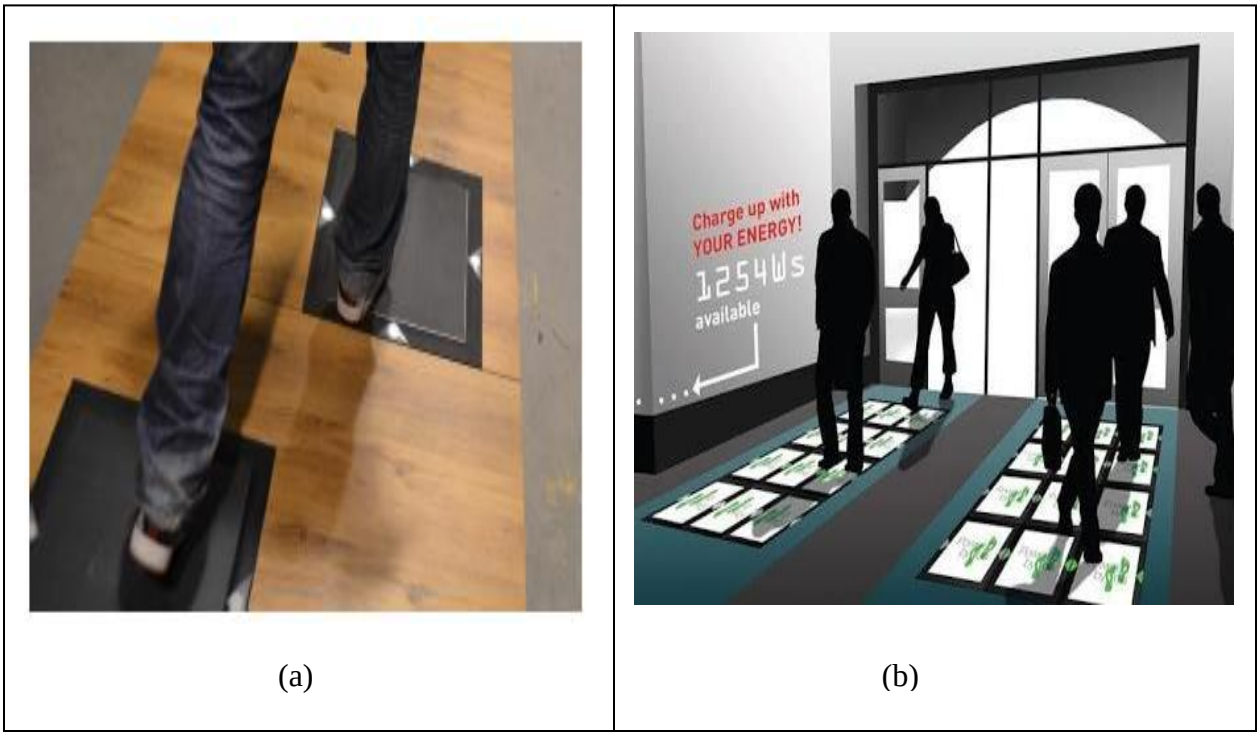

(a) (b)

Figure 11. - Sustainable dance floors and walkways [37], [40].

A summary of international power generation projects presently underway is enumerated in table 3.2

Table 3.2.- Current international piezoelectric power-generating projects.

Project	**Power generation**
Innowatchtech project - energy harnessing from highways - Israel [115]	Up to 400 KW per Km along dual carriageway for traffic volume > 600 per hour
	Up to 250 KW per Km along single lane for traffic volume > 500 per hour
Innowatctech project Energy harnessing from Rail tracks – Israel [6]	120 KWh
POWERleap Inc. San Francisco, California & Treevolt located in Columbia [29]	720 KW
Ticket gate area Tokyo Station by East Japan Railway Company (JR East) [118]	0.14 KWhr from 90 m^2
Digital Safari Greenbizz Company, Public buildings: Libraries [29]	17.5 W from a single step, 1.1 MWh annually
Public places: Pedestrian crossings [103]	6.8 V with 0.000319 Watts of power per step. 7 Watts from one person

2.4 Future applications

Tire energy harvesting has been researched in recent years. Research in [66] and [67] revealed how piezoelectric materials could generate power when assembled within the insides of a vehicle's wheel. In [53] the capabilities of a piezoelectric transducer to harness electric power from the vibrations of an engine of an automobile are explored. The dependency of current hybrid cars on conventional fuels to charge their batteries can be drastically reduced if these ideas are developed. In [66] and [67], experiments generated approximately 2.3 watts of power

by this experiment with around 160 piezo elements boned to the interior of a 185/65R14 tire, traveling at a speed of 100 Km/hr and powering a load of 1000 Ω. New ideas to improve energy harvesting from low frequencies were developed in [2]. In [69] whether centripetal force could be used to generate an impact on piezoelectric transducers is investigated. This system produced 4 mW of electrical power at a rotational speed of 800 rpm.

The harvesting of waste energy by piezoelectric materials has the potential to replace batteries and reduce costs of battery replacement and disposal, accompanied by almost zero maintenance. This provides advantages in several applications, use in wireless sensor nodes being one important area. This creates environmental friendliness as the disposal of batteries is eliminated. Batteries are known to contain materials harmful to the environment and damaging to human health [59], [93], [95]. The battery-less self-powered systems could lead to becoming the technology of the future, and more research is being done towards achieving sufficient efficiency.

Piezoelectricity has found potential in applications to monitor remote or underwater locations. Patterned ionic polymer metal composites were used to research harvesting of energy from underwater torsional vibrations in [12].

In [15] it was explained how hazardous wind turbines could be in terms of damage to fauna. According to [28], visual and acoustic manifestations of wind turbine farms have to be addressed as possible areas of concern. This is of course not to underestimate this vast source of energy-producing methodology but to be taken as a hint that venturing into other approaches to energy harvesting wouldn’t hurt.

Experiments have been conducted in wind-harvesting plants, and in these schemes, the electro-mechanical coupling has been achieved by piezoelectric elements hung on faux plants. Small

strips of plastic with piezo properties inside the leaf stalks generate electrical charge as a result of being bent by air drafts [71].

In [21] it was suggested that because human joints/organs are in almost-continuous motion (e.g., elbow, wrist), Piezoelectric Energy Harvesters (PEH) can play an influential role in human-based nano-electronics. This concept could be extended to giving mobile devices (i.e., laptops, cellular phones, etc.) the extended battery life they need. In contemporary machine-induced motion, vibration occurs in the low-frequency range of 1-100 Hz [57].

	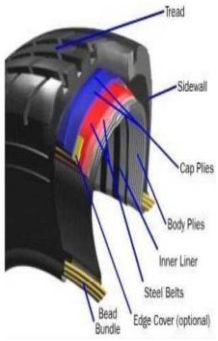	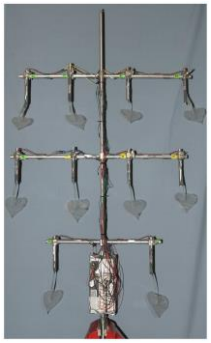	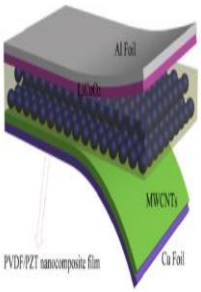
Underwater Sensors (2013) [12]	Piezoelectric tires [53]	Faux Plants [71], [99], [101]	Self-Charging Battery [100]

Figure 12. - Future applications of piezoelectric energy harvesting.

Researchers at the Massachusetts Institute of Technology developed a battery-free underwater communication system that utilizes almost zero power to transmit sensor data. Scientists envision their system being made use of in monitoring sea temperatures, studying climate change, and tracking marine life over prolonged time spans. [38]. Underwater applications which are sonar-based mostly rely on ultra-sonic piezo transducers in generating sound waves and

pulses. Navigation, communication with, or detection of objects, on or under the surface of the water, such as fish or other vessels, is done using this methodology [43].

2.5 Choice of material

Most piezoelectric energy harvesters have a power output that ranges from nanowatts to milliwatts. The use of all four types of piezoelectric materials i.e. single crystals, polymers, piezoelectric ceramics, and quartz, has been explored by researchers, testing their performance in various harvester configurations. The two widely known single crystal Ferro-electrics i.e. PZN-PT (Lead Zinc Niobate- Lead Titanate) and PMN-PT **(**Lead Magnesium Niobate-Lead Titanate) have a high piezoelectric performance; however, their wide use for energy harvesting is limited by their high cost. Piezoelectric polymers PVDF (Polyvinylidene fluoride), considered Ferro-electrets, are flexible when it comes to function and usage due to their tender nature, which helps them to withstand considerable strain and is, therefore, better suited for applications requiring the device to undergo considerable bending. However, their piezoelectric properties are found to be weak, and harvesting devices utilizing these materials generate power outputs in order of milli to microwatts. PZT ceramics, though brittle and non-flexible, have piezoelectric properties of 600 pC/N been reported, which is superior to composites and polymers and is also of low cost. According to [59], and [64], there are five widely acknowledged types of piezoelectric material, as listed below, with some examples.

Out of all materials listed below, Quartz is naturally occurring, and the other four are synthetic. These other materials generate a noticeable amount of electricity even with a 1% change in dimension. This gives rise to ruggedness and remarkably high natural frequencies with a very good linear response, operating over a wide amplitude range. Ferro-electric material and Ferro-electret material are worthy of comparison.

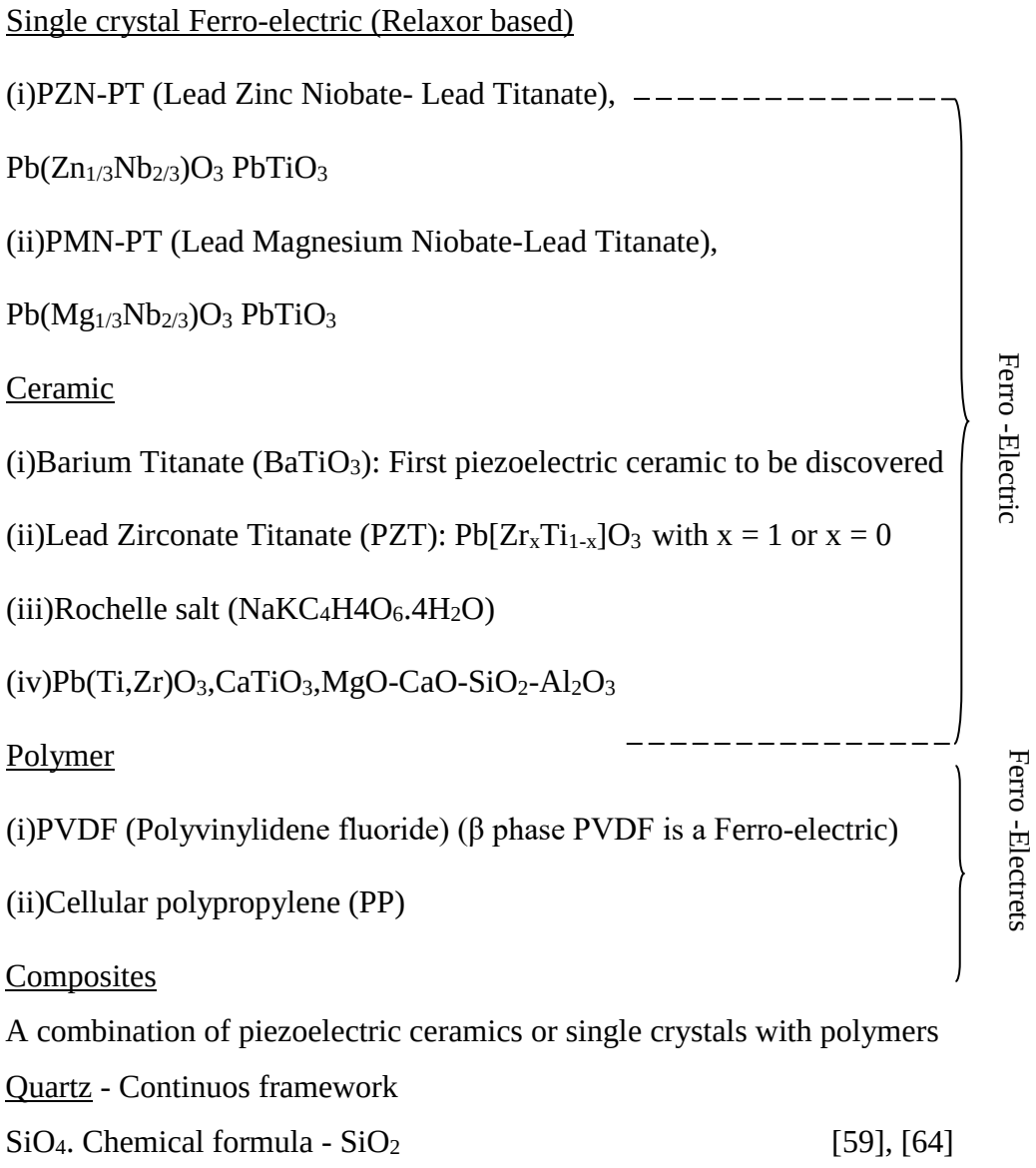

[59], [64]

In [110] a very comprehensive investigative report was produced about vibration-based energy technologies, encompassing theory, mathematical modeling and implementation of piezoelectric materials. Their findings showed that piezoelectric energy harvesters have relatively low coupling coefficients, but it was also shown that they have many advantages over other energy harvesting technologies. Among them is the fact that piezoelectric materials are least affected by electro-magnetic waves compared to most other energy harvesters.

Table 3.3 compares the piezoelectric charge constant (d_{33}) of known piezoelectric material. d_{33} is a measurement of how much polarization is generated (in Coulombs) per unit of mechanical stress (in Newton).

By definition of d_{ij} (piezoelectric charge constant), the subscript 'i' is for the direction of induced polarization, with electrodes to measure it perpendicular to that direction when used in direct mode (see Section 4.5.1) or applied field when used in the reverse mode (see Section 4.5.2). The subscript 'j' is for the direction of external stress applied, when used in the direct mode or induced strain when used in the revere mode. Therefore, in the context of the direct mode, the first subscript in $d_{33,}$ will mean that the induced polarization is along axis 3 (the electrodes will be placed perpendicular to axis 3), and the applied stress also would be applied along axis 3. Whenever there is only one subscript it means that the electrodes are placed perpendicular to the direction indicated.

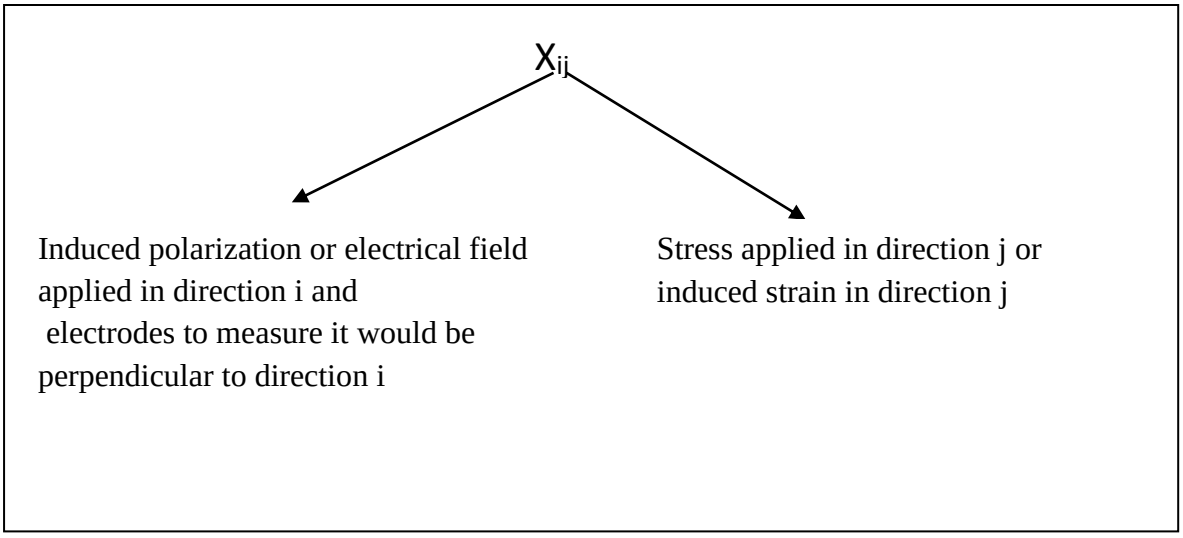

Figure 13. - Notation for direction of induced polarization/applied electric field and direction of applied stress/induced strain **[**16], [26].

For a piezoelectric material, when used in the direct mode, meanings of d_{33} and d_{13} would be as shown in figure 14.

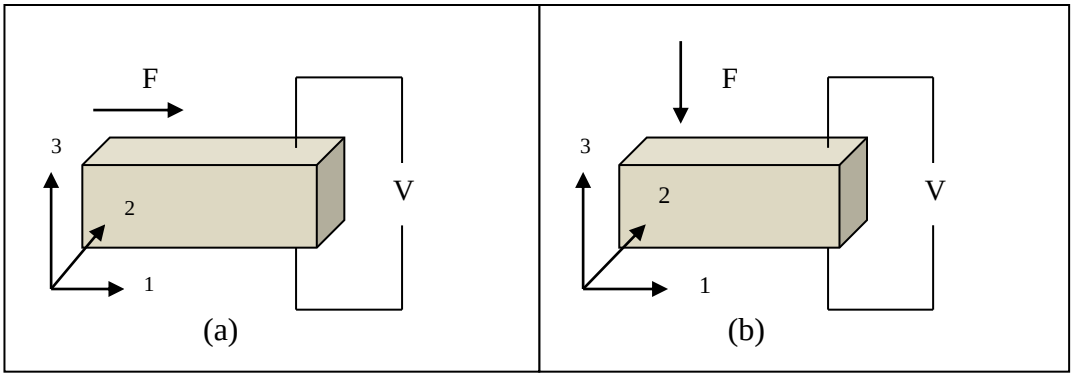

Figure 14. - d_{31} mode and d_{33} mode (a) d_{31} mode: Induced polarization is along axis 3 and applied stress is in directions 1 (b) d_{33} mode: Induced polarization is along axis 3 and applied stress is in directions 3. [114].

Table 3.3. - A comparison of the piezoelectric d_{33} coefficient for most common piezoelectric materials.

Material	d_{33}(pC/N)
Ceramic: Lead Zirconate Titanate (PZT) [85],[86]	170-600
Ferroelectrics: β-PVDF (homopolymer) [59], [61]	25-33
PVDF –TrFE (copolymer) [72], [116]	33.5-72
PVDF (composite) [79], [85],[86], [107] - [109]	30-87
Ferroelectrets: Optimized cellular polypropylene (PP) (single) [105]	1400
Optimized cellular polypropylene (PP)(multi) [74],[75]	2010
Optimized cellular PETP polyethylene terephthalate[107]- [109]	15
Optimized cellular PTFE [92]	220
Optimized cellular fluoroethylenepropylene (FEP) (single) [85],[86]	40
Crystal: quartz [72]	2.3

Table 3.4. - Vital properties of certain selected piezoelectric ceramics, single crystals, PZT-polymer composites and polymers. Source: Li H. et al (2014) [59].

Parameter	PMN-32PT (Single crystal) [81]	PZT -5H (Ceramic) [96]	PVDF (Polymer) [8], [9], [99]	PZT – (Polymer composite) [27]
(i) Density (g/cm^3)	8.1	7.65	1.78	3.08
(ii) Dielectric constant (Ɛ)	7000	3250	6.0	380
(iii) Young's modulus Y_{33} (GPa)	20.3	71.4	2	
(iv) Mechanical quality factor Q_m		32	10	
(v) Piezoelectric charge constant d_{33} (pC/N)	1620	590	25	375
(vi) Piezoelectric charge constant d_{31} (pC/N)	-760	-270	12-23	30-87
(vii) Electro-Mech coupling factor k_{33}	0.93	0.75	0.22	

Table 3.5. - Comparison of vital characteristics of major piezoelectric materials.

	Ease in fabrication	Rigidity/ robustness	Piezoelectric Properties ($d_{33}$and k_{33} combined)	Fundamental Frequency	Cost	Overall Ranking
Single Crystals (Relaxor based) (PZN,PMN)	Less than moderate	Moderate	Best	Moderate	High	1
Polymers (PVDF)	Less than moderate	Lowest	Lesser than some others	Lowest(good)	Low	4
Ceramics (PZT)	Moderate	Highest (Fragile)	Better than Polymers	Highest	Low	2
Composites	Less than moderate	Moderate	Moderate	Low	Moderate	3
Quartz	Natural	High	Lowest	Moderate	Low but more than ceramics	5

d_{33}, the piezoelectric coupling coefficient is also known as the charge constant and gives an idea of how much electricity is generated for a unit amount of force applied. k_{33} is the electro-mechanical coupling coefficient and measures the efficiency of transformation of mechanical energy into electrical energy. Table 3.5 gives a relative comparison of common piezoelectric materials with an overall ranking assigned to each material from a suitability point of view for this project. Table 3.6 gives the definition of symbols of major piezoelectric properties.

In [54], a comparison is provided about the performances of PMN-PT and PZN-PT single-crystals. They concluded seeing no significant differences (regarding amplitude of desired output against frequency bandwidth) between these single-crystal transducers, whose fabrication conditions were the same. However, both PMN-PT and PZN-PT single-crystal materials have shown better electro-mechanical coupling coefficients than PZT ceramics, as expected, with better bandwidth and sensitivity too. The negative aspects were, however, significantly higher costs and complexities in the manufacturing process. The work in [65] agrees with this view and in addition, say that single crystals have strong anisotropy of their properties, which offer new opportunities for device design. In [4], a finite element model each for PZT and PMN-33% PT was implemented to compare their performances. For the configuration selected PZT delivered the best energy transformation efficiency, which is interesting but not a reason to discard other materials as they exhibited reasonably satisfactory performances in some other respects.

In [7] it is highlighted that among the several materials earmarked for the implementation of a nano-generator, PVDF is the most promising material due to its good Ferro-electric, piezoelectric, and pyro-electric properties, flexibility, biocompatibility, and nontoxic nature and could therefore tap the micro-power generated by body movements. The work in [59] make a good comparison as far as the most vital characteristics of major piezoelectric materials are

concerned, and they are tabulated in table 3.4 above. Giving due consideration to the above PZT ceramics becomes the most suitable candidate with advantages over criteria (i), (iii), (v), and (vii). The second choice would be piezoelectric polymers, not withstanding criteria (v). For this project, piezoelectric ceramics were chosen.

Table 3.6. - Important parameters associated with piezoelectric materials.

Symbol	Name	Description	Units
ρ	Density	The ratio of the mass to volume of the material	Kg/m^3 (Kilo gram per cubic meter)
d	piezoelectric charge constant	Field induced by applied stress or mechanical strain produced by an applied electric field	C/N (Coulombs per Newton)
k	Coupling coefficient	Efficiency of conversion of mechanical energy into electrical energy or vice versa.	No Units
G	Voltage co-efficient	Ratio of the electric field produced to the mechanical stress applied	Vm/N Voltmeter per Newton
Y	Young's modulus	Ratio of stress (force per unit area) to strain (change in length per unit length).	GPa (Giga Pascals)
σ	Tensile strength	maximum load that a material can support without fracture when being stretched, divided by the original cross-sectional area of the material	N/m^2 or MPa (Newtons per square meter)
ε_r	The relative dielectric constant	Ratio of the permittivity of the material, ε, to the permittivity of free space, ε_0, in the unconstrained condition, i.e., well below the mechanical resonance of the part.	No Units
C	Capacitance	Relative dielectric constant multiplied by the permittivity of free space and electrode surface area, then dividing by the distance between the electrodes.	F (Farads)
T_c	Curie temperature	temperature at which the crystal structure changes from a non-symmetrical (piezoelectric) to a symmetrical (non-piezoelectric) form	°C (degrees Celsius)
P	Poling direction	The direction in which poling has being done. A material could be x- poled or z-poled.	No Units
T	Thermal stability temperature	Temperature range across which stable piezoelectric operations could be achieved	°C (degrees Celsius)

The following are trade-offs when selecting a suitable piezoelectric material.

(i)Ability to sustain larger strain at the optimum resonance frequency

(ii) Flexibility

(iii) Lightweight

(iv) Excellent environmental resistance

(v) Exceptional piezoelectric properties including power output

(vi) Formability into a complex shape

(vii) Workable power output at low frequencies

(vii) Cost-effectiveness

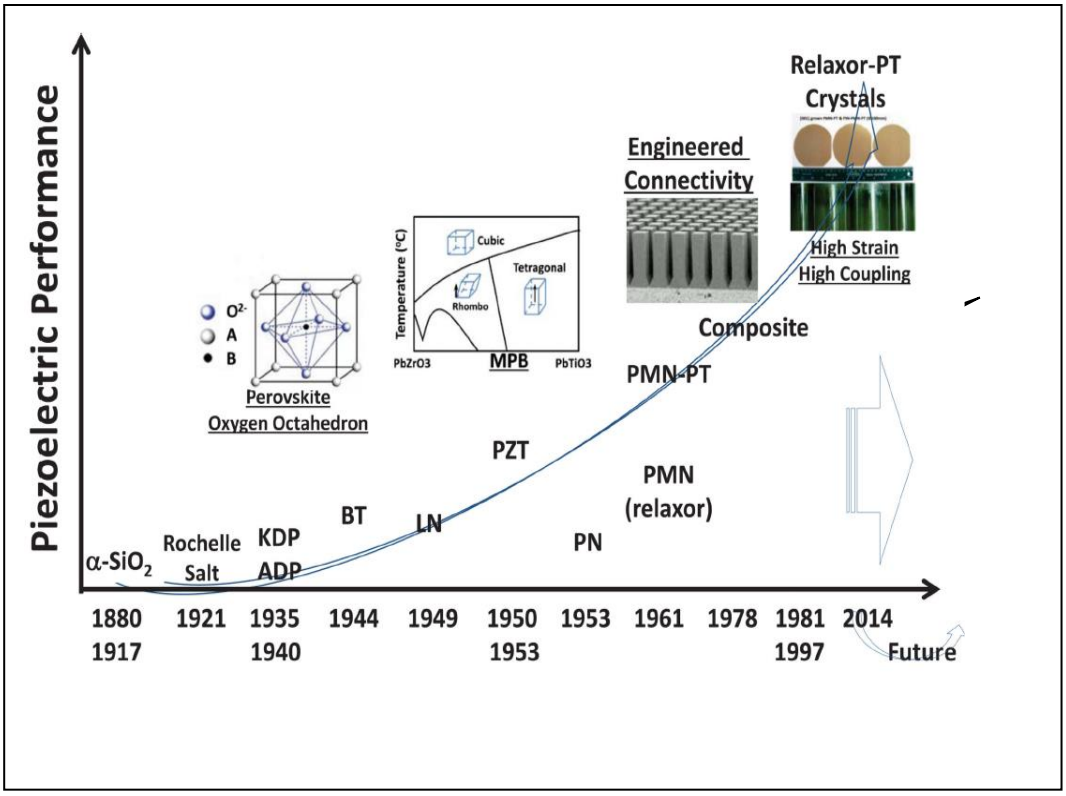

Figure 15. - The evolution of piezoelectric transducer material
KDP/ADP: $KH_2PO_4(NH_4)H_2PO_4$; BT: $BaTiO_3$; LN: $LiNbO_3$; PZT: $Pb(ZrTi)O_3$; PN: $PbNb_2O_6$; PMN:$Pb(Mg_{1/3}Nb_{2/3})O_3$; PNM-PT: $Pb(Mg_{1/3}Nb_{2/3})O_3$-$PbTiO_3$ [117].

2.6 Piezoelectric inter-relationships

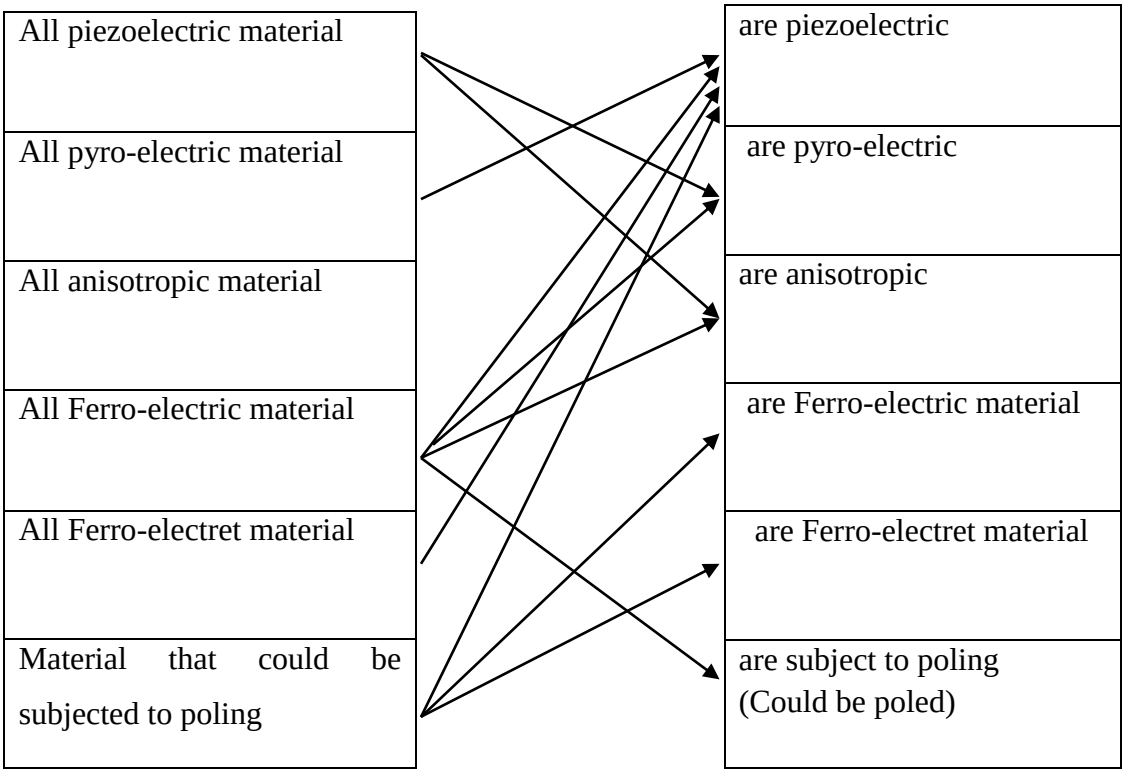

Figure 16. - Relative relationships between piezoelectric materials [16],[17].

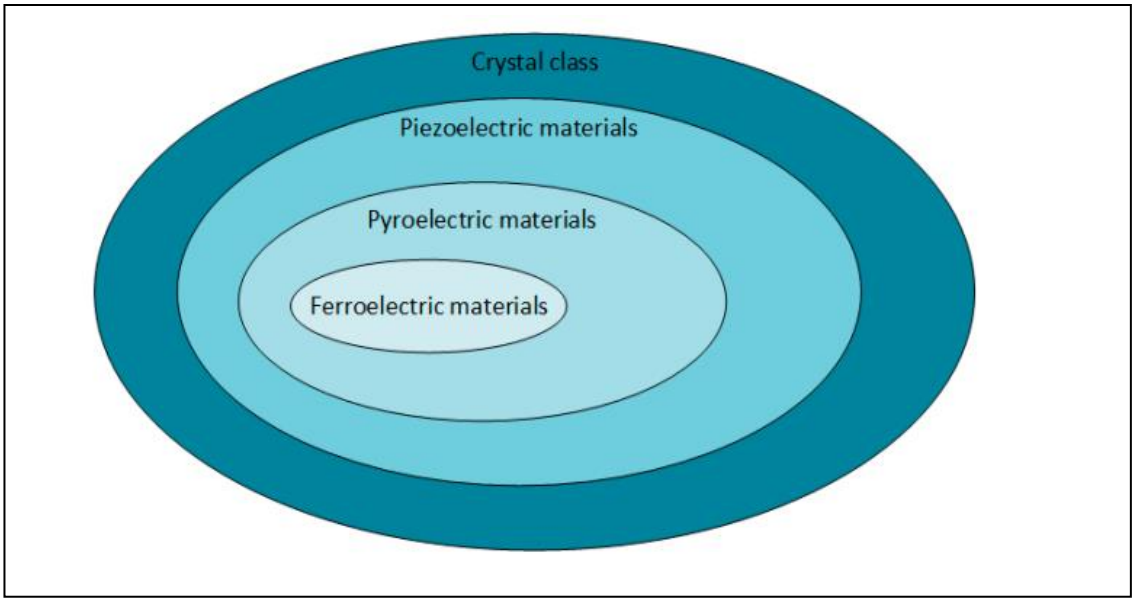

Figure 17. - The relationship between piezo-, pyro-, and Ferro-electric materials shown in a Venn diagram.

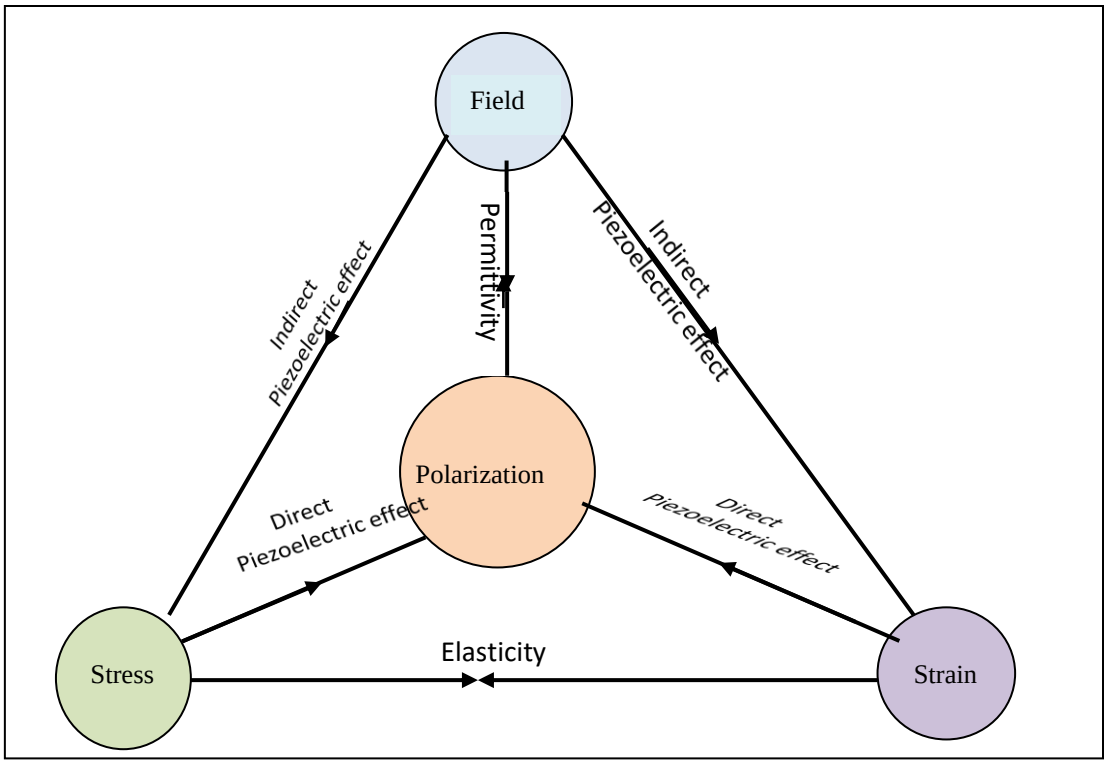

Figure 18. - Inter-relationships in piezoelectricity [16].

2.7 Choice of geometry of structure

Different factors influencing the output of piezoelectric harvesters are geometry, type of material, the resonance frequency of the piezoelectric material [110], and associated electric circuitry [60].

Piezoelectric materials though of low power and efficiency could be improved by modification to the materials, changing the stress direction, selection of a proper coupling mode of operation, adopting suitable construction architecture, and incorporating improved electronic circuitry. To achieve practical worthiness of piezoelectric micro-electro-mechanical systems (Piezo-MEMS), an energy harvester in the order of a quarter size dollar coin measuring 24.26 mm in diameter and 1.75 mm in thickness should be able to produce about 100 μW continuous power from low-frequency ambient vibrations of order 10^2 Hz. Talking about the 'choice of a coupling mode of

operation' two fundamental modes exist. The first mode, the 31 mode, has the excited vibration force applied perpendicular to the poling direction. In the other mode, the 33 mode, the direction of force applied and the poling direction are the same. Of the two modes, the 31 mode is widely used, which produces a lower coupling coefficient "k" than the 33 mode, but however, has other advantages. Figure 14 shows the two modes. However, as they are very thin, the piezo discs used in this project are of coupling mode 33.

2.7.1 The plucked method

In an experiment performed in [87], a two-staged piezoelectric energy harvester was designed for considerably low-frequency vibration environments. (range 0.2-0.5 Hz). They called it the 'Plucked method.' The two parts contained in this design is firstly, the mechanical energy transfer unit which is attached to a vibration platform, and the next, a secondary vibration unit composed of piezoelectric elements and vibrating beams as shown in figure 19. Due to the initial impact on the platform, the mass attached to the mechanical energy transfer unit vibrates at a low frequency. This low-energy vibration then excites the piezoelectric beams as the transfer unit traverses within the secondary vibrating unit.

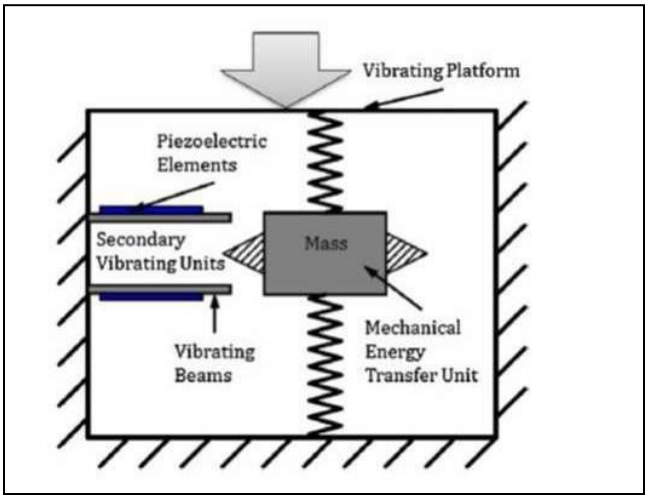

Figure 19. - The plucked method [87].

The energy yielded is directly proportional to the duration that the piezoelectric elements remain activated. The units are placed about five centimeters below the surface where movement takes place. However, due to design complexities, it was decided not to pursue the plucked method in this research.

2.7.2 Cantilever beams

A cantilever can be built with a thin layer of piezoelectric ceramic, bonded to a non-piezoelectric layer (usually metal), serving as a conductor of the generated charge. One end would be fixed to give a flexural mode to the structure. With only one active piezoelectric layer, such a configuration would be called a "unimorph". A cantilever made by bonding two thin layers of piezoelectric ceramic on either side of the same metal layer is called a "bimorph".

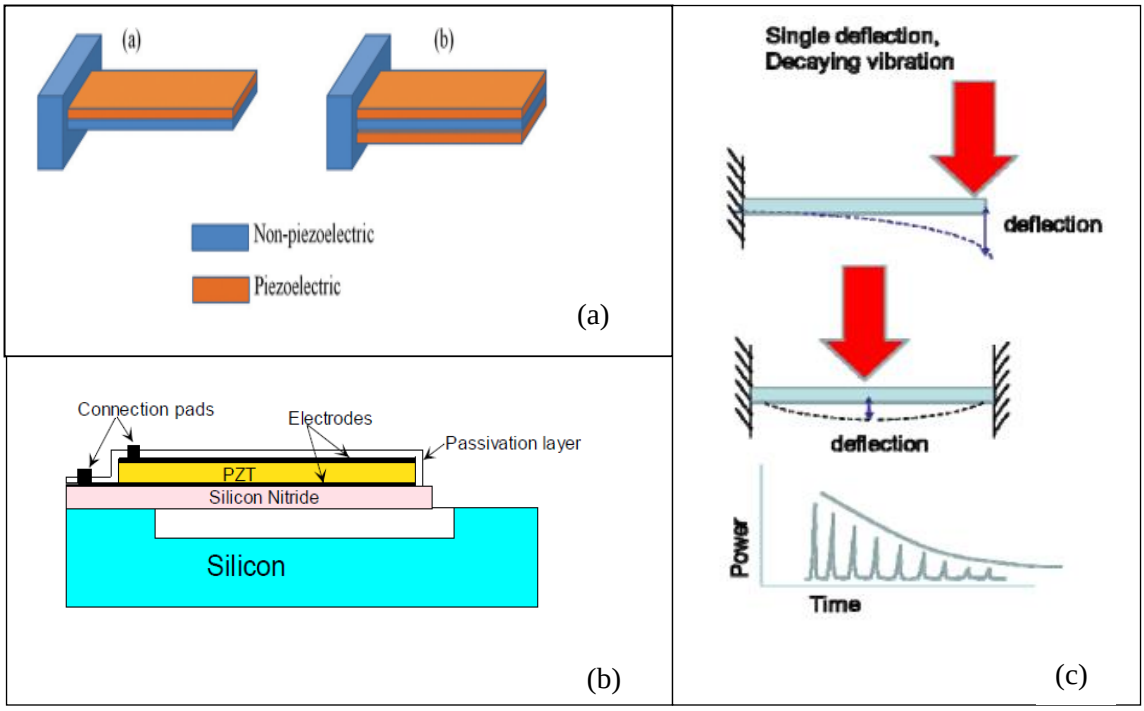

Figure 20. - Cantilever structure construction and employment in low-frequency energy harvesting.
(a) Unimorph and bimorph cantilever architecture [59].
(b) Construction of a simple piezoelectric PZT- on- Si cantilever resonator.
(c) Performance characteristics of a unimorph energy harvester. Source: DNV KEMA Ca. U.S.

As two active layers are used in this structure, the power output would be obviously higher. The two structures are shown in Figure 20(a).

In [89] and [90] piezoelectric generators were developed based on this two-layer bender (bimorph) architecture. Piezoelectric materials are on the opposite planes (faces) of the device. A downward bend of the beam would produce tension due to elongation in the top layer and compression in the bottom layer. The voltage developing across each layer could be tapped off in series or in parallel [91], [104].

Cantilever geometry is one of the most indulged geometries. Therefore, most often, the sought-after structure in piezoelectric energy harvesters, especially for harnessing mechanical energy from vibrations because it is able to withstand large mechanical strain, has high responsiveness to small vibrations, and simple in construction. Moreover, the fundamental flexural frequency of a cantilever is much lesser than the other vibration modes of the piezoelectric element itself. Therefore, most piezoelectric energy harvesting devices reported today incorporate a unimorph or bimorph cantilever design [59], as shown in figure 20.

Bimorph piezoelectric cantilevers may be a better choice in piezoelectric energy harvesting applications because it gives a double portion of energy as output without a significant increase in the device volume.

However, the work in [48] demonstrated that the unimorph cantilever beam configuration also could generate high power under lower excitation frequencies and load resistance. Two Macro Fiber Composite (MFC) materials attached in parallel onto the beam could increase the current. A maximum voltage of 50 V ac could be generated at resonance frequency which could be converted to DC by using a suitable rectifier circuit. Finally, energy is saved in capacitors or batteries.

2.7.3 The Moonie

Poled ceramic Lead Zirconate Titanate (which is of PZT-5H category) is sandwiched between two specially designed metal end caps to create the "Moonie." [58]. The energy output recorded from one step (one foot down) was 81 µJ which translates to 162 µW for both feet when walking at a rate of 2 Hz (meaning 2 feet contacting the ground per second). The power output at 1Hz step frequency was measured to be 56 µW.

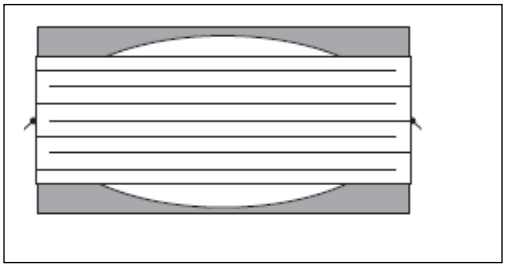

Figure 21.- The Moonie [58].

2.7.4 Compression-based energy harvester systems

In compression-based energy harvesting systems, the piezoelectric material is subject to direct vertical mechanical force which in turn induces an electric field at the opposite faces of the

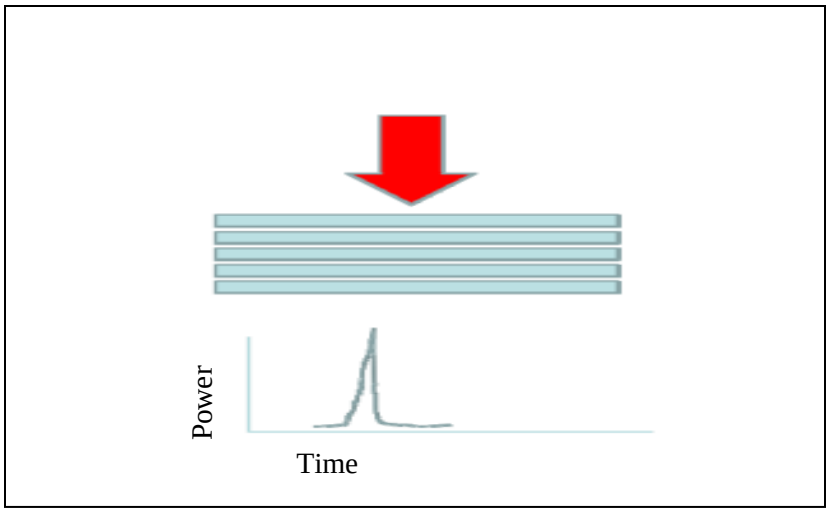

Figure 22. - Performance characteristics of a multi-layer compression-based energy harvester. Source: DNV KEMA, California.

material. The harvesting unit could consist of a single layer or multiple layers of piezoelectric material. This simple construction of such a contraption is shown in figure 22.

The piezoelectric energy harvesting systems that would be considered in this project caters to low motion frequencies. The thinner and flatter a piezoelectric element is, it allows ready interaction with the motion of the host structure. The overall dimensions and weight of the energy harvester are reduced by such a geometrical form. Thus, a thin-layer geometric shape stands out in this regard. The mode of operation for piezo discs for this project would be 33 mode.

2.8 Rectification and power management circuits

2.8.1 Rectification

In many areas, the energy generated is in the micro to milli range. Hence a boost up in the primary voltages before it could be put into use in a system is very pertinent. In [93] DC-DC Step-Up Converter of 1.67 V is simulated with an overall circuit efficiency of about 80%. In [3] it is demonstrated that a Dynamic Threshold –Voltage MOSFET (DTMOS) is ideal for low-power, low-voltage operation as it has a good operating threshold (cut-in) and higher carrier mobility than the standard MOSFET. The research done in [5], proposed a DTMOS-based voltage differencing buffered amplifier (VDBA) circuit which could work with 0.4 V voltage while consuming just 6.22 nW, thus qualifying for ultra-low voltage and ultra-low power operations. In [49] a low voltage rectifier with high power conversion efficiency (PCE) is propose based on SMIC (Semiconductor Manufacturing International Corp., Shanghai, China) 0.18 μm standard CMOS technology for PE energy harvesting. This application facilitates the rectifier with dynamic control over the threshold voltage as shown in figure 23 (a) and (b). Their simulations showed that both the voltage conversion efficiency and the power conversion

efficiency can achieve 95.5% respectively with an input voltage of 0.2 V, operating at 100 Hz and a load resistance of 50 kΩ. They further demonstrated that rectification could be affected on input voltages with frequencies as low as 10 Hz–1 kHz.

In [113] a rectifier is proposed to deal with very low voltages produced by a PE energy harvester, consisting of diodes integrated with a parallel Synchronous Switch Harvesting on Inductor (SSHI) technique, yielding a high efficiency (figure 23(c)).

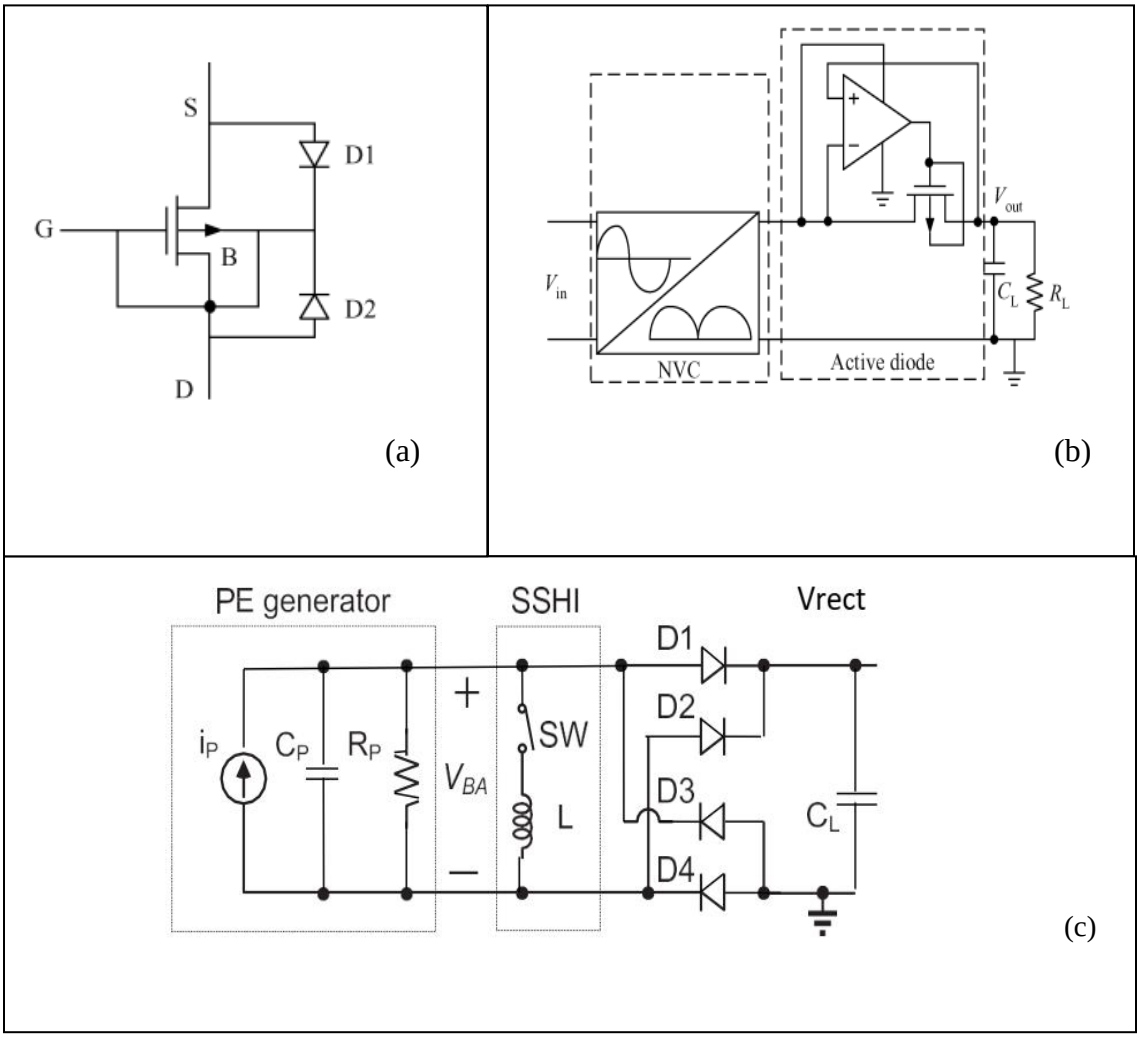

Figure 23. - DTMOS architecture and SSHI circuit
(a) The basic building block of DTMOS architecture.
(b) The proposed active rectifier [49] .
(c)Parallel SSHI circuit followed by a diode bridge rectifier [113].

2.8.2 Power management

The DC-DC converters usually fall into the category of boost, buck, or buck-boost. These converters act on the principle that the output voltage magnitude increases or decreases when compared to the input voltage [95]. DC-DC converters when operated under an open loop condition, offer poor voltage regulation and a tangible outcome to work with. However, if used in a closed-loop feedback control system, (with the duty cycle being adjusted due to the converter switching on and off) it (the controller) passes on optimal output voltage to the load. Power flow regulation is achieved through switching the MOSFETs (in the circuitry of the DC-DC converter) ON and OFF which is equivalent to pulse width modulation (PWM). The advantage of a single-phase DC-DC converter is the need for just a single MOSFET to be switched, causing small losses, thus promoting its suitability for energy harvesting applications [94].

It could be proved that the optimal power transfer to the battery occurs when the rectified output is half the open circuit voltage of the piezoelectric element [73]. Experimental results have proved that adaptive DC-DC converters increases power transfer by over 400% as compared to circuits that don't use them.

There are two types of power management circuits that could be employed as shown in figure 24.

(a) Step–up circuits, also known as Boost converters

(b) Step-down circuits, also known as Buck converters

The Buck converter is a step-down converter which offers a lower voltage at the output compared to what's available before the controller and the Boost converter is a voltage step-up converter. The Boost converter is used to 'step up' the voltage available from the source, to some higher

level, required by a load. This is achieved by the stored energy in the inductor being released so that the load sees a higher voltage Hence a Boost converter is the complement of a Buck. A Buck converter is just a step-down chopper. It's just like a transformer, but the conversion is in DC.

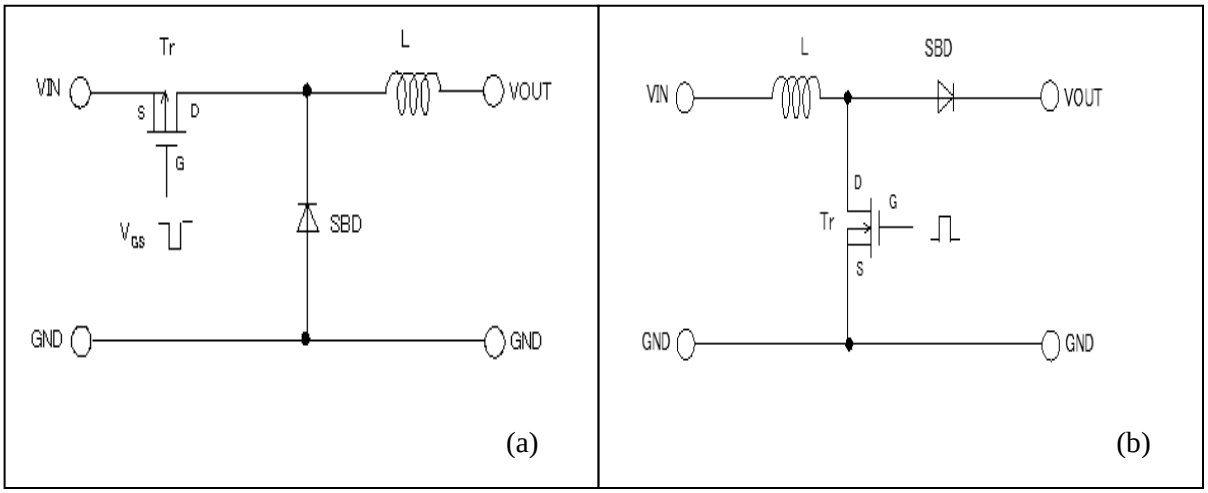

Figure 24. - Buck and Boost converters (a) A step-down DC-DC converter (Buck Converter) (b) A step-up DC-DC converter (Boost Converter) [10].

An advantage of using a Buck converter is that; the inductor is placed on the load side, which makes the ripple in the output current i.e. load current be reduced, thereby giving fruitful operation of the load. The capacitor helps here by limiting the ripples in the output voltage. It is called a Buck converter because the voltage across the inductor opposes or 'bucks' the supply voltage. Switching converters such as buck converters, provide much greater power efficiency in their role as DC-DC converters than their linear counterparts, which are of course simpler circuits that steps down voltages by dissipating power as heat but do not step up output current. The efficiency of Buck converters can reach as high as 90%. [32]. This project uses a Buck converter with the series-parallel configuration and the Boost converter with the all parallel configuration due to the aforesaid reasons.

2.8.2.1 Power losses

Since the order of power generated by the proposed system is small, other power losses are of concern. However, they are inevitable as discussed in sections 3.8.2.1 to 3.8.2.4

2.8.2.1.1 Power loss in an inductor

An inductor (coil) consists of a number of turns of wire. Since all this wire possesses some resistance, inductors definitely offer a certain amount of resistance. Usually this resistance is small which is neglected in solving various types of ac circuit problems. The reactance of the inductor (the inductive impedance or opposition to a.c.) is so much greater than the resistance, that the effect of resistance on the current is negligible.

The losses that an inductor offers as a virtue of its Ohmic resistance is called 'Copper losses' (I^2R) and are disregarded, as explained above. In addition, an inductor has two other losses called 'iron losses', namely 'Hysteresis Loss' and 'Eddy-Current Loss.' All these losses dissipate power in the form of heat and hence are lost power. (Power Loss in an Inductor [45]). Inductors of higher value have a larger number of turns and therefore have larger DC resistance and vice versa. For higher operating frequencies, the value of the inductance needed goes low and vice versa. D.C. resistance proportionally affects losses. Therefore, there has to be a tradeoff between the operating frequency and the value of inductance chosen. In our case, the operating frequencies are low. This should not necessarily mean that an inductor of a large value is selected, which would lead us to larger losses. Therefore, the inductors selected would be of mid/moderate magnitude.

2.8.2.1.2 Power losses in the capacitor

Power loss in a capacitor takes place within the dielectric. They are namely 'dielectric hysteresis' loss and 'dielectric leakage' loss. Dielectric hysteresis and the hysteresis found in a magnetic

material bear a similarity. It results from the rapid reversals of the polarity of the line voltage. Even though there is an assumption that the dielectric virtually prevents the flow of current through the capacitor because of the extremely high resistance of the dielectric, a minute amount of current will still flow, causing dielectric leakage losses. However, this current is so minute that for all practical purposes, it is neglected, and it is assumed that the capacitor returns the total charge back to the circuit [46].

2.8.2.1.3 I^2R losses (resistive losses)

All conductors do pose some resistance and therefore incur resistive losses, which are equal toI^2R but these are considered to be negligible for our calculations.

2.8.2.1.4 Power losses in synchronous Buck/Boost converters

There are three main sources of power loss in synchronous buck converters: quiescent losses (static losses), switching losses, and conduction losses. Quiescent losses generally represent only a small percentage of the total losses when the load at the output of the converter is above a few tens of milliamps and, therefore, can be neglected. In applications of relatively higher currents, switching and conduction losses play a much bigger factor than the quiescent losses. Switching losses in synchronous buck converters are the result of charging and discharging the capacitances that exist between gate-to-drain and gate-to-source of the power MOSFETs, which comes into effect when they are turned on and off. One part of the conduction losses (Joule losses) in a buck converter is due to the drain-source on-state resistance of the power MOSFETs. These losses listed from 8.2.1 up to 8.2.4 are liable to reduce the power available at the output of the piezoelectric system. However, they are considered inevitable.

2.9 Weather and climate considerations

Electrical circuits and components deployed in sub-zero temperatures could be pushed to their extremes. The properties of the materials used in the construction of electrical equipment could be altered or negatively affected by low temperatures and therefore its smooth functionality could be hindered.

Though often, temperatures during winter will be within operating ranges of much electrical equipment, there may exist intermittent periods of extremely low temperatures that fall outside of the standard operating temperature ranges of many common electrical equipment. –50°C temperatures, are not an impossibility in some areas, even for a short period of time. In Nova Scotia temperatures can vary rapidly and take any value from 10°C to -10°C within a single day.

The material used in electrical circuits could lose strength rendering them more brittle at lower temperatures. This indicates that low temperatures can change the properties of materials used in the construction of electrical equipment and hence require changes to be made in installation and operation to be affected to them in order to negate the effects of low temperatures. In addition to low temperatures prevalent in cold weather regions, low humidity, wind, snow, and ice formation are some other conditions that can also influence electrical equipment [51].

Metals can become less ductile and more brittle at very low temperatures. This impacts their ability to withstand impact. ‘Embrittlement’ which is the tendency to become brittle, is more characteristic in some materials than others. The crystal lattice structure of the metal is a strong determinant of the effects that temperatures has on the ductility of metals.

The decrease in ambient temperature leads to the insulation on wire and cable to harden and become brittle. Cables can experience damage during the process of being installed at low

temperatures. Standards regarding cable installations say that they be installed at a temperature range between their certified cold bend temperature up to 15°C in excess. It is also recommended that before installing cables in a cold atmosphere, they be stored at temperatures over 10°C, for one day. Impacting, dropping, or sharply bending cables should be avoided during installation and cables should be pulled slowly with care and trained (to remain in the path it is supposed to) the same day that it is removed from warm storage [51].

Figure 25 shows the three primary crystal structures for metals, body-centered cubic (BCC), face-centered cubic (FCC), and hexagonal close-packed (HCP) [51]. Commonly used industrial metals have BCC and FCC lattice structures. Metals with a crystal lattice structure of the BCC type lose their ductility easily compared to other lattice types due to low temperature.

Perovskite material which is known to have a molecular structure that is a combination of BCC and FCC exhibits almost negligent changes to subzero temperatures. Hence the employment of piezoelectric material itself in low temperatures experienced in Nova Scotia doesn't pose a major concern. But however, the effects of temperature on other components such as wire and cable will have to be taken into consideration.

Even though low temperatures would only have a negligible effect on the ductility of majority of metals used for electrical enclosures and fittings, care needs to be taken in selecting mounting structures, fasteners, equipment housings, and terminal, and all other parts that are made of materials that may experience embrittlement at low temperatures.

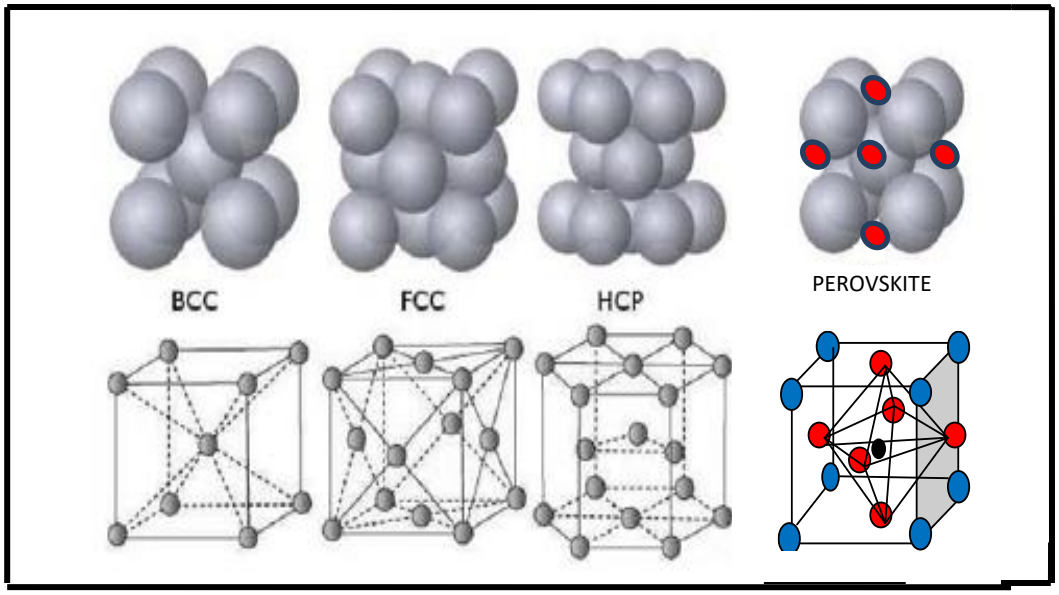

Figure 25. - BCC, FCC and HCP and Perovskite lattice structures [51].

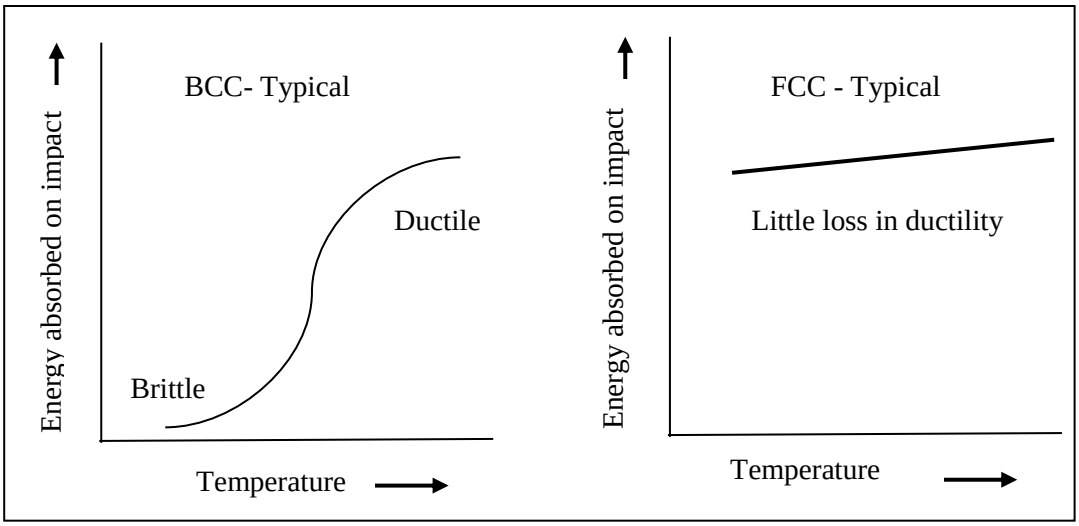

Figure 26. - Ductile to brittle transition [51].

Although materials used for components installed within enclosures are protected from impact they may be negatively affected by low temperatures and if made brittle by the low temperatures, could face fracture as a result of vibration, expansion, contraction or other occurrences that bring about stress.

Solder materials have problems too. Standard lead-tin solder and certain non-lead solders can have a fairly high ductile-brittle transition temperature (DBTT). It is vital to ensure that the solder materials used too are suitable for operating ground temperatures [51].

Differential expansion and contraction occurs because different materials have different coefficients of expansion. This could pose potential problems with both metals and non-metals and is encountered when alloys are used.

When equipment have to be explosion-proof and flame-proof, mating parts made of different materials should meet the requirement that the minimum flame path gap must be held across the entire range of ambient temperature. Tight tolerances on flameproof joints could bring that joint out of tolerance due to differential expansion or contraction at low temperatures. Differential expansion, if not given due consideration could cause electronics to fail.

Lubricants, unless specifically fabricated for low temperatures, can freeze and cause equipment to malfunction. In instances where it is required to use a lubricant, the manufacturer's guidelines should be faithfully followed with regard to use at low temperatures.

Installations and assemblies practically launched for the harnessing of piezoelectricity hitherto have been in mostly hot and humid environments or indoors. Our weather here in Nova Scotia is a distant contrast to these tropical or dry conditions and therefore special consideration has to be given to making installations sufficiently rugged. This will help them to withstand inclement or harsh weather conditions and unpredictable atmospheric disturbances.

Further study is required to come up with exact measures which need to be taken to make energy harvesting installations withstand extreme weather conditions and this project will undertake to

identify gaps in the study and practical manifestations of quantitative methods available for assessment of component vulnerability, and its application.

According to [78], the determinants of vulnerability to climate and weather hazards include exposure, sensitivity, and adaptive capacity. As per the papers presented at the 2014 Inter-governmental Panel on Climate Change (IPCC), the two factors are just sensitivity and adaptive capacity as shown in figure 27.

Even though these concepts were first introduced to discuss eco-systems and habitats they equally well apply to structures and composite hardware systems. The degree to which infrastructure is exposed to hazards is simply known as 'Exposure' and can change as the frequency and intensity of hazards change. The degree to which electricity systems and infrastructure are affected by a hazard is known as 'Sensitivity'. Adaptive capacity is the ability to adjust to potential hazards or respond to consequences.

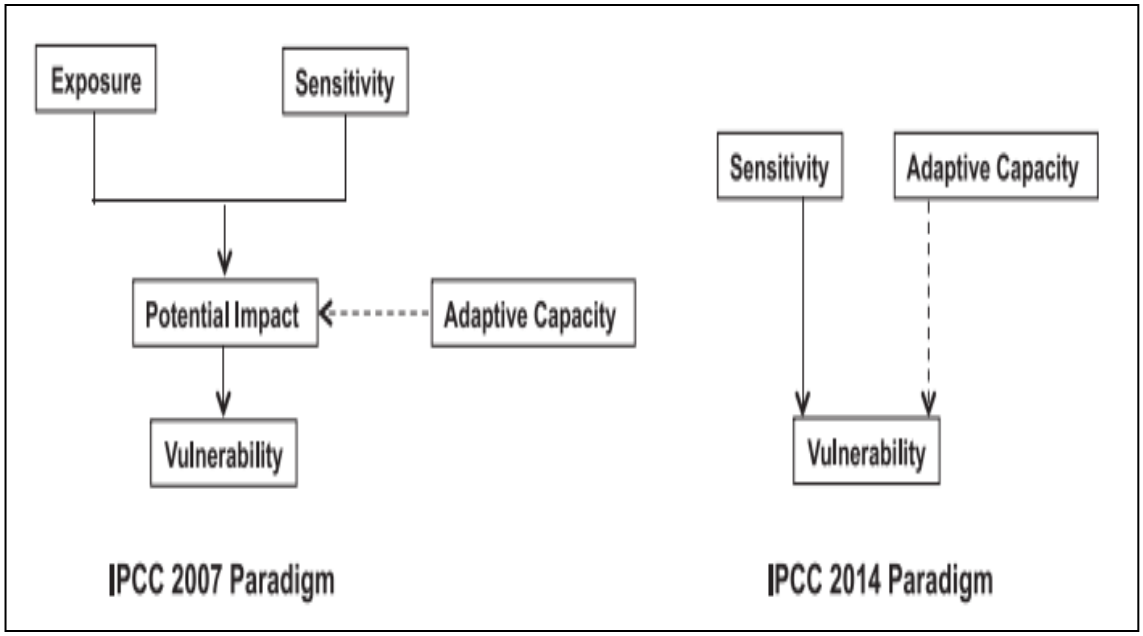

Figure 27. - The concept of vulnerability as presented in the IPCC 2007 and 2014 reports [97].

The review in [78] provides a collection of quantified relationships for determining grid (electrical) component sensitivity to extreme weather and climate hazards i.e. providing relationships between a potential environmental threat to a specific component and how that threat could snowball to affect consequences on the entire system (e.g., damage to equipment, duration of outages, etc.). The outlining of these mathematical formulae is beyond the scope of this project.

3. TECHNICAL CONTENT

3.1 What is piezoelectricity in detail

Certain materials, when subjected to physical distortion (changes to its dimensions as a result of external force) produces an electric charge across parallel opposite planes oriented in the conventional x,y or z axis. While this is what piezoelectricity is, the occurrence just mentioned in the previous sentence is called the direct piezoelectric effect. The opposite or the inverse effect (also called the reverse effect) is about deformation (changes to dimensions) of the material when it is connected to an external electric field. The word piezoelectricity is made of two Greek words: 'piezein' which means squeeze and 'elektron'. Piezoelectricity was first discovered by two French physicists Jacques Curie and Pierre Curie in 1880 but it was only in the '50s that it was used in industrial applications. In 1881 inverse piezoelectricity was mathematically deduced by Lippmann using fundamental thermodynamic principles. Later the inverse piezoelectric effect was confirmed by the Curies to be a fact [70].

Piezoelectric materials used today range from naturally occurring substances to synthesized substances. Each material has its own unique performance and there is an indication that the later discoveries being made with the passage of time are yielding better outcomes with their superior properties. The fundamental principle of operation and activity at the molecular/atomic level remains the same in almost all of these materials.

A good understanding of a piezoelectric material's behavior at the molecular level is needed to comprehend the causes that make a material possess piezoelectric properties.

What causes the piezoelectric effect is a phenomenon called 'spontaneous polarization' [83]. Two effects are contributory to this phenomenon. First is that the electron clouds in the atoms of the piezoelectric material displace onto one side of their positively charged nucleus. The second

is that positive ions in the crystal structures of the material distance themselves relative to their negative ions. Both of these effects create tiny electric dipoles within the crystals. In a piece of untreated or unpoled (poling explained in section 4.4) piezoelectric ceramic, all dipoles are oriented in random directions, so that no real piezoelectric effect is witnessed.

Figure 34 (a) presents a schematic view where a cross-section of a piezoelectric material is shown with dipoles, randomly oriented. Poling it (say below Curie temperature for now) gives it a macroscopic piezoelectric effect as shown in figure 34 (b). A poled piezoelectric material is one which has its dipoles remain aligned in the poling direction, even after the poling process is complete, as shown in figure 34(c)

The two electric fields i.e. polarization voltage and the polling voltage occur in the same direction in all materials with the exception of piezo-electrets where a third voltage comes into play known as the 'electet' voltage. The piezoelectric phenomenon too has a different explanation in these materials.

The ultimate deciding factors of a piezoelectric material will be its electro-mechanical coupling co-efficient, flexibility, frequency response, thermal stability, and cost. All known piezoelectric materials compete very closely in many of these areas but it's imperative that a clear winner is chosen in order that the optimum results are delivered in an individual's project/application.

3.2 Ferro- electrets

Piezoelectricity in Ferro-electrets is a result of deformation of charged voids. The dynamics of piezoelectricity in Ferro-electrets is illustrated in figure 28. Polymer films with closed internal voids are subjected to an electrical field. This makes the gas inside the voids to break down. The piezoelectricity in these films manifests from the macroscopic dipoles created due to the separated positive and negative charges positioning themselves at the gas/polymer interface on

the opposite boundaries of the voids. Upon metallization, compensating charges are seen on the electrodes with the polarity opposite of the polarity of the dipoles closest to that side as shown in figure 28(a). Under the influence of an externally applied stress, the Ferro-electret's experiences a volume decrease. A decrease in the dipole distances results in a decrease in dipole moments. On the other hand the decrease in the whole film volume, leads to an increases in dipole density. The extent of the dipole moment reduction is however, more contributory than the increase in dipole density. Therefore the amount of compensating charges on the metal electrode decreases and the change in dipole moment causes the flow of charges as displayed in figure 28(b). The special aspect of the electret effect is that it is the surface charges that are responsible for the electret effect. Because the surface charge is opposite in sign from that associated with the polarization (taking place within the voids) and the electret voltage is measured at the surface, the electret voltage polarity is opposite to the polarization voltage polarity (polarization voltage as applicable also to Ferro-electric material) and is the same as the poling voltage polarity as shown in figure 29 [64].

Even though very good piezoelectric properties have been displayed by Ferro-electrets their manufacture and commercial use faces a few challenges such as very poor charge stability at high temperatures, random individual void geometry, and irregular overall cellular structure. Therefore, the material is still under experimentation. This project limits itself to Ferro-electric material.

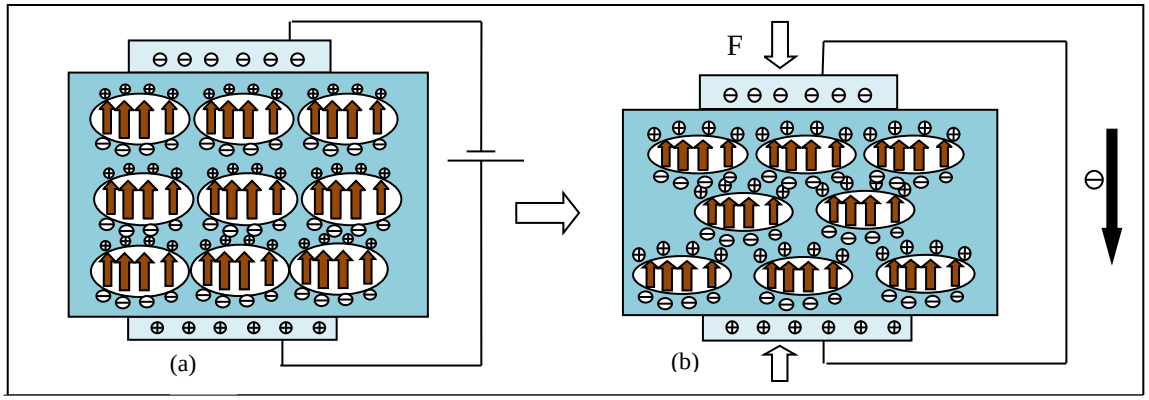

Figure 28. - Ferro-electret poling and charge movement [64].
(a) Macroscopic dipoles are formed in the voids at the gas/polymer interface after charging.
(b) Under mechanical stress, change in dipole moment causes the flow of charges.

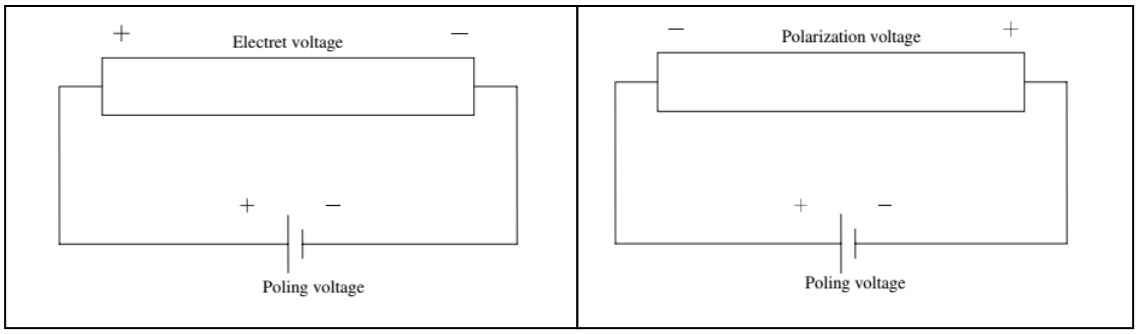

Figure 29. - Poling voltage, electret voltage and polarization voltage in Ferro - electrets [64].

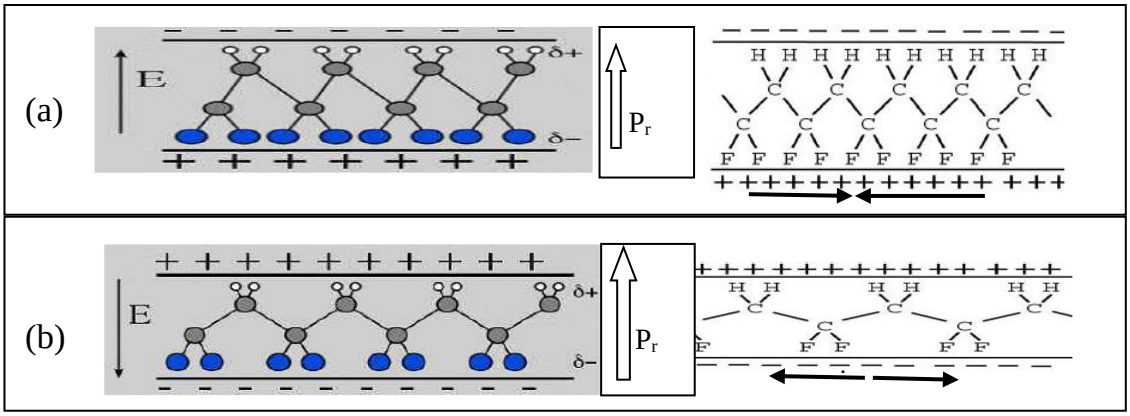

Figure 30. - Molecular behavior β PVDF during reverse piezoelectric effect [7].
(a) When the applied electric field is of the same polarity as the poling voltage the material is contracted (elongation in the direction of applied field).
(b) When the applied electric field is of opposite polarity to the poling voltage the material is stretched. (Contraction in the direction of applied field).

Figure 30 shows the molecular behavior of β PVDF during the reverse piezoelectric effect. β PVDF is a polymer but however, unlike other polymers behaves like a Ferro-electric.

3.3 Ferro-electrics

In Ferro-electric material, the unit cells (the basic repeating unit) inside the crystal may not be symmetrically arranged unlike in most other crystals. The crystal itself will still remain electrically neutral with a net non-zero charge in each unit cell of the crystal. Ideally, the centers of the positive and negative charges of each molecule should coincide resulting in electrically un-polarized molecules. However, as a result of the Titanium or the Zirconium ion occupying a slightly off-center position, an electrical polarity develops; effectively turning the unit cell into an electric dipole. These dipoles would be randomly oriented due to the unit cells themselves being randomly oriented.

With no external pressure (Stress) and the structure therefore undisturbed, electric dipole moments would cancel each other with no change to the charge distribution.

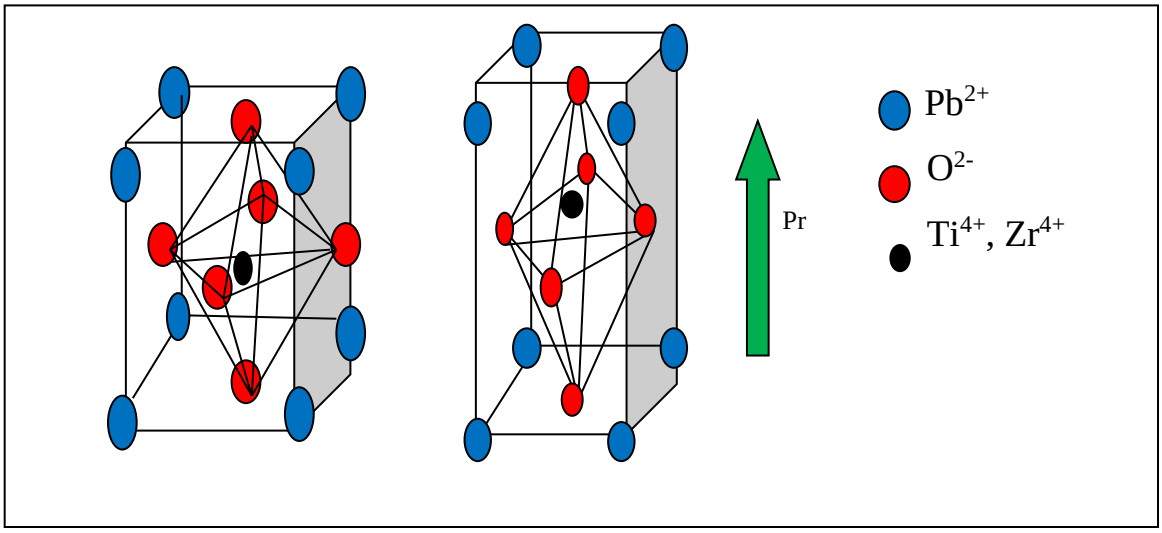

Figure 31. - Perovskite structured tetragonal unit cell of Lead Zirconate Titanate, $Pb(Zr,Ti)O_3$ [112].

Piezoelectricity occurs due to an external stress that is applied which deforms the structure. This displaces the Ti or Zr ionic charges as shown in figure 31. When charges get displaced the charge distribution which so far was symmetric will no longer remain so.

The Piezoelectric material will now possess a lattice structure in which the centers of positive and negative charges aren't overlapping anymore. When each dipole rotates from its original orientation towards another direction, the overall electrical and mechanical energy stored in them is minimized [19]. This re-orientation pushes some of the atoms closer together or further apart and while this effect propagates throughout the whole structure, net positive and net negative fixed charges appear on the opposing faces of the crystal, i.e. net polarization occurs as shown in figure 33. The poles facing each other with opposite polarity inside the material will still cancel each other and the crystal as a whole will still remain neutral.

The spatially separated charges at the two opposite surfaces result in an electric field and in turn a potential difference across them. The 'free charges' available at the opposite faces are now ready to flow through an externally connected conductor. Thus the electric field generated could be instrumental in transforming the mechanical energy that was used to deform the material into electrical energy.

Lead Zirconate Titanate is said to have a Perovskite structure. Originally the crystal structure of calcium titanium oxide ($CaTiO_3$), was named the 'Perovskite structure', or $A^{2+}B^{4+}X^{2-}{}_3$ with the oxygen(X) in the edge centers as shown in figure 32. This mineral was first discovered in the Ural Mountains of Russia by Gustav Rose in 1839 and its structure got its name after Russian mineralogist L. A. Perovski. Now any material with this same type of structure is called a Perovskite [112].

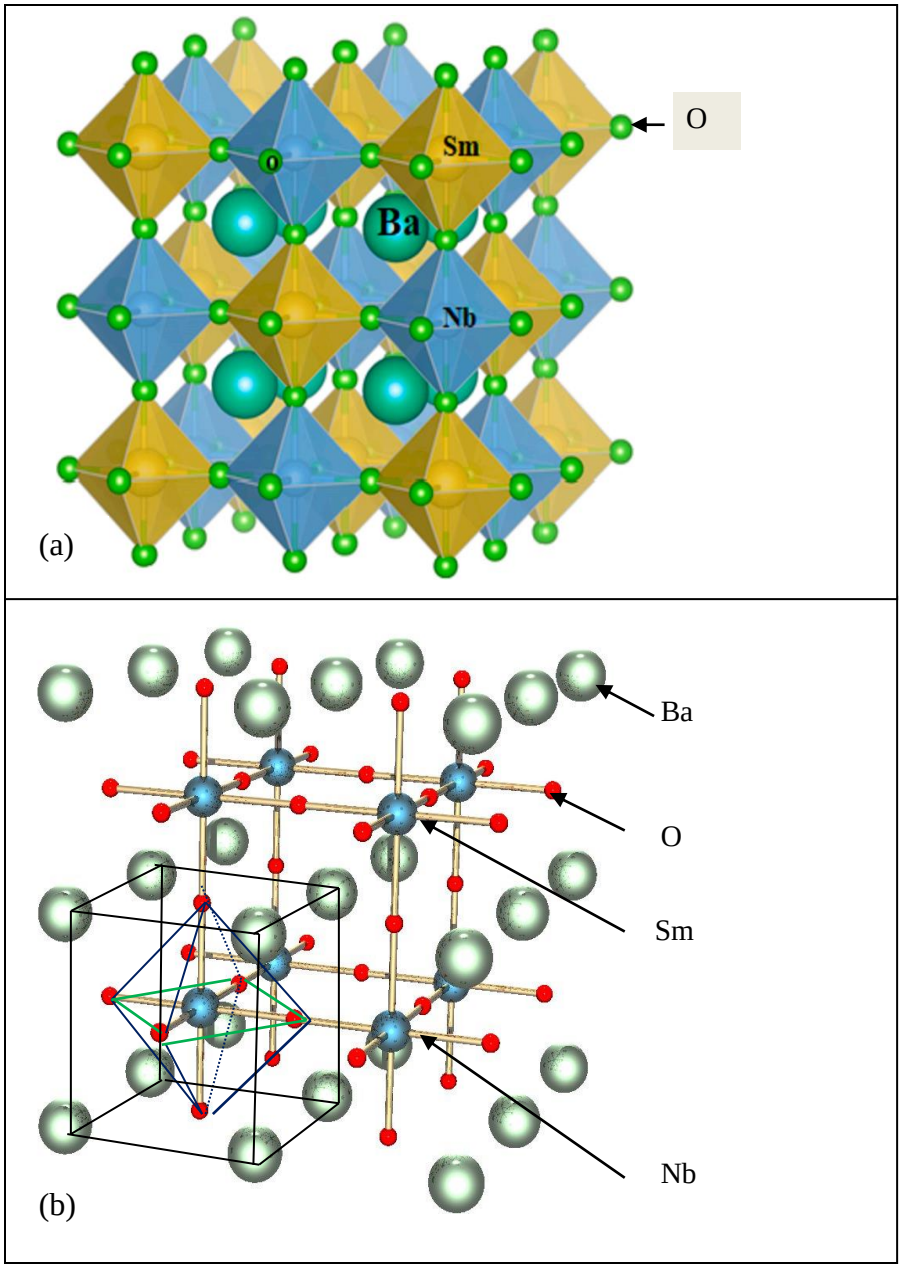

Figure 32. - Perovskite structured Barium Samarium Niobate crystal (Ba_2SmNbO_6) [52].
(a)Three-dimensional cubic crystal structure of typical ordered Perovskite.
(b) Skeletal cubic crystal structure of typical ordered Perovskite.

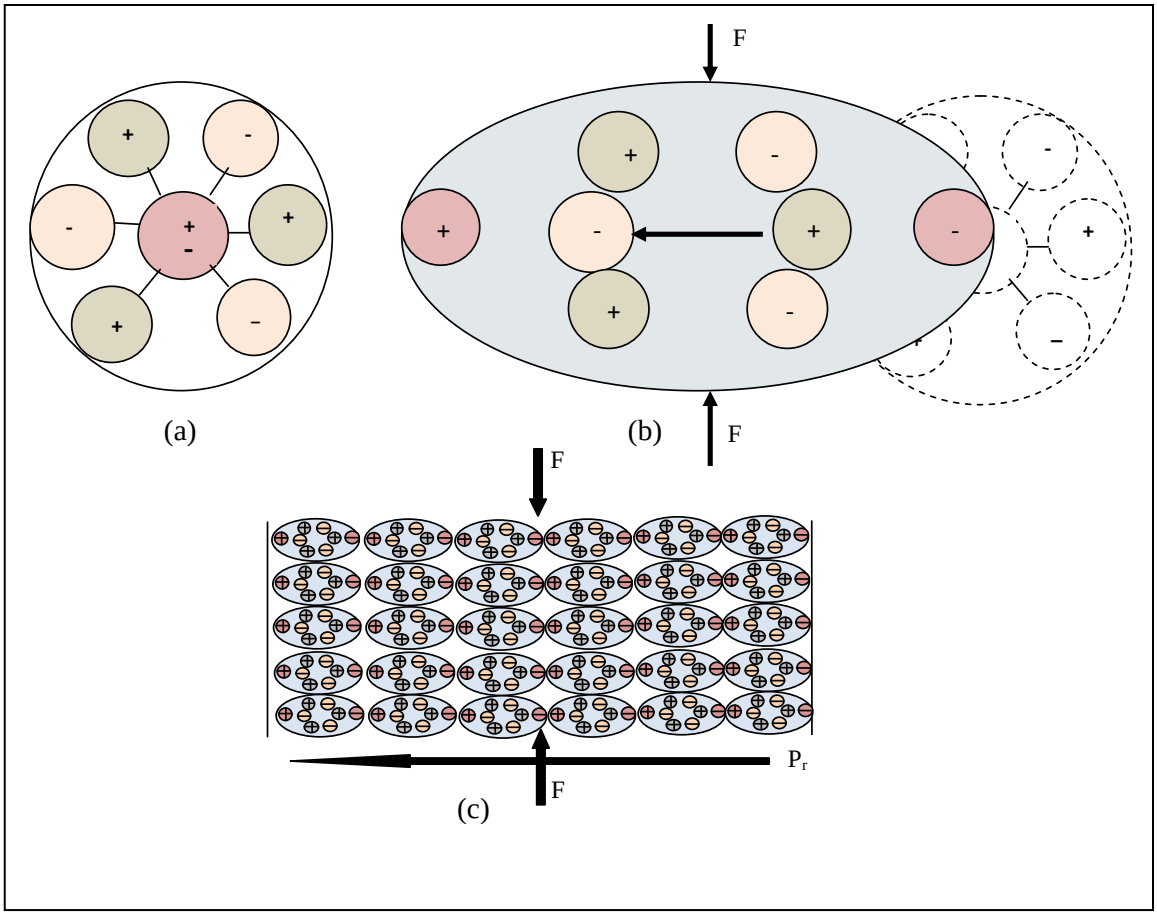

Figure 33. - Molecular behavior in Ferro-electric material [16].
(a) An undisturbed molecule with no piezoelectric polarization.
(b) A molecule subjected to an external force resulting in polarization.
(c) Polarization effect when piezoelectric material is subject to external force.

Incidentally, Ferro-electret polymers and Ferro-electric polymers have d_{33} (PZ coupling co-efficient) of opposite signs. In Ferro-electrets the most common effects referred to as the direct and inverse effects, behave in a way different from the corresponding mechanisms in Ferro-electric polymers. In Ferro-electric polymers, a compressive stress in the 3-direction causes a decrease of distance between the molecular chains. This is due to the relatively weak Van Der Waals and electrostatic interaction between chains in comparison to the strong covalent bonds within the chain. The thickness decrease causes an increase of dipole density and then an

increase of the charges on the electrodes, yielding a negative d_{33} coefficient. In Ferro-electrets polymers, a compressive stress in the 3-direction also decreases the thickness of the sample. With this decrease of thickness occurring dominantly across the voids, the macroscopic dipole moments also decrease, and so do the electrode charges, yielding a positive d_{33} [30], [63].

3.4 Poling

Since all dipoles are initially randomly oriented (i.e. a net polarization of zero) before poling, the piezoelectric effect exhibited will be negligible. (Figure 34 (a)) The decisive criterion of the piezoelectric effect is the change (increase or decrease) in polarization when subjected to mechanical stress. Therefore, creating an initial state in the material where most dipoles are more-or-less oriented in the same direction would be helpful, making it more piezoelectric sensitive, i.e. yield more polarization when mechanically stressed.

The material could be yielded to such an initial state by poling it. Poling is done by applying a strong electric field across the material while the material remains at an elevated temperature known as the Curie temperature. The heat enables the free movement of the molecules and the electric field forces the dipoles to align themselves in accordance with it.

After cooling while the electric field still remains, and then the subsequent, complete removal of the electric field, not all dipoles return to their original direction. This results in what's called 'remnant polarization' denoted by P_r which will be a permanent feature of the material and qualifies it to the status of a poled material. It is now ready to produce electricity; piezoelectricity [64].

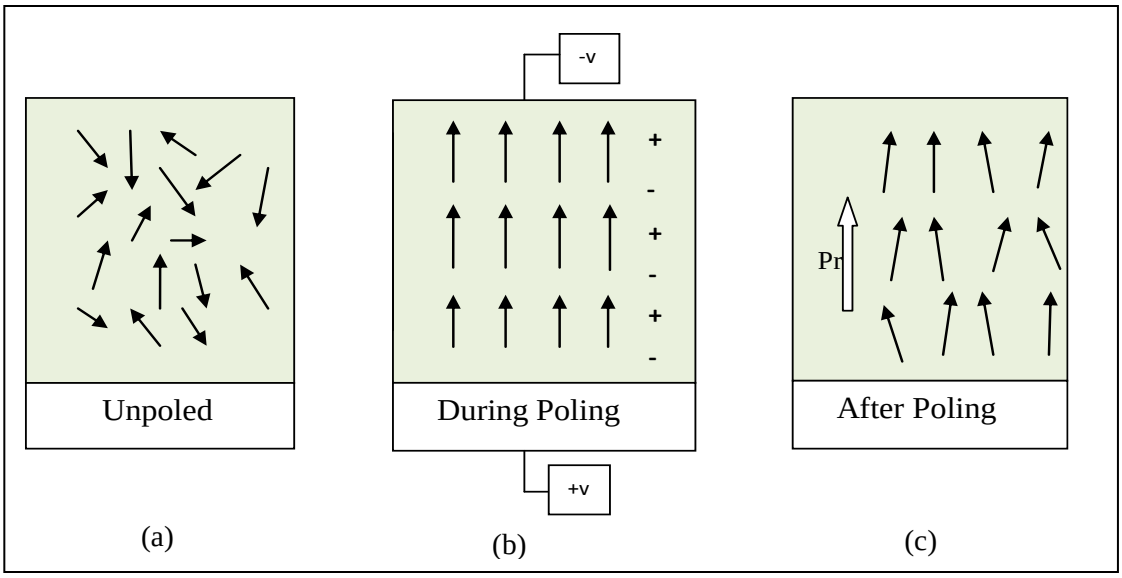

Figure 34. - Dipole orientation during the process of poling [35], [84].
(a) Dipoles in an un-poled piezoelectric material.
(b) Alignment of dipoles during poling.
(c) Alignment of dipoles after poling.

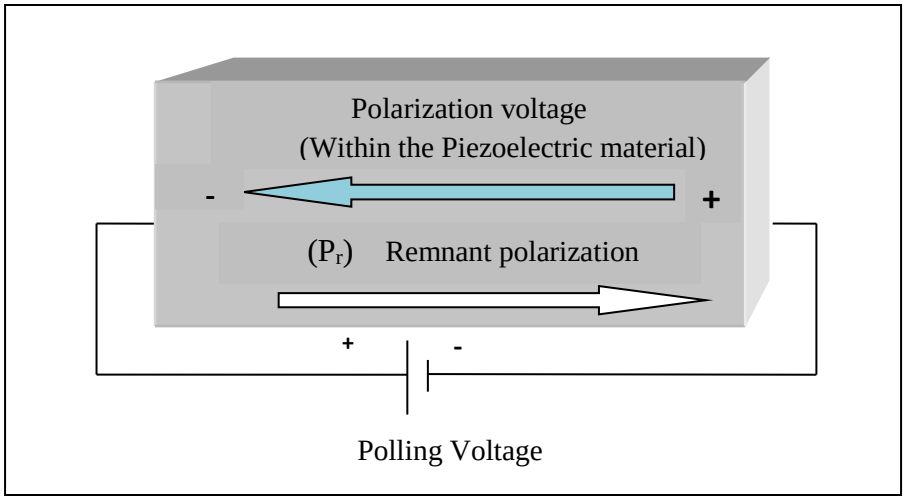

Figure 35. - Polling voltage, polarization electric field and remnant polarization [64].

The positive and negative signs in figure 34 (b) represent dipole orientation. Since the negative ions are attracted towards the positive end of the applied electric field and the positive ions are attracted towards the negative end of the applied electric field, the electric field created within

the material due to poling, opposes the applied electric field. The direction along which the dipoles align themselves is known as the 'poling direction' and the remnant polarization (P_r) would remain in this direction as shown in figure 34(c) and figure 35. Terms such as 'Polarization vector' (P_L) and 'Polarization axis' are also used and are marked in the same direction as P_r. The small arrows showing dipoles and the arrow showing Pr shouldn't be confused with the convention used to mark electric fields.

During the poling process dipoles not only rotate, they also stretch and this dipole activity causes the material to expand in the poling direction, as shown in figure 36. In keeping with Poisson effects, contraction occurs in the transverse directions. This results in permanent alterations to the dimensions of the piezoelectric material i.e. the dimension between the poling electrodes increases and the dimensions parallel to the electrodes decreases. The piezoelectric nature of the material will remain as long as the material is not de-poled, due to for example operating at a temperature which is in excess of the Curie point, or being subjected to extreme electric or mechanical conditions.

The phenomenon of piezoelectricity occurs when a poled piezoelectric material experiences mechanical stress which causes it to get electrically polarized. However, it is interesting to note that all piezoelectric materials cannot be poled.

A poled piezoelectric material displays different electro-mechanical properties in different directions depending on the axis along which electrical and mechanical excitations are applied. This is the property of being 'anisotropic'. Incidentally, there are no isotropic piezoelectric materials. The axis which gives optimum results should be selected before selecting a material for any particular practical purposes and this would decide the application of the poling field and

therefore the poling axis. Conventionally, the poling direction is considered to be the 3rd axis (z-axi), except in quartz where the polarity is considered to be along the 1st axis [19].

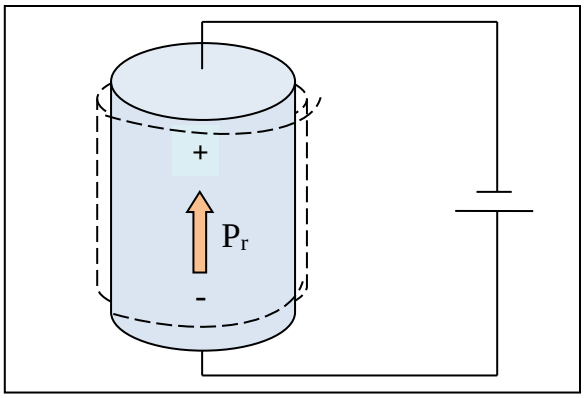

Figure 36. - Dimensional changes to piezoelectric material before (dotted line) and after poling (thick line) [16].

The dipole model is a simplification of the true piezoelectric mechanism in two ways. The first simplification is that in the actual case, electric dipoles with like orientation group themselves into tiny domains and it is these domains that get aligned with the electric field when polarized. The second simplification is that not all of these domains are able to completely align themselves with the electric field due to micro-mechanical effects.

However, enough does align to deliver the desired piezoelectric effect [76]. A material with randomly oriented grains (unsymmetrical) must be Ferro-electric, to be able to be poled. Being 'Ferro-electric' means the dipole moment could be nullified when an external electric field in the opposite direction is applied. Ferro-electric crystals exhibit electric dipoles even before being poled, because the center of the positive charge(s) of the crystal does not coincide with the center of the negative charge(s). This tells us that dipoles thus exists even before poling, they are just not aligned.

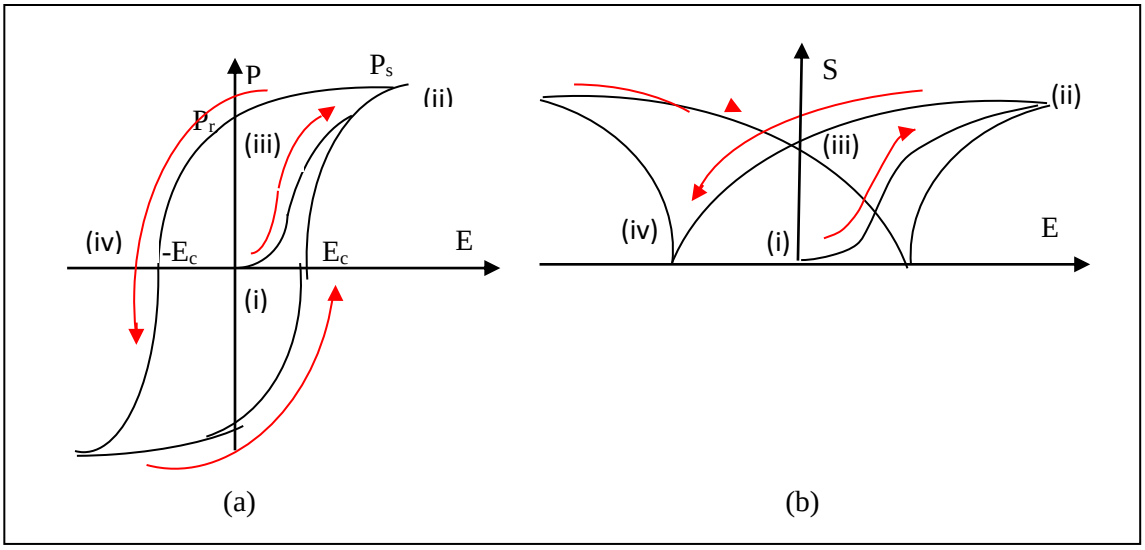

Figure 37. - Hystersis behavior of Ferro-electric material [16].
(a) Typical Polarization (P) Vs Applied Electric Field (E) hysteresis plot.
Ps: saturation polarization; Pr: remnant polarization. Ec: coercive field.
(b) Strain (S) versus Electric Field (E) plot of a piezoelectric material.

All Ferro-electrics are pyro-electric. Pyro-electricity is the capability of a material to generate a temporary voltage when it is subjected to a temperature which is a fair departure from ambient temperature. They have the additional property that their natural electrical polarization is reversible.

3.5 Basic behavior of piezoelectric material (static action)

The basic behavior of piezoelectric material could be categorized into direct behavior and reverse behavior.

3.5.1Direct piezoelectric effect

When a compressive force is applied parallel to the poling axis, or a tensile stress perpendicular to the poling axis, a voltage would be generated between the electrodes which would have the same polarity as the poling voltage.

Alternatively when a tensile force is applied parallel to the poling axis or a compressive force perpendicular to the poling axis a voltage would be generated between the electrodes which would have opposite polarity to the poling voltage as shown in figure 38(a) and figure 38(b). The solid arrow indicates the direction of the current flow. The plus and minus signs near the ammeter show the correct meter polarity for the current measurement. An ammeter is always connected so that the current will flow into the positive terminal and out of the negative terminal. A galvanometer doesn't have this restriction.

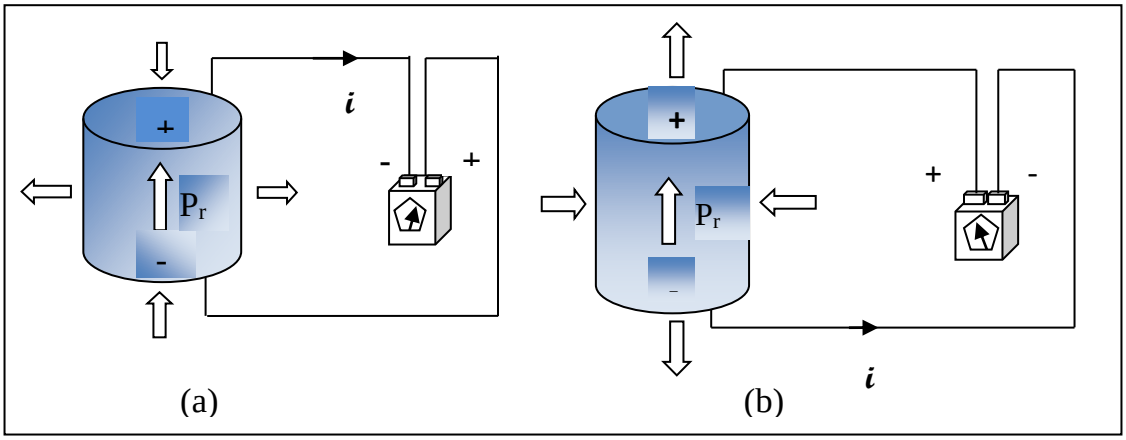

Figure 38. - Direct piezoelectric effect [24].
(a) Generated voltage with polarity similar to the poling voltage due to longitudinal compressive stress.
(b) Generated voltage with polarity opposite to the poling voltage due to longitudinal tensile stress.

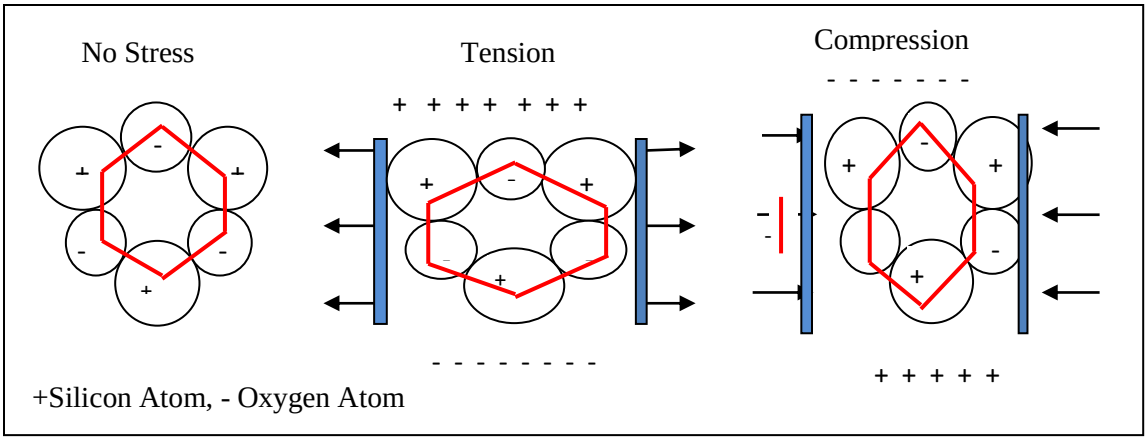

Figure 39. - Molecular behavior during direct piezoelectric effect in Quartz [98].

3.5.1.1 Direct piezoelectric effect explained in terms of longitudinal and transverse piezoelectric effect

Longitudinal piezoelectric effect (as shown in figure 40)

When a force is applied to a piezoelectric material in the longitudinal direction (parallel to the axis of polarization- z-axis), a voltage is generated across the two opposite faces along the 'z' axis. This voltage tries to restore the piece to its original thickness.

Transverse piezoelectric effect (as shown in figure 41)

When the force is applied along the neutral axis, say 'x' or 'y' (perpendicular to the axis of polarization: z-axis) charges are displaced along the z-axis so that a voltage is generated across the two opposite faces along the z-axis. This voltage tries to restore the piece to its original length and width.

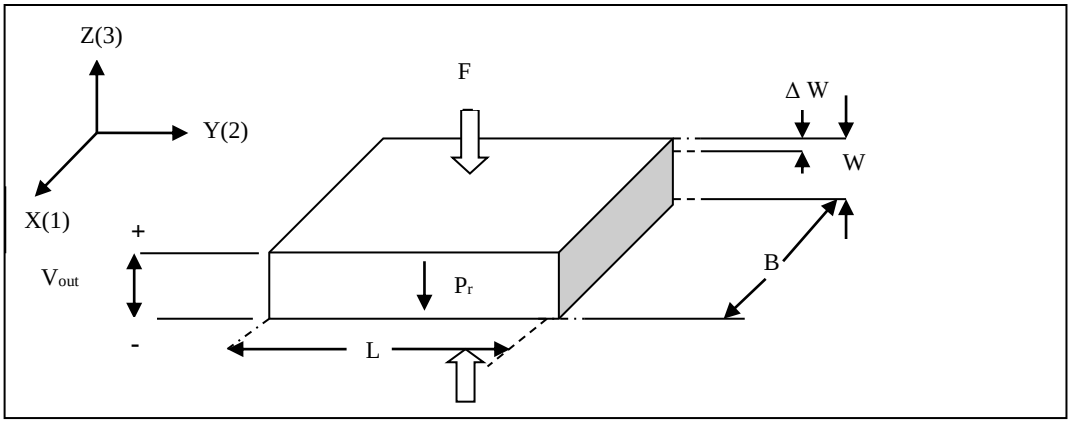

Figure 40. - Longitudinal piezoelectric effect.

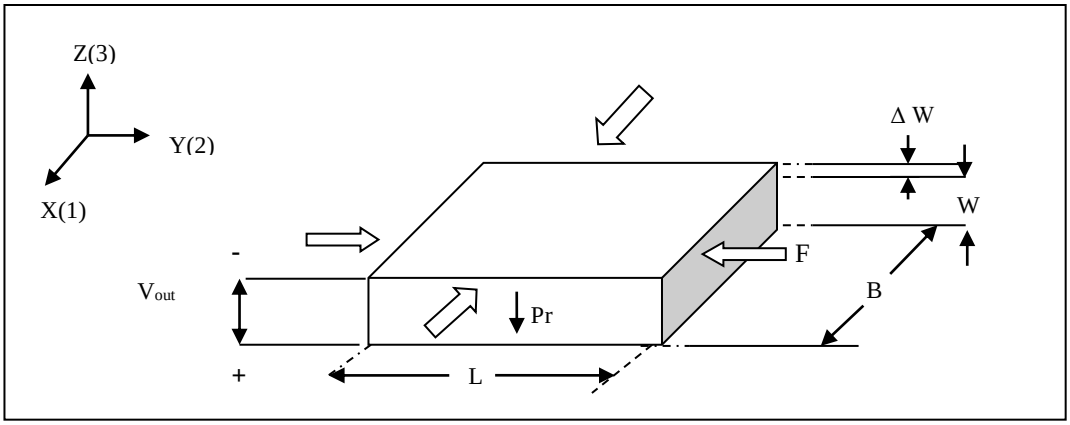

Figure 41. - Transverse piezoelectric effect.

A point to note is when mechanical stress (compression or tensile) is applied longitudinally (same direction as polarization) the voltage generated is such that, if that voltage were to be applied externally it would try to bring the material to its original length. A similar argument exists when stress is applied in a transverse direction (perpendicular to polarization) [82]). This is in line with the fact that the material is trying (or would try) to resist external effects to try to regain its original dimensions, akin to the action of an inductor.

3.5.2 Reverse piezoelectric effect

After the poling process is complete, even a voltage lower than poling voltage will cause a dimensional change in the piezoelectric material. This effect of reverse piezoelectricity was first discovered by Lippman during the study of thermodynamic principles and was further confirmed by the Curie brothers.

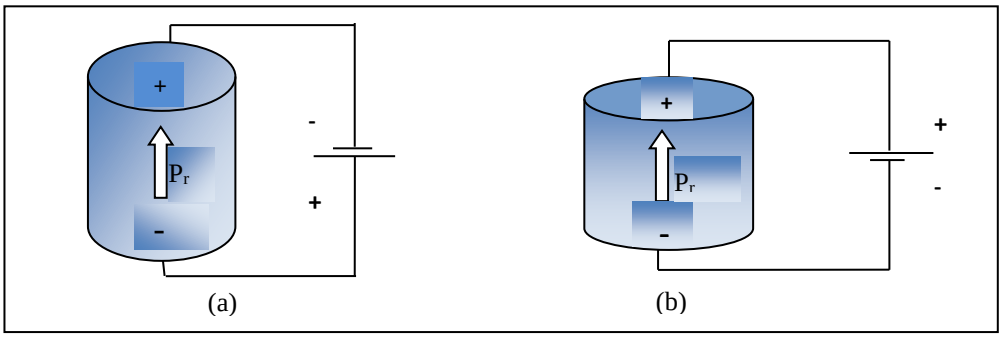

Figure 42. - Reverse piezoelectric effect [24], [50].
(a) Expansion of material when externally applied voltage has same polarity as poling voltage.
(b) Contraction of material when externally applied voltage has opposite polarity to poling voltage.

A voltage applied externally with the same polarity as the poling voltage will cause expansion of the material along the poling axis and contraction perpendicular to the poling axis.

A voltage applied externally with polarity opposite to the poling voltage will cause contraction of the material along the poling axis and expansion perpendicular to the poling axis.

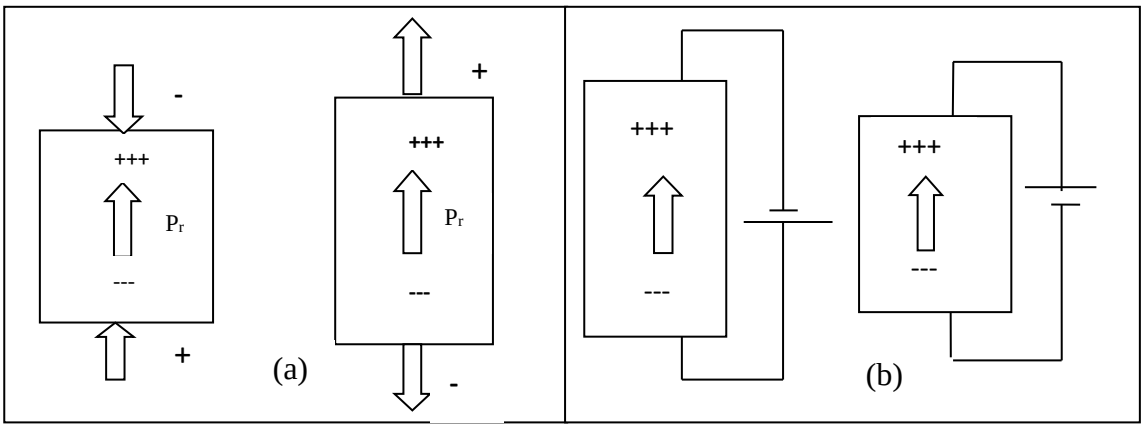

Figure 43. - Schematic diagram of (a) Direct piezoelectric effect and (b) Reverse piezoelectric effect.

3.6 The basic mathematical relationships governing piezoelectricity

(1) Relationship between charge generated and force

The basic mathematical relationship of a piezoelectric material, between its charge generated and force applied, is given by

$$C_x = (d_{xy})(F_y)(b/a)(n) \quad (4.1)$$

Where

C_x = Amount of charge generated in Coulombs

d_{xy} = Piezoelectric coefficient in C/N (Coulombs/Newton)

- Electric polarization generated per unit of mechanical stress applied

F_y = Applied force in N (Newton)

a = The dimension in line with the neutral axis (the axis along which the pressure is applied. Here it is 'y'

b = The dimension in line with the charge-generating axis (Perpendicular to dimension 'a'). Here it is 'x'.

n = number of elements in electrical parallel

(2) Piezoelectric linear constitutive relations

Linear piezoelectricity is a combined or cross-coupling effect of

(a) The linear electrical behavior of the material:

$$D = \varepsilon E \Longrightarrow \boldsymbol{D_i = \varepsilon_{ij} E_j} \tag{4.2}$$

Where D is the electric charge density and ε is the permittivity and E is the electric field strength.

And also, where ∇ . D = 0 and ∇ x E = 0 (the dot product and the cross product);

and

(b) Hooke's law for linear elastic materials

$$S = sT \quad \Longrightarrow \quad \boldsymbol{S_{ij} = s_{ijkl} T_{kl}} \tag{4.3}$$

Where S is strain, s is compliance and T is stress.

And also, where ∇ . T = 0 and $S = \frac{\nabla u + u\nabla}{2}$

These may be combined into so-called coupled equations of which the strain-charge form is

$$S = sT + \partial^t E \tag{4.4}$$

$$D = \partial T + \varepsilon E \tag{4.5}$$

In matrix form it is

$$\{\boldsymbol{S}\} = \left[s^E\right]\{\boldsymbol{T}\} + \left[d^t\right]\{\boldsymbol{E}\} \tag{4.6}$$

$$\{\boldsymbol{D}\} = [d]\{\boldsymbol{T}\} + \left[\varepsilon^T\right]\{\boldsymbol{E}\} \tag{4.7}$$

Where

$\{S\}$ is the strain matrix

$\{D\}$ is the electric charge density matrix

$\{E\}$ is the electric filed strength matrix

$\{T\}$ is stress matrix

s is compliance

$[d]$ is the matrix for the direct piezoelectric effect

$[d^t]$ is the matrix for the converse piezoelectric effect

ε = permittivity

The superscript E indicates a zero or constant electric filed

The superscript T indicates a zero or constant stress field

The superscript t stands for the transpose of a matrix

Considering tensor directions, the constitutive relations (or coupling) between mechanical stress, mechanical strain, electric field and electric displacement could be given by the following equations

$$S_p = s_{pq}^{E} T_q + d_{pk} E_k \quad (4.8)$$

$$D_i = d_{iq} T_q + \varepsilon_{ik}^{T} E_k \quad (4.9)$$

Where

S_p : mechanical strain in the p^{th} direction, S= F/A; F is stress and A is area

s_{pq}^{E} : elastic compliance tensor under constant electric field

T_q : mechanical stress in the q^{th} direction

d_{pk} : piezoelectric constant tensor (not to be confused with piezoelectric charge constant)

E_k : electric field in the k^{th} direction

D_i : electric displacement or charge density in the i^{th} direction, where in general $D = Q/A_r$;

Where Q = Charge in Coulombs and A_r = Area

d_{iq} : transposition of d_{pk}

ε_{ik}^{T} : dielectric constant tensor under constant stress

and where

p: $1 \leq p \leq 6$

q: $1 \leq q \leq 6$

k: $1 \leq k \leq 3$

i: $1 \leq i \leq 3$

The equation for the direct piezoelectric effect is

$$\begin{bmatrix} D1 \\ D2 \\ D3 \end{bmatrix} = \begin{bmatrix} d_{11} & d_{12} & d_{13} & d_{14} & d_{15} & d_{16} \\ d_{12} & d_{22} & d_{23} & d_{24} & d_{25} & d_{26} \\ d_{31} & d_{32} & d_{33} & d_{34} & d_{35} & d_{36} \end{bmatrix} \begin{bmatrix} T1 \\ T2 \\ T3 \\ T4 \\ T5 \\ T6 \end{bmatrix} + \begin{bmatrix} \varepsilon_{11}\varepsilon_{12}\varepsilon_{13} \\ \varepsilon_{21}\varepsilon_{22}\varepsilon_{23} \\ \varepsilon_{31}\varepsilon_{32}\varepsilon_{33} \end{bmatrix} \begin{bmatrix} E1 \\ E2 \\ E3 \end{bmatrix} \qquad (4.10)$$

And the equation for the converse piezoelectric effect is

$$\begin{bmatrix} S_1 \\ S_2 \\ S_3 \\ S_4 \\ S_5 \\ S_6 \end{bmatrix} = \begin{bmatrix} s_{11}^{E} & s_{12}^{E} & s_{13}^{E} & s_{14}^{E} & s_{15}^{E} & s_{16}^{E} \\ s_{21}^{E} & s_{22}^{E} & s_{23}^{E} & s_{24}^{E} & s_{25}^{E} & s_{26}^{E} \\ s_{31}^{E} & s_{32}^{E} & s_{33}^{E} & s_{34}^{E} & s_{35}^{E} & s_{36}^{E} \\ s_{41}^{E} & s_{42}^{E} & s_{43}^{E} & s_{44}^{E} & s_{45}^{E} & s_{46}^{E} \\ s_{51}^{E} & s_{52}^{E} & s_{53}^{E} & s_{54}^{E} & s_{55}^{E} & s_{56}^{E} \\ s_{61}^{E} & s_{62}^{E} & s_{63}^{E} & s_{64}^{E} & s_{65}^{E} & s_{66}^{E} \end{bmatrix} \begin{bmatrix} T1 \\ T2 \\ T3 \\ T4 \\ T5 \\ T6 \end{bmatrix} + \begin{bmatrix} d_{11} & d_{12} & d_{13} \\ d_{21} & d_{22} & d_{23} \\ d_{31} & d_{32} & d_{33} \\ d_{41} & d_{42} & d_{43} \\ d_{51} & d_{52} & d_{53} \\ d_{61} & d_{62} & d_{63} \end{bmatrix} \begin{bmatrix} E_1 \\ E_2 \\ E_3 \end{bmatrix} \qquad (4.11)$$

Processing conditions such as extrusion and particular crystal symmetry of piezoelectric material determine which components of the dielectric constant, piezoelectric and elastic compliance tensors are non-zero and unique. As such for most common piezoelectric material the above equations could be re- written as follows.

$$\begin{bmatrix} D1 \\ D2 \\ D3 \end{bmatrix} = \begin{bmatrix} 0 & 0 & 0 & 0 & d_{15} & 0 \\ 0 & 0 & 0 & d_{24} & 0 & 0 \\ d_{31} & d_{32} & d_{33} & 0 & 0 & 0 \end{bmatrix} \begin{bmatrix} T1 \\ T2 \\ T3 \\ T4 \\ T5 \\ T6 \end{bmatrix} + \begin{bmatrix} \varepsilon_{11} 00 \\ 0 \varepsilon_{22} 0 \\ 00 \varepsilon_{33} \end{bmatrix} \begin{bmatrix} E1 \\ E2 \\ E3 \end{bmatrix} \quad (4.12)$$

$$\begin{bmatrix} S_1 \\ S_2 \\ S_3 \\ S_4 \\ S_5 \\ S_6 \end{bmatrix} = \begin{bmatrix} {s_{11}}^E & {s_{12}}^E & {s_{13}}^E & 0 & 0 & 0 \\ {s_{21}}^E & {s_{22}}^E & {s_{23}}^E & 0 & 0 & 0 \\ {s_{31}}^E & {s_{32}}^E & {s_{33}}^E & 0 & 0 & 0 \\ 0 & 0 & 0 & {s_{44}}^E & 0 & 0 \\ 0 & 0 & 0 & 0 & {s_{55}}^E & 0 \\ 0 & 0 & 0 & 0 & 0 & s_{66}^E \end{bmatrix} \begin{bmatrix} T1 \\ T2 \\ T3 \\ T4 \\ T5 \\ T6 \end{bmatrix} + \begin{bmatrix} 0 & 0 & d_{13} \\ 0 & 0 & d_{23} \\ 0 & 0 & d_{33} \\ 0 & d_{42} & 0 \\ d_{51} & 0 & 0 \\ 0 & 0 & 0 \end{bmatrix} \begin{bmatrix} E_1 \\ E_2 \\ E_3 \end{bmatrix} \quad (4.13)$$

Where $s_{66}^E = 2(s_{11}^E - s_{12}^E)$

When a piezoelectric material is used in the thickness mode i.e. both stress and electric field are along the 3-direction, as in figure 14 (b), the equations can be expressed as

$$D_3 = d_{33} T_3 + \varepsilon_{33}^T E_3 \quad (4.14)$$

$$S_3 = s_{33}^E T_3 + d_{33} E_3 \quad (4.15)$$

A piezoelectric material's position is specified by the Material Coordinate System, which are the universally accepted XYZ axes (denoted in Capital). Therefore, while simulating piezoelectric materials, its spatial orientation and poling direction should be considered correctly in order to interpret the material properties. If the principal axes of the crystal do not align with the axes of the Material Coordinate System, an appropriate user-defined coordinate system would be created to provide a mapping function for appropriate transformation and interpretation of the material's properties.

The direction along the 'z' axis is considered the positive direction in a rectangular cardinal system, which comprises 'x', 'y', 'z' axes. Subscripts 1, 2, and 3 represent these global axes

directions and shear related to these axes are represented by ‘4’, ‘5’ and ‘6’. The direction of positive polarization usually is made to coincide with the Z-axis of a rectangular system of X, Y, and Z axes as shown in figure 44.

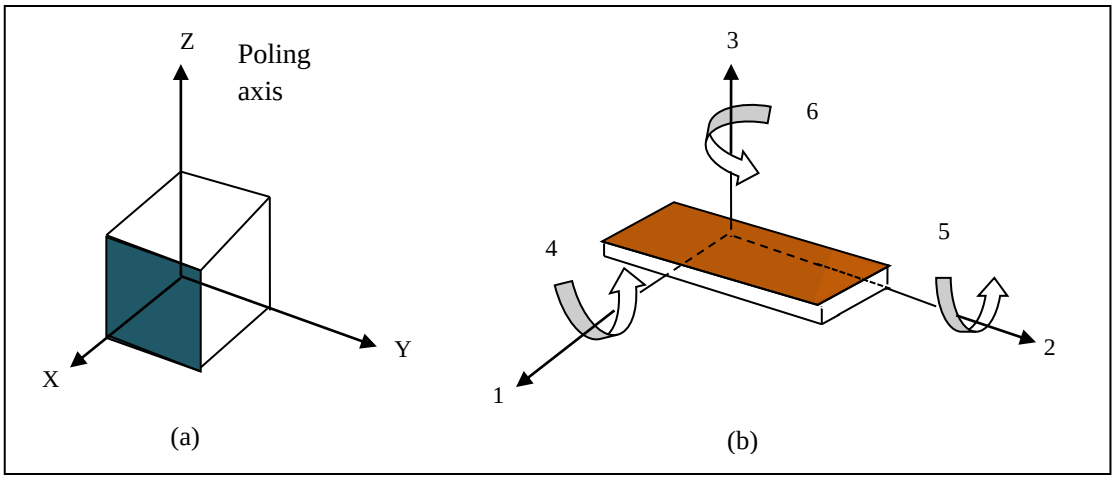

Figure 44. - Tensor directions for defining the constitutive relations [16], [26].
(a) Universal x,y,z coordinate directions.
(b) 1 corresponds to the draw direction. 2 to the transverse direction, 3 to thickness.

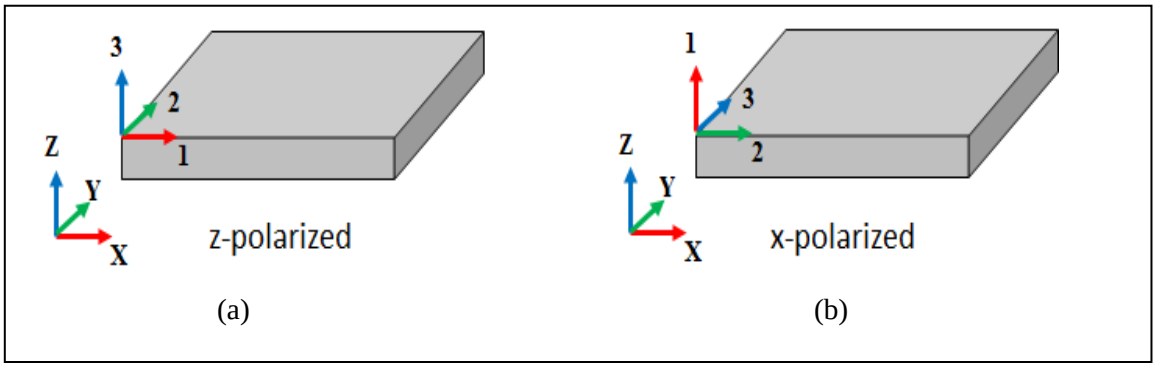

Figure 45. - z-poled and x-poled piezo material [36].
(a) Pictorial representation of a z-poled piezo where the principal crystal directions 123 are aligned with XYZ axes of the material coordinate system.
(b) An x-poled piezo is represented differently such that the 1st principal direction is aligned with the Z-axis of the material coordinate system.

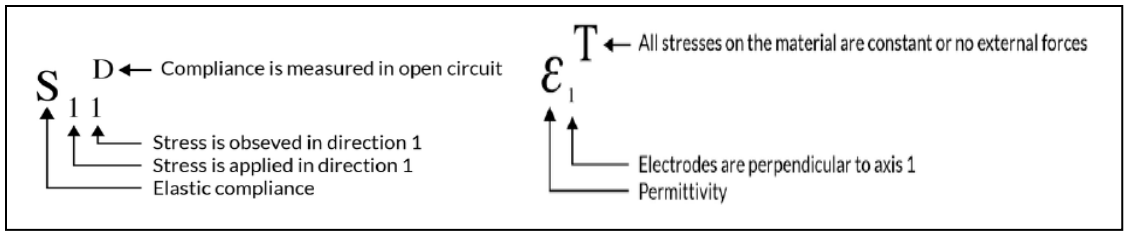

Figure 46. - Subscripts of coefficients s_{ij} and ε_{ij} have special meaning [35].

Note that the axis directions 1.2.3 in figure 44 and 45 might not be pointing the same way; however their relative orientation is the same.

3.7 Piezoelectric sensor response with respect to frequency

Piezoelectric materials produce a characteristic response which is analogue in behavior when subjected to a varying mechanical force. The peak of the response curve would correspond to some frequency named resonance frequency (Fr). Maximum energy conversion takes place for this value of frequency. A replica of the Voltage Vs frequency response is shown in figure 47 [18]. But quite often the working frequency for many a practically implemented structure is outside this resonance frequency, mainly towards the lower region. It's in the flat region between the high-pass cutoff (point A) and left of resonance (point B) in the frequency response plot that a sensor is typically used.

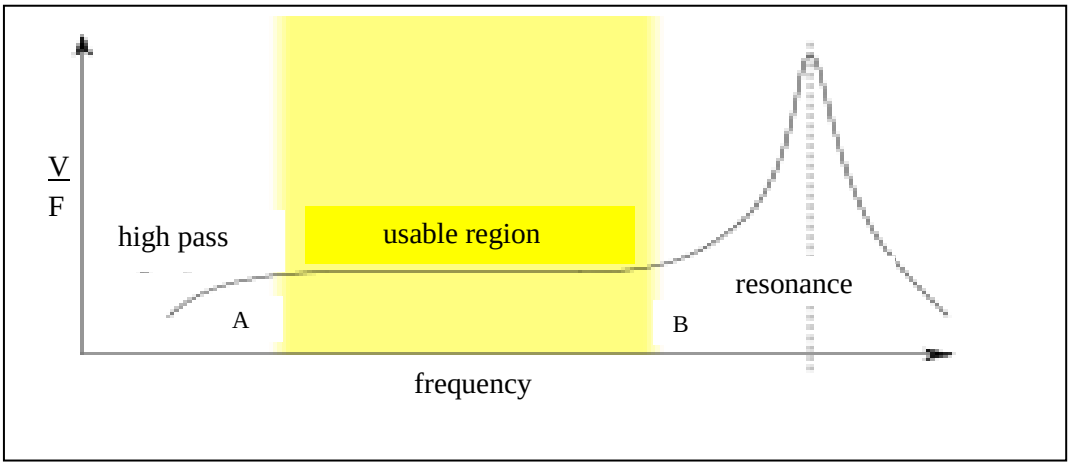

Figure 47. - Voltage response of a piezoelectric against frequency of applied force [111].

3.8 Matching the resonance frequency of the piezoelectric element to input frequency of the host structure

The biggest challenge in piezoelectric energy harvesting is low input frequencies. To get piezoelectric harvesters to yield an appreciable power output at these low frequencies is where the hump point lies. Different types of piezoelectric materials, harvester contraptions and new techniques were considered in this project in order to seek ways to achieve optimum performance in the mechanical-to-electrical energy conversion.

The fundamental frequency that the host is going to operate at has a direct relationship to the type, size and numbers of the basic piezoelectric element chosen, in creating the finished contraption. Most vibrational energy harvesting applications work with frequencies of hundred or below, which rather a mismatch with the natural resonance frequency of small piezoelectric harvesters.

Hence a broad spectrum of frequencies, in the low frequency range though, will have to be catered for. Ideally several frequency tuning and bandwidth enhancing techniques will have to be employed in order to improve the efficiency of piezoelectric energy harvesters. This, it is anticipated, would add to the complexity, and therefore the cost, of the harvesting systems. Therefore, such considerations have been set aside as far as this project is concerned, but nevertheless archived for future investigation. In [89] and [90] it is identified that the low frequency fundamental mode should be targeted in the design rather than the higher harmonics because the potential output power is proportional to $1/\omega$, where ω is the frequency of the fundamental vibration mode. The various techniques to be considered in achieving a lower resonance frequency in a relatively small package size, apart from the choice of piezoelectric

material used, configuration and design of the energy harvesting element, are also parameters archived for future investigation.

While most machinery operate at frequencies 100 Hz or higher, human activity is usually within the 1–30 Hz range. Piezoelectric ceramics which are metal oxides, exhibit much higher fundamental frequencies than composites and polymers of comparable size and geometry, with the same vibration mode. If monolithic piezoelectric ceramics are used as the energy harvesting element, the lowest resonance frequency mode is in the kilohertz range or higher, significantly beyond the frequency range of vibration of human sources. The lower the frequency of the vibration source, the more complex it becomes to design the energy harvesting unit using piezoelectric ceramics, as dimension and weight constraints could be limiting factors towards achieving the desired fundamental frequency. Under these situations even though piezoelectric composites and polymers seem to be the ideal 'material' candidates, in this project ceramics are selected for reasons enumerated in section 3.5 with table 3.5 cited.

3.9 Physical implementation and distinct stages in the energy harvesting system

A schematic diagram showing the basics of a piezoelectric energy harvesting system is shown in figure 48 and a block diagram of such a system in detail is shown in figure 49. Generally it

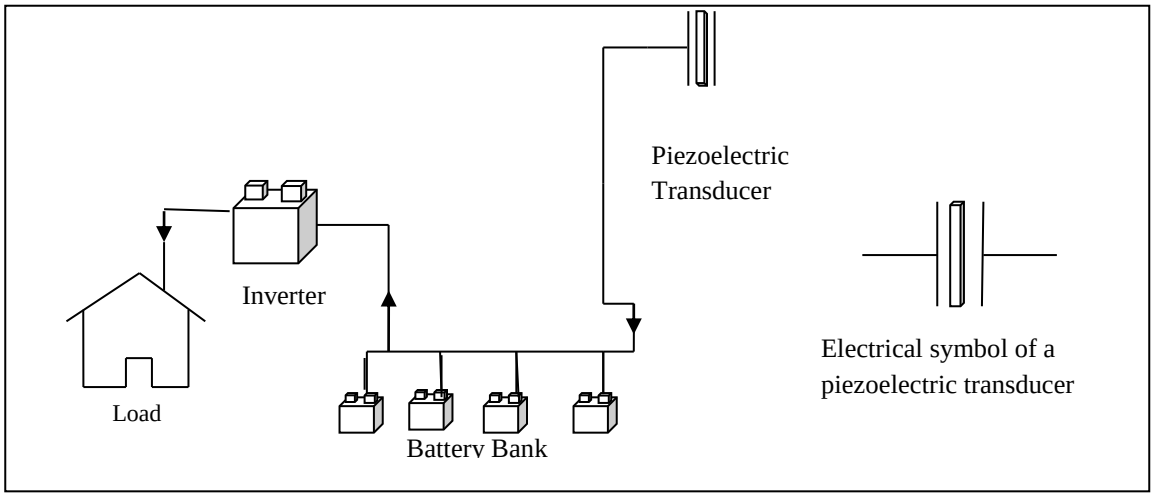

Figure 48. - Schematic diagram showing the basics of a piezoelectric energy harvesting system.

contains four main electronic units: an ac-DC rectifier, a voltage regulator, an energy storing device and an inverter.

The functions of the blocks shown in figure 49 are respectively as follows:

(a) The Piezoelectric harvester platform

(b) Converting voltage output from the piezoelectric material from ac to DC

(c) Regulating/conditioning the DC power supplied to the external load or the storage device

(d) Storage of energy harvested

(e) Inverting the DC voltage once again to ac as required

(f) The Load

Circuit design has a lot to play in the overall efficiency of power conversion. Various methods and designs have been looked into in improving the efficiency of rectifier and regulator circuits. Now with the advancement of micro-electronic technology, there exists small energy harvesting interface circuits, successfully mounted on a single chip which has low quiescent currents too. This project looks at both building a regulator circuit from basic components and also using a single power conditioning chip.

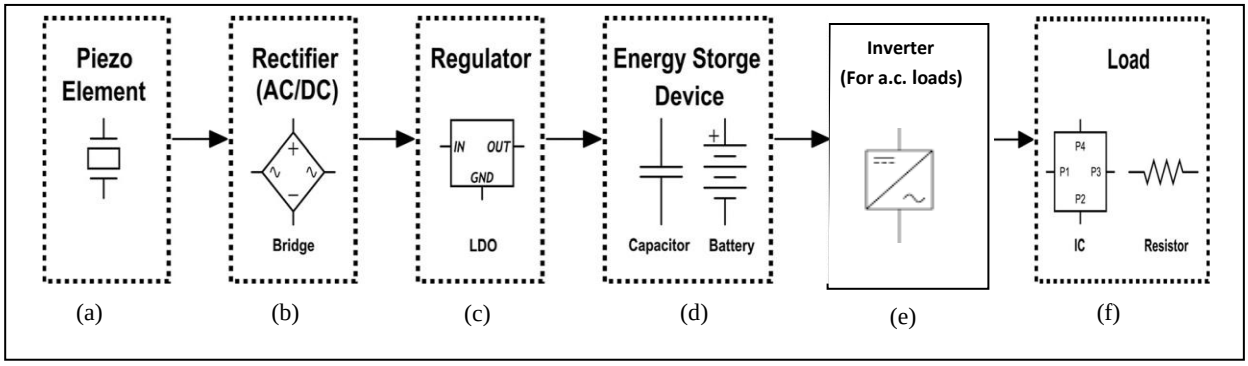

Figure 49..- Block diagram of a general electrical circuit for piezoelectric energy harvesting systems.

3.9.1 The piezoelectric unit (The basic element)

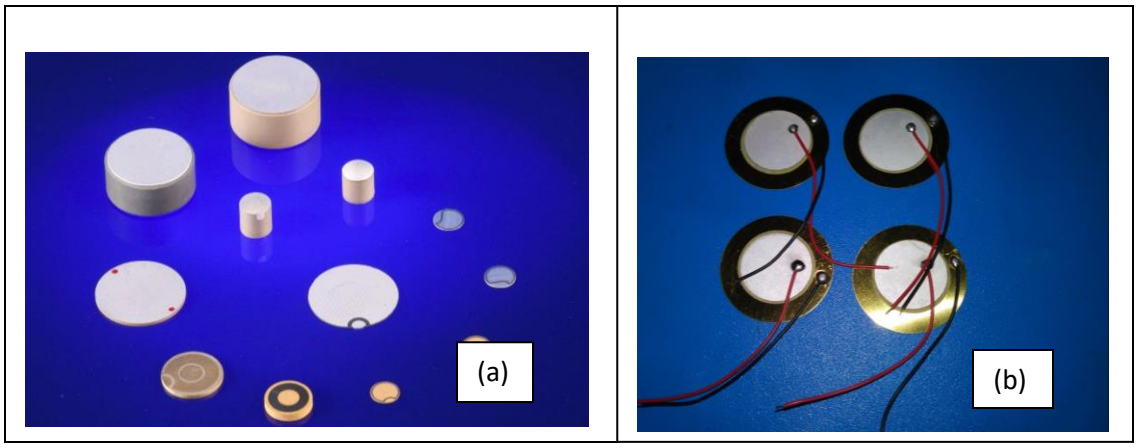

Figure 50. - Piezoelectric discs of various sizes and shapes.
(a) Piezoelectrics discs usable in harvesting energy from pedestrian traffic [31].
(b) The basic piezoelectric transducer discs used in this project for fabrication of the piezoelectric sub-assembly (27 mm outer diameter, D).

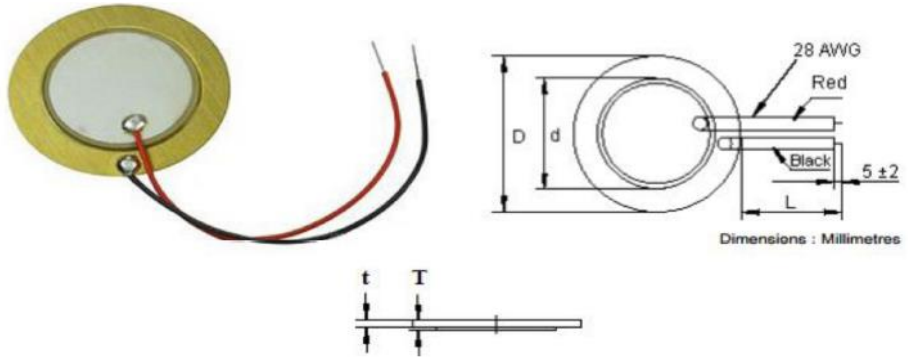

Plate size diameter, D (mm)	20.0	27.00
Element size diameter, d (mm)	14.0	19.7
Electrode size diameter, b (mm)	12.8	18.2
Thickness, T (mm)	0.42	0.54
Metal plate thickness, t (mm)	0.20	0.30
Resonance frequency, f_r (KHz)	6.3±0.6	4.6 ± 0.5
Capacitance, C (nf)	10.0 ± 30%	20.0 ± 30 %
Dielectric constant, ε_r	1510	1510
Resonance impedance, R (Ω)	≤ 300	≤ 300
Input voltage, V_{pp} max (V)	30	30
Operating temperature, (°C)	20 ~ 70	20 ~ 70

Figure 51. - Data sheet for commonly used 20 mm and 27 mm piezo discs [77].

3.9.2 Construction of the piezoelectric transducer sub-assembly

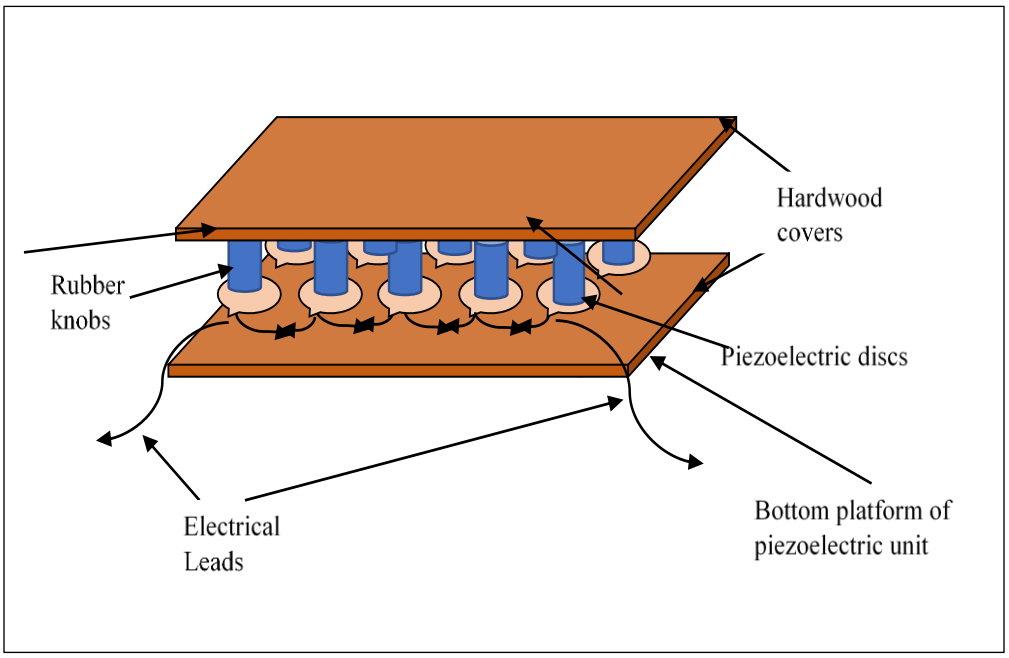

Figure 52. - Exploded view of a single piezoelectric transducer sub-assembly.

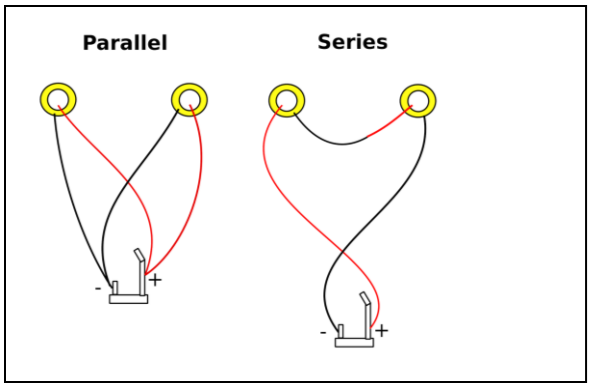

Figure 53. - Basic configurations of piezoelectric elements: parallel and series.

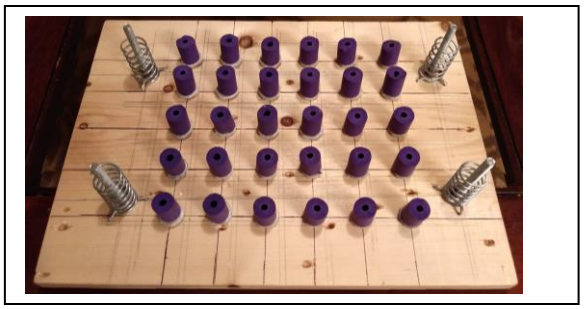

Figure 54. - Contact pods attached to the upper layer of the piezoelectric sub-assembly.

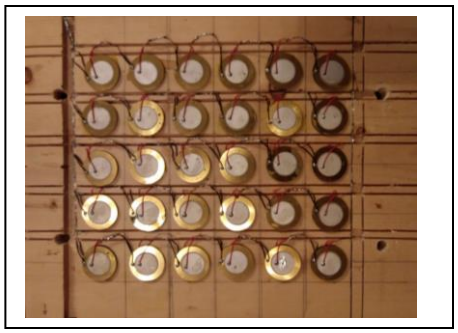

Figure 55. –Piezoelectric elements attached on wooden platform of piezoelectric sub-assembly.

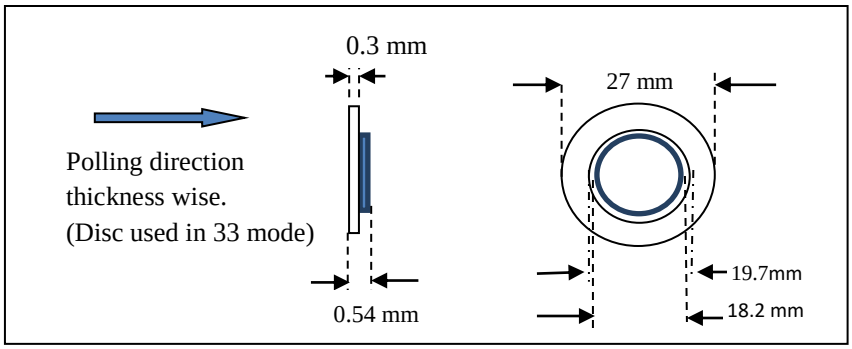

Figure 56. - Polling direction and dimensions of piezo discs

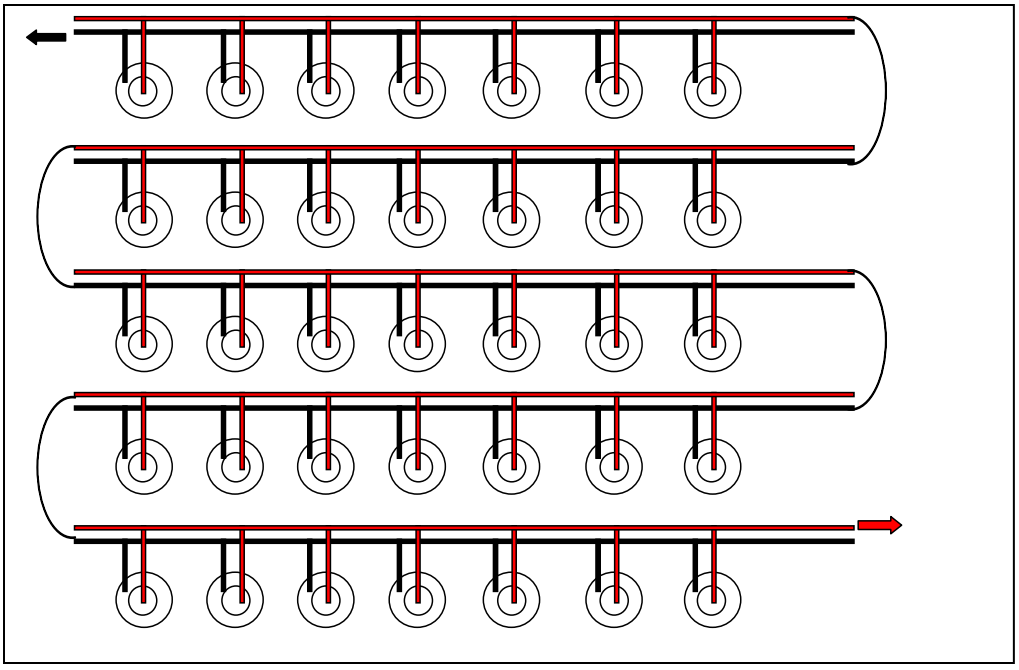

Figure 57. - Electrical connections of piezoelectric discs in the hybrid parallel-series configuration.

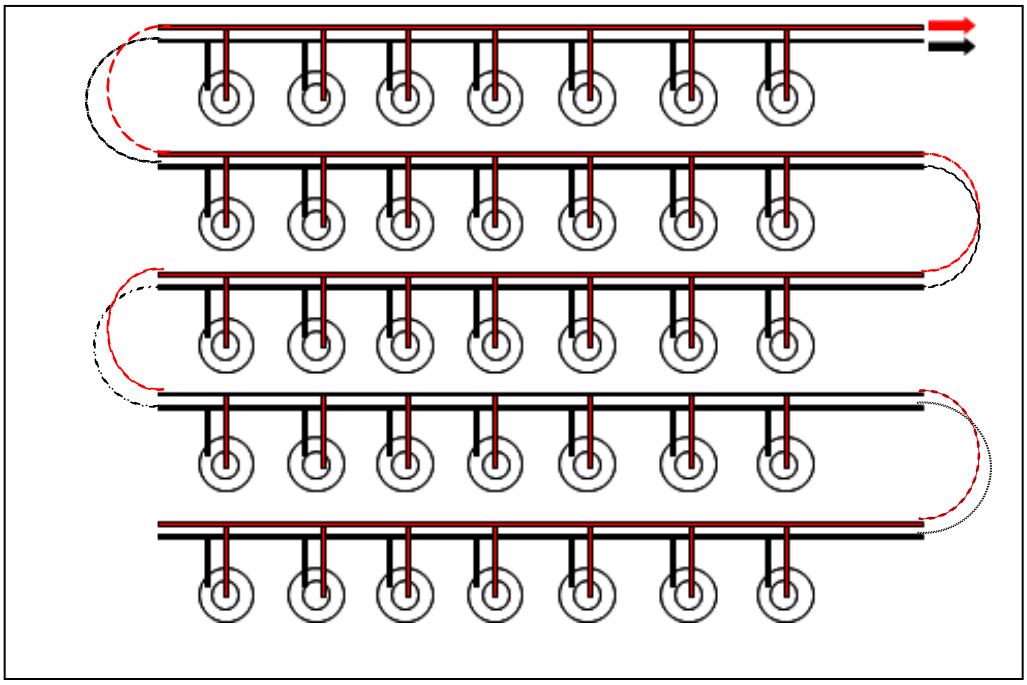

Figure 58. - Electrical connections of piezoelectric discs in all-parallel Configuration.

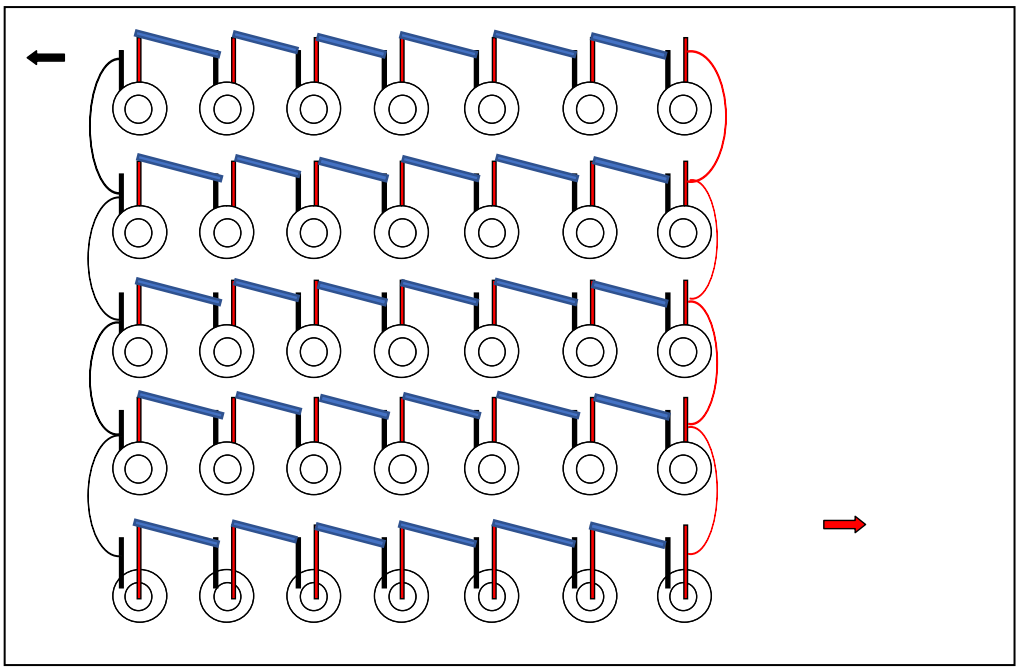

Figure 59. - Electrical connections of piezoelectric discs in the hybrid series - parallel configuration.

3.9.2.1 Stacked configurations of the basic piezoelectric transducer unit (discs)

The stacked piezoelectric configuration could consist of two or more basic piezoelectric transducer elements, which in this project are ‘discs’ and two of them are used. An alternate configuration as shown in figure 61could be adopted for a single tier or multiple tier arrangement which gives more space efficiency and material saving.

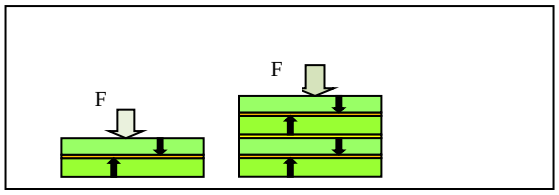

Figure 60. - Basic piezo transducer unit (disc) used in two-tier or multiple-tier configuration.

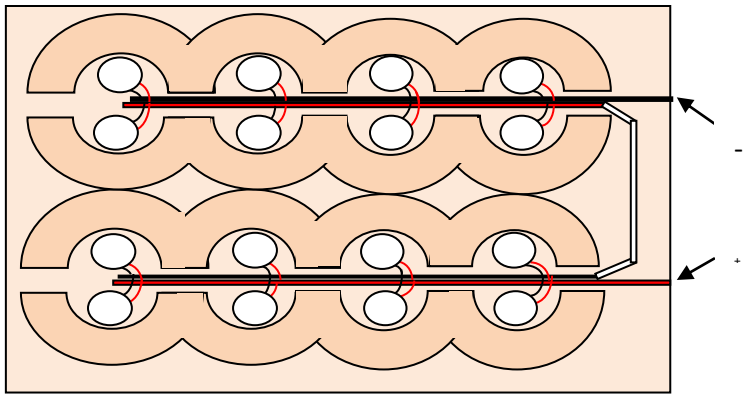

Figure 61. - Alternate configuration for stacked basic piezoelectric transducer units (discs).

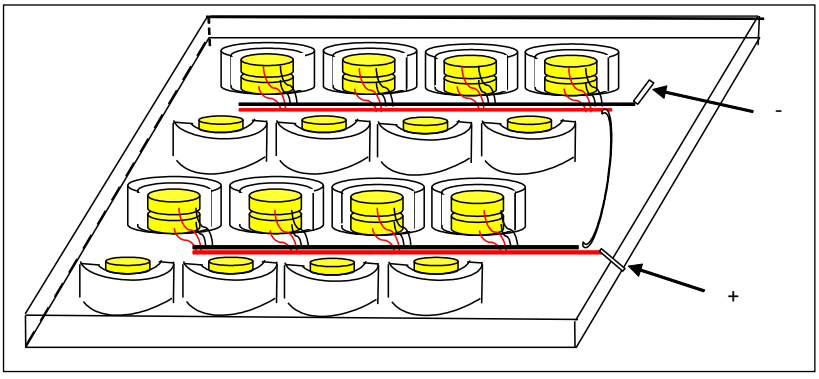

Figure 62. - 3D view of alternate configuration shown on figure 61.

In this project multiple layers of the basic piezoelectric discs were used using configurations given in figures 57, 58 and 59.

3.9.3 Empirical formula to calculate efficiency

The following formula could be used to calculate the average efficiency of a piezoelectric harvesting unit if the energy is directly supplied to a load

$$\eta = \frac{P_{out}}{P_{in}} x100\%$$

$$= \frac{1}{m} \sum_{n=2}^{m} \frac{\frac{(V_n + V_{n-1})^2}{R}}{[(F_n + F_{n-1})(d_n - d_{n-1})]/(t_n - t_{n-1})} \quad (4.16)$$

Where η is the efficiency, V is the voltage drop across load resistance R, F is the force applied to the base of the plate, d is the displacement of the plate, t is the time increment between data points, n is the data point index, and m is the total number of data points measured [100].

The efficiency figure we obtain here is not the efficiency of the sum piezoelectric discs but the efficiency of the entire system as a whole, because the experimental set up involves i^2 R losses (along connecting wires) and mechanical losses in the form of energy absorbed by springs. This could be considered the most universal form of efficiency calculation. The power in and power out calculation would depend on the method adopted.

As such in this project a more subjective approach would be adopted where the electricity generated by each piezoelectric unit would be calculated and then multiplied by the number of piezoelectric units being utilized to come with an estimate of the final value of electricity generated.

Many other formulae could be brought forward for calculation/prediction of amount of electricity generated based on the method employed i.e. landing of aircraft, athletes footsteps, internal pneumatic tire pressure, motor vehicle pressure exerted on road etc., but these are outside the scope of this project.

3.9.4 Additional electro-magnetic induction sub-assembly

Four EM units made of magnetic bolts are screwed onto the underside of the piezoelectric unit as shown in figure 63. When the external mechanical vibrations are applied to the upper platform (the primary system) of the PE harvester, the magnetic units follow this same motion of displacement and make the magnets move in and out of copper coils placed below. The central axis of the coils is in line with the axis of motion of the magnets. Therefore, when external mechanical vibrations are applied to the PE harvester base, the primary system oscillations are transferred to the electro-magnetic system at the same frequency i.e. the EM generators follow the same reciprocating movement as the PE generators. The relative motion of the magnets causes the magnetic flux density to change through the coils and hence induce an electromotive force (emf) inside the conductive coils by Faraday's law of electro-magnetic induction. When in operation, the system is excited as a whole. The overall system then exhibits MDOF (Multiple degree of freedom) behavior [102].

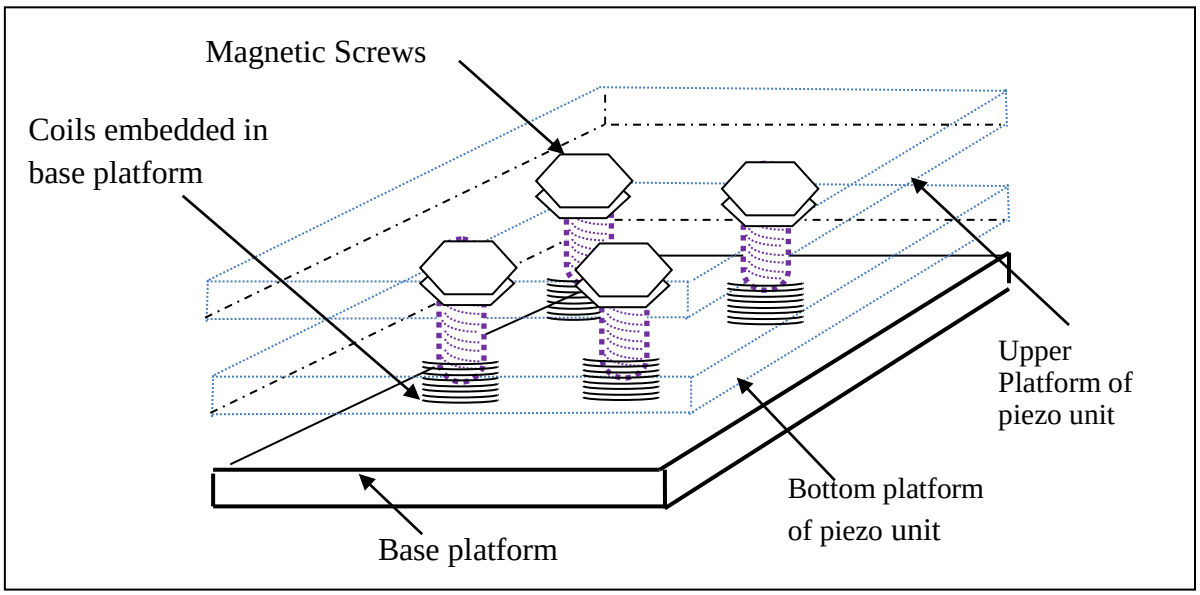

Figure 63. - Additional electromagnetic sub-assembly to be used in conjunction with the PE harvesting sub-assembly.

Electro-magnetic generators work on the principle of electro-magnetic induction which is Faraday's law of induction. It states that the electro-motive force around a closed path (loop) is equal to the negated rate of change of the magnetic flux enclosed by that path.

$$emf = -\frac{d\psi}{dt} \tag{4.17}$$

where emf is in volts, and ψ is the magnetic flux expressed in Weber as though the coil is a one-turn coil. The negative sign on the right side together with Fleming's right hand rule ensures that Lenz's law is always satisfied. Lenz's law states that the sense (direction) of the induced electro-motive force (emf) is such that any current it produces tends to oppose the (change of) the very magnetic flux producing it. If the loop contains more than one turn, (say N_t turns) then this is the same as having N_t separate, identical, single-turn loops stacked tightly one on topf of the other, so that the emf induced in the N_t turn coil is N_t times that induced in one turn. So it follows that for an N_t turn coil,

$$emf = -N_t \frac{d\varphi}{dt} \tag{4.18}$$

Figure 64 shows the dimensions of a cylindrical magnet involved in the calculations of its magnetic flux density

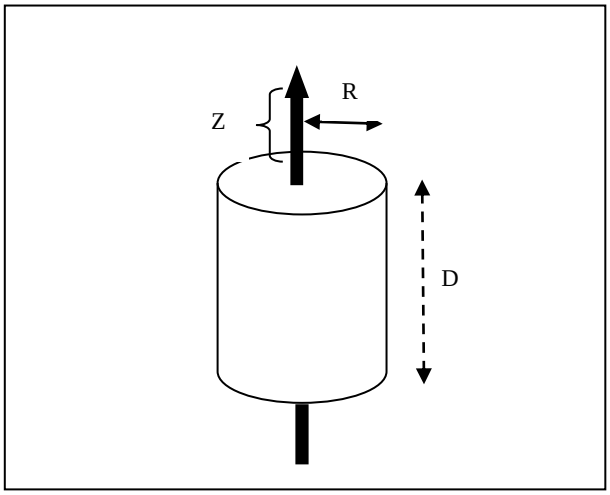

Figure 64. - Dimensions involved in calculating the flux density of a cylindrical magnet [44].

The formula for calculating B field (magnetic flux density) on the symmetry axis of an axially magnetised cylinder magnet (disc or rod) is as follows

$$B = \frac{Br}{2}\left[\frac{D+Z}{\{R^2+(D+Z)^2\}^{\frac{1}{2}}} - \frac{Z}{\{R^2+Z^2\}^{\frac{1}{2}}}\right] \quad (4.19)$$

Where;

B_r: Remnant field (flux density), independent of the magnet's geometry

D: Thickness (or height) of the cylinder

Z: Distance from a pole face on the symmetrical axis

R: Semi-diameter (radius) of the cylinder

The unit of length can be selected arbitrarily, as long as it is the same for all lengths.

NdFeB and SmCo are both known as rare-earth magnets because they are composed of materials from the Rare Earth group of elements. The magnets used in this project are made of rare earth material.

Table 4.1. - Remnant magnetic field for rare earth magnets [41].

Material	Grade	Br (Gauss)	Hc	Hci	BHmax	Tmax (°C) *
NdFeB	39H	12,800	12,300	21,000	40	150
SmCo	26	10.500	9.200	10.000	26	300

Using a typical value for Br = 11650 Gauss (1.165 Wb/m^2) and equation 4.19 to calculate the magnetic flux density with R= 0.5 cm and D= 0.75 cm

$B = \frac{1.165}{2} \times \frac{1}{\sqrt{(0.5)^2+1^2}}$ = 0.521 Wb/m^2 ; the Z dimension being regarded as zero.

In this project the formula for induced e.m.f. in a conductor moving in a fixed magnetic field will be used.

An emf induced by motion relative to a magnetic field is called a motional emf. Quantitatively it is represented by the equation

$$emf = -Blv \qquad (4.20)$$

Where;

B = strength of the magnetic field in Weber/m^2 (Webers per square meter) or T (Tesla)

l = is length of the conductor in m (Meters)

v = speed of moving conductor relative to the magnetic field in m/s (Meters per second)

The minus sign in the above equation is because the induced e.m.f. is in such a direction that would attempt to negate the very flux change that is causing it.

Substituting values in the above formula as follows;

B = 0.521 Wb/m^2; l = 2 m; v = 0.4 m/s; 2 m being the extended length of one coil.

The induced e.m.f work out to be 0.4168 Volts per coil. As there are 4 coils the total induced e.m.f. would be 4 x 0.4168 = 1.6672 V. The four coils are connected in series so that the e.m.f.'s generated would add up and create an e.m.f. that would be larger than that produced just by one coil magnet assembly.

The extending leads were configured in series and then in parallel to the leads of the piezoelectric sub-assembly and was checked as to which configuration gave a larger total e.m.f. for the composite assembly. The individual waveforms of the piezoelectric sub-assembly and the EM sub-assembly are identical except for the fact that they have different amplitudes a shown in Figure 65.

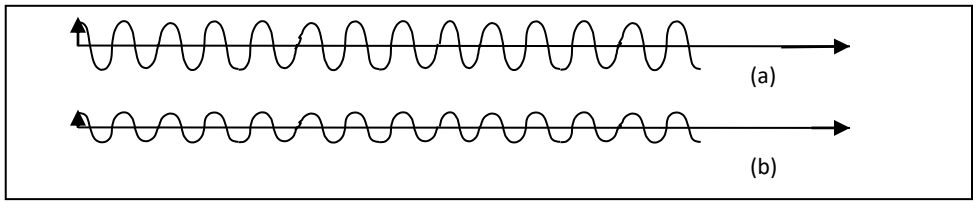

Figure 65. **-** Replica of e.m.f. wave patterns (a) Theoretical e.m.f. wave pattern generated by the piezoelectric sub assembly. (b) Theoretical e.m.f. wave pattern generated by the electro-magnetic induction sub assembly.

Figure 66. - Four permanent magnets mounted on insulator stubs.

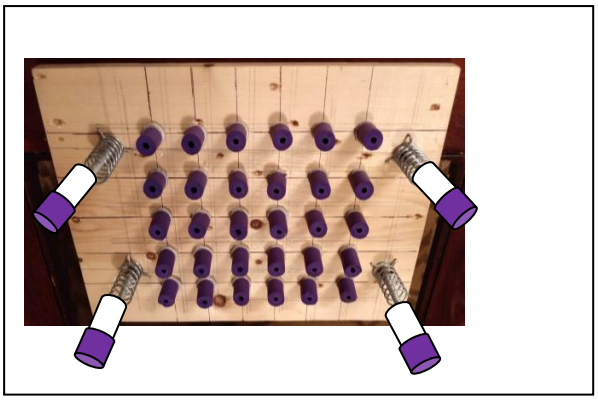

Figure 67. - Screw and spring assembly to attach the permanent magnets.

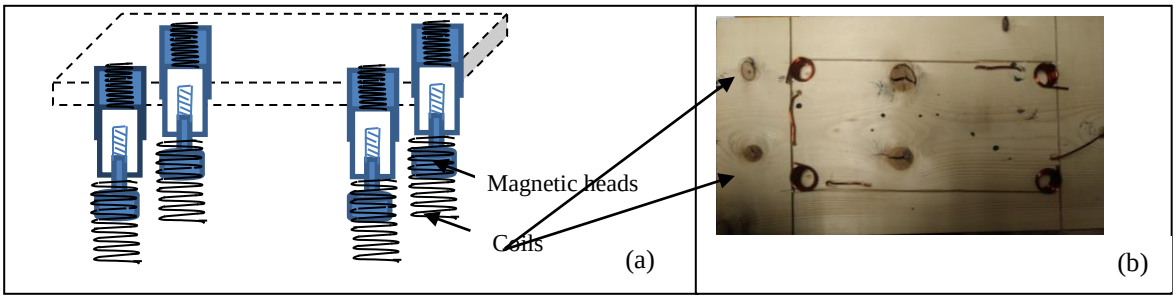

Figure 68. - Electro-magnetic sub-assembly.
(a)Arrangement of electromagnets.
(b)Coil arrangement on the bottom board.

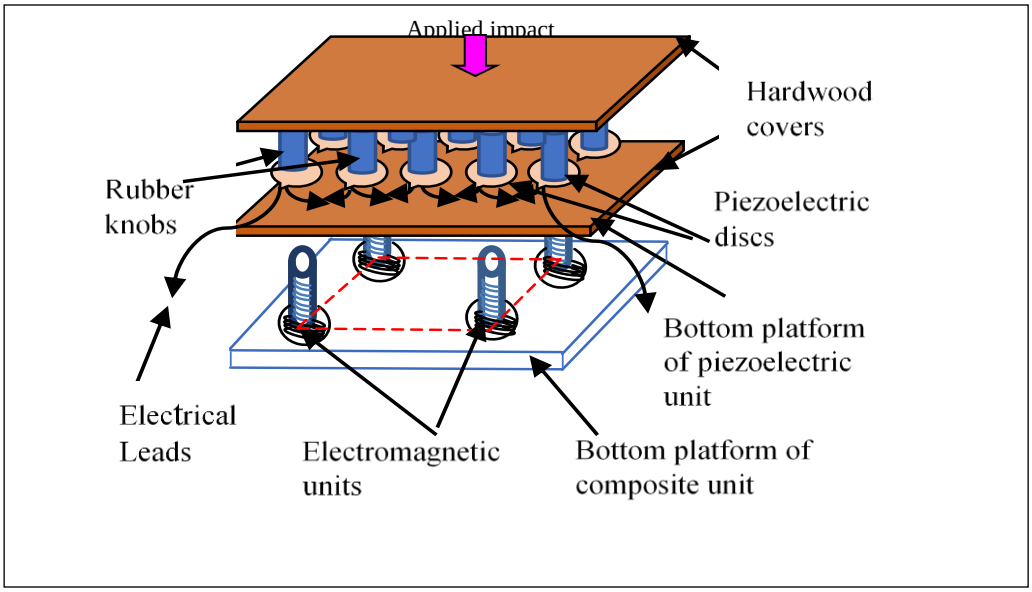

Figure 69. - The blown-out image of the combined PE harvester sub-assembly and electro-magnetic sub-assembly (composite energy harvester).

(a) Parallel –Serial configuration

(b) Serial-Parallel configuration

(c) All Parallel configuration

(a)

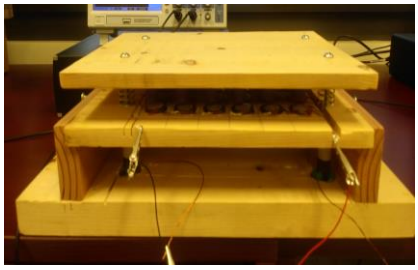

(b)

(c)

Figure 70. - The three different configurations of the composite energy harvester.

3.9.5 Rectifier stage

Efficient rectification is an essential part of an electrical energy harvesting system and the rectification process plays a critical role in overall conversion efficiency. The idea is to pass over as much generated energy as possible from the source for the consumption of the load.

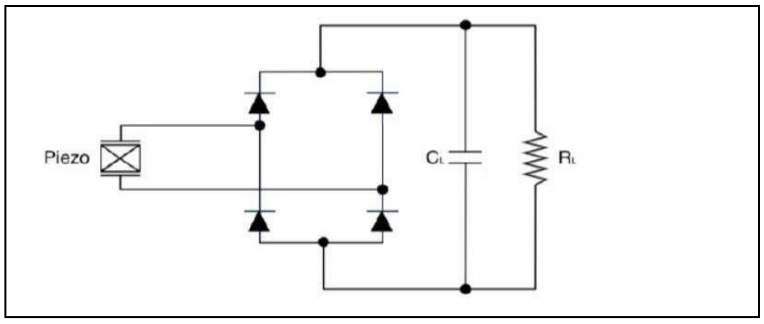

Figure 71. - A simple diode bridge rectifier [11].

The electricity generated by piezo films, vibrating in a simple harmonic motion is unarguably ac in nature. This ac electrical energy is required to be converted into usable DC power and a

passive rectifier is needed for this conversion. The most commonly used passive rectifier in energy harvesting is the full-wave bridge rectifier as shown in figure 71. One of the important factors that affect the conversion efficiency in a diode-based rectification process is the turn-on voltage (or cut-in voltage or threshold voltage). This is because until the diode reaches the 'turn-on voltage', it remains 'off'. As a result, up to the turn-on voltage, no voltage would be available to the load for that duration of time. Therefore to construct rectifier circuits, especially for low energy harvesting systems, diodes of lower turn-on voltages are preferred. Schottky diodes have the lowest turn-on voltage when compared with Si, Ge diodes [68].

It has been experimentally shown that Schottky diodes can be used to obtain usable dc energy from mechanical vibration. Though the conversion efficiency of Schottky diode is better in comparison to other diodes, it has, however, its own limitations. For example, the turn-on voltage of a Schottky diode is about 0.2 V and thus the bridge rectifier remains off from the beginning of an a.c. input cycle (voltage 0V, time = 0 s,) until it reaches a magnitude of 0.4 V (or 2×0.2 V, i.e. 2 diodes have to be traversed). Another limitation of the Schottky diode is its reverse saturation current which is high and about three orders higher than that of other diodes. This gives rise to a higher energy loss through the reverse-biased diodes during the rectification process.

To overcome the limitation of bridge rectifiers a more efficient rectifier circuit is needed. This project will use the low voltage rectifier with high power conversion efficiency (PCE) based on SMIC 0.18 μm standard CMOS technology for PE energy harvesting as proposed in [49] and shown in Figure 23(b) for reasons mentioned in paragraph 3.8.1.

3.9.6 Employing a power management circuit (DC-DC conversion)

A power management circuit is another important stage in any energy harvester system. This is employed with an intention of maximizing the 'raw power harvested' to 'net energy harvested' ratio. The power management circuit of a small-scale energy harvester should dissipate minimal power in addition to ensuring maximum power is transferred to the load side. Its special circuit design will include a simple maximum power point tracking scheme. The power management circuit in the dashed frame as shown in figure 72 consists of a single stage DC-DC converter with a controller.

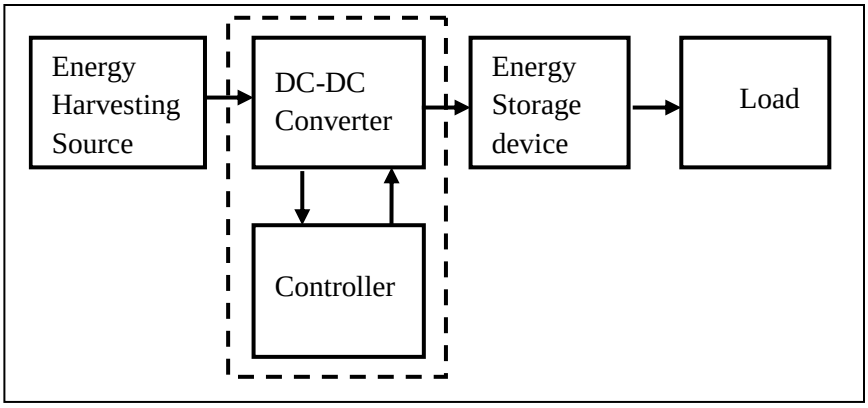

Figure 72. - Block diagram of a DC-DC power.

The difference between a typical electrical power source and a vibrating piezoelectric device used in the low frequency region is that it (the piezo device) is considered as having capacitive rather than inductive source impedance. This fact is used in deriving formulae to arrive at the maximum power transfer condition.

Usually harvesting circuits simply consist of an ac–dc rectifier which converts the a.c. into D.C. so that the storage battery can be charged. However, in the case of piezoelectric energy harvesting, the rectified DC voltage may not be constant as it depends on the vibration frequency and intensity experienced by the piezoelectric harvesting unit. This calls for adaptability of the

circuit i.e., to provide an optimum voltage to the load by making adjustments (compensation) to the output voltage of the rectifier. In other words, the adaptive control technique would facilitate the attainment of optimum voltage, which in turn would ensure continuous, maximum power transfer to the load or storage unit.

To achieve this, a switched-mode dc–dc converter together with control circuitry is placed at the output of the rectifier, which would control the energy flow from a vibrating piezoelectric transducer into the electro-chemical battery (Figure 73, 75). As battery voltages change very slowly, this maximization of energy transfer we speak about amounts to maximizing the current into the battery. The controller monitors the output power, i.e., in actual reality, the current into the battery, and dynamically adjusts the duty cycle of the DC-DC converter to maximize the current and therefore the power transfer [56]. This procedure is somewhat similar to maximum power point tracking employed in solar power harvesters. A super capacitor could be employed as the storage device for the proposed system due to less stringent requirements for charging compared with rechargeable batteries and having virtually infinite life cycles.

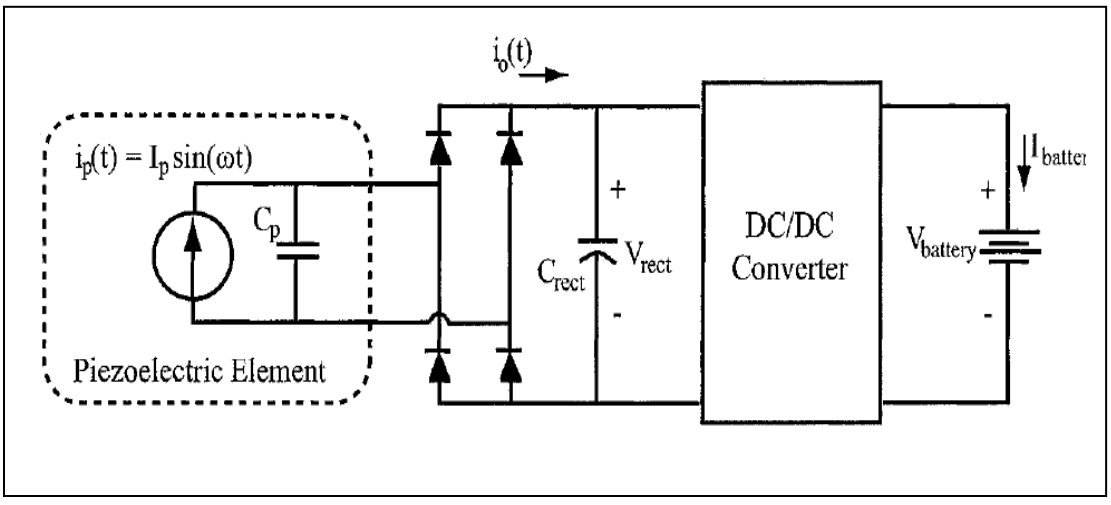

Figure 73. - Adaptive energy harvesting circuit [73].

In this project both step up (Boost converter) and step-down (Buck converter) circuits will be used. The first one will be used with the 'all serial' configuration and the second one will be used with the 'series –parallel' configuration. However due to space constraints only the operation of the Buck converter is explained as below.

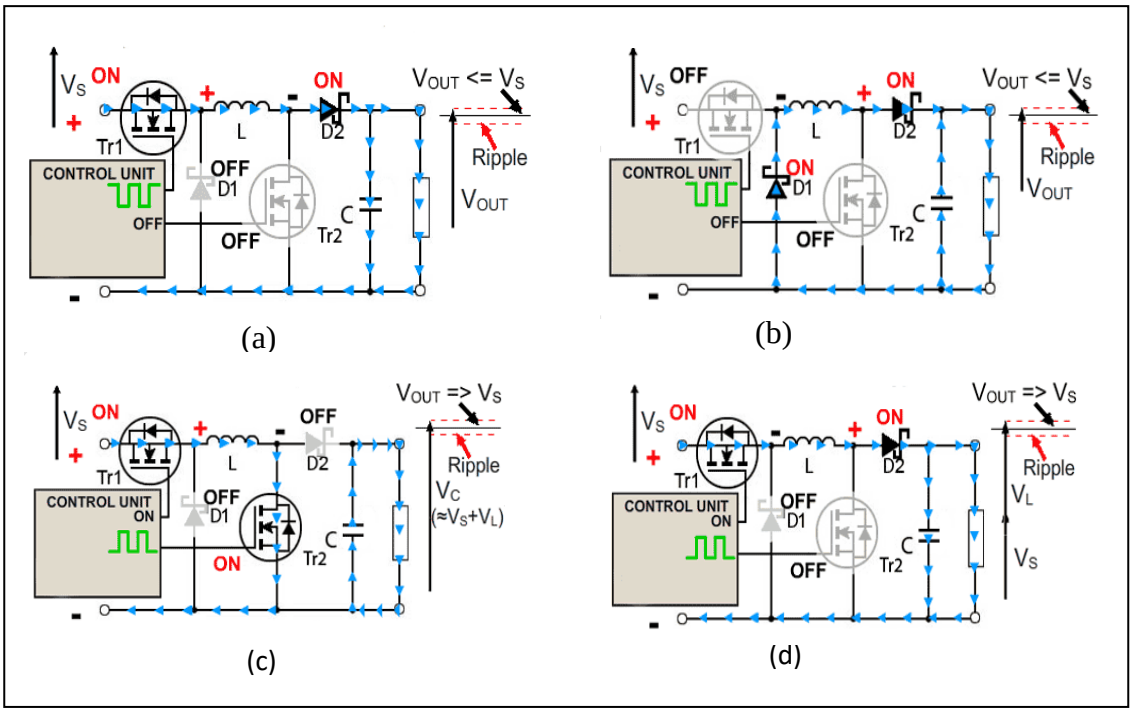

Figure 74. - Buck-Boost converter [10].
(a) Operation as a Buck Converter during Tr_1 'ON' Period.
(b) Operation as a Buck Converter during Tr_1 'OFF' Period.
(c) Operation as a Boost Converter during Tr_2 'on' Period.
(d) Operation as a Boost Converter during Tr_2 'off' Period.

In a buck converter Tr_2 is going to be always 'OFF'. Therefore, it might as well be removed and short circuited so that a constant 'OFF' pulse from the control unit doesn't have to be supplied to it. A MOSFET serves dual purposes i.e., high speed switching of the output voltage and providing high current with less dissipation of heat.

During the period when Tr_1 is 'ON' it conducts with the input current passing through the inductor L, energizing its magnetic field, charging C and supplying the load. The current then

flows back to the supply negative terminal. While this is happening D_1 cannot conduct as its anode is being held at a positive potential by the heavily conducting Tr_1.

During the period that Tr_1 is "OFF' the initial source of current is now the inductor L. With its magnetic field collapsing, the back e.m.f. generated reverses the polarity of the voltage across L, which turns on D_1 and current passes through D_2 and the load ensuring a smooth supply of current to the load. Schottky diodes have a property that they dissipate very low heat and work fine at higher frequencies than regular diodes. The Inductor is used to control voltage spikes which can otherwise damage the MOSFET. Since operating frequencies are low, the value of the inductance required for this purpose would be high. (around 0.95 H).

As the current decreases along with the discharge of L, the charge accumulated in C during the 'ON' period of Tr_1 now adds to the current flowing through the load, keeping V_{OUT} faithfully constant during the Tr_1 'OFF' period. This helps to keep the ripple to a minimum and V_{OUT} as close to V_S as possible.

Figure 75 shows elaborate circuitry of a more complex DC-DC converter (incorporating a Buck converter) which could take the place of the broken lined box in figure 73. In this circuit Tr_2 of a conventional buck-boost converter has been removed.

The fact that all piezoelectric elements used in the experiment are of the same characteristics and therefore possess the same resonance frequency; the use of one and same rectifier circuitry for the composite structure becomes possible. If in case piezoelectric elements of different resonance frequencies were used a separate rectifier circuit would have to be used for each different group because their peak powers would occur at different frequencies. Also, each 'piezo group-rectifier circuit' combination having its own inherent output impedance might lead to impedance mismatches if they are all connected in parallel at the load or storage device.

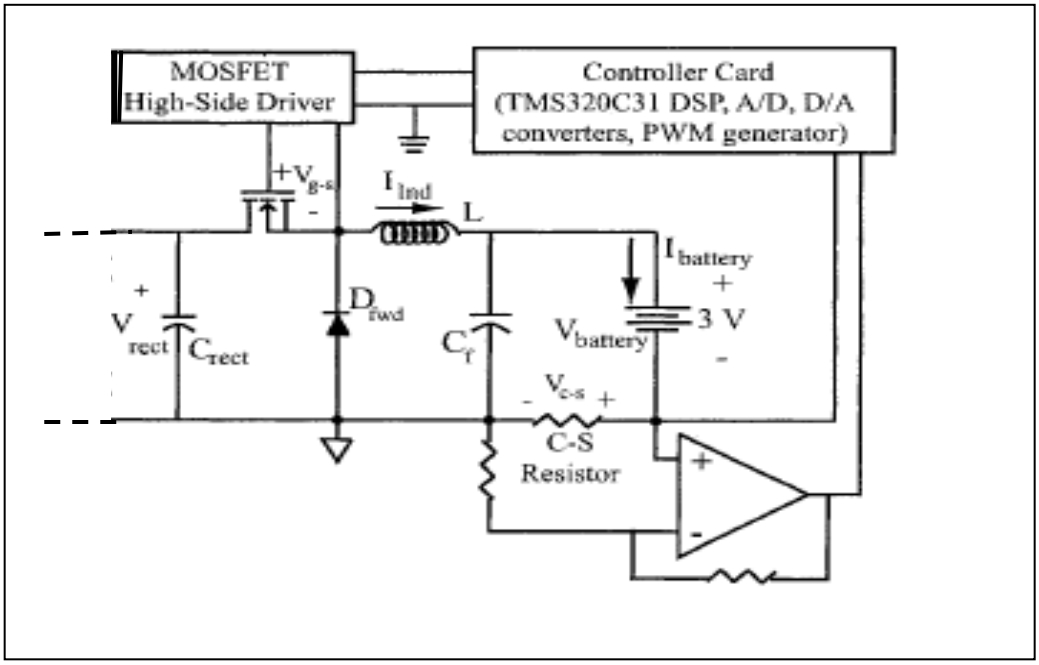

Figure 75. - Circuitry of a more complex DC-DC converter (employing a Buck converter) [73].

Figure 76 shows the discrete components required for the power management circuitry shown in figure 75.

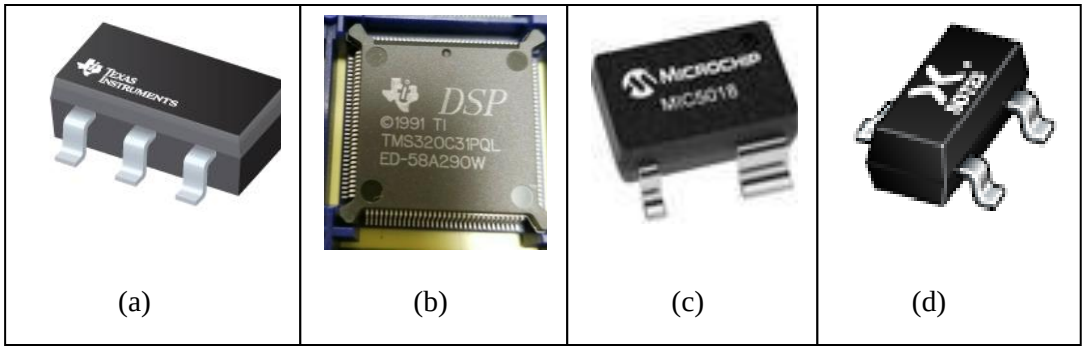

(a) (b) (c) (d)

Figure 76. - Components of the DC-DC converter and power management circuit.
(a) OP-AMP (296-TLV9061SQDBVRQ1CT-ND).
(b) DSP (TMS 320LC31).
(c)MOSFET High Side Driver (MIC5018YM4-TR).
(d) P Channel MOSFET (BSH205G2AR).

3.9.7 Regulator stage

The rectified voltage of the AC-DC converter is dependent on the Copper distance from the source and the amplitude of the input signal. A simple regulator could be employed in place of the sophisticated circuitry given in section 4.9.6 to overcome the loss of voltage that's dropped along lengthy circuitry. This will minimize any variation caused by fluctuations in the input voltage or the load. However, due to limitation on available power, the regulator must be efficient and must be able to work with low voltage levels. An Integrated circuit (IC) could be employed for this purpose. A linear voltage regulator comprises of an active (BJT or MOSFET) pass device (series or shunt) controlled by a high gain differential amplifier. It does a comparison of the output voltage with a precise reference voltage and adjusts the pass device to provide a constant output voltage [93]. The circuit diagram of a voltage regulator is shown in figure 77(a). Figure 77(b) is a picture of a real voltage regulator.

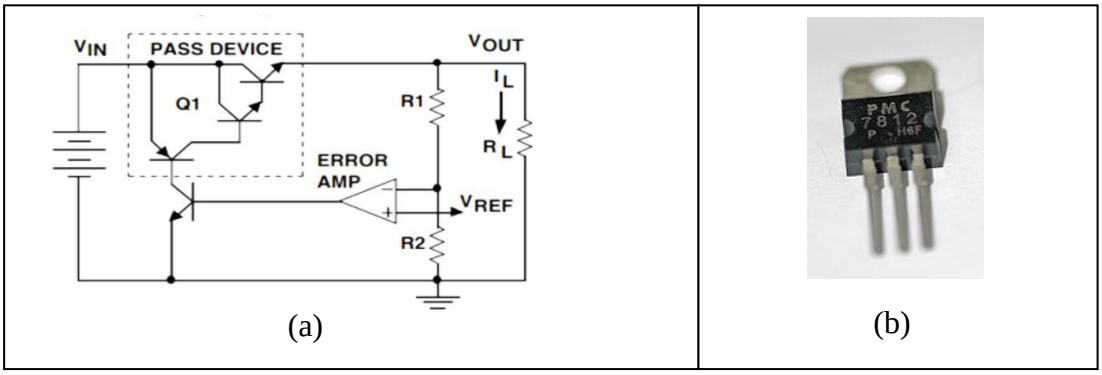

Figure 77. - A voltage regulator (a) A circuit diagram of a typical linear voltage regulator. (b) A voltage regulator in real life.

In this project, for voltage conditioning (power management) Buck or Boost circuitry will be used as appropriate with closed loop feedback through a comparator which will provide the dynamic adjustment to the duty cycle of the DC-DC converter. This amounts to a combination of components mentioned in section 4.9.6 and this section.

3.9.8 Energy storage stage

The energy generated by piezoelectric systems are not sizeable enough to be able to deliver power to consumer electronics directly. Therefore, for power harvested through piezoelectricity to fit into the commercial market, there should be means for gathering and storing it, until enough can be made available to power consumer electronics [100].

Capacitors and rechargeable batteries both could be used for energy storage. Capacitors do not require a minimum voltage to start charging unlike rechargeable batteries. Charging and discharging can take place very quickly due to their high power density, making instantaneous provision of the accumulated energy possible. However, compared with batteries the energy density of capacitors is lower; thus, they lose their voltages quickly as they discharge. Therefore, they find their suitability in applications that require rapid energy transfers and not for applications where an almost constant output voltage or a steady energy supply is required. Only continuous physical vibrations experienced, which can generate sufficient energy, will help them sustain constant operation of the load.

Batteries, could boast of being free of this shortcoming. As widely known they can store the energy from the PE harvester for subsequent use and thus are capable of supplying constant voltage and power even with intermittent energy generating physical vibrations experienced by the piezoelectric unit. The limited number of charging cycles is however, the main disadvantage of rechargeable batteries when used for piezoelectric energy harvesting applications. 300–1000 charging cycles is the average for both nickel metal hydride (NiMH) batteries and lithium-based rechargeable batteries, after which the capacity of the battery becomes significantly reduced and renders the battery unusable.

One large battery could be employed for storage or a battery bank consisting of multiple batteries could be employed for larger systems, to store the electricity generated by the piezoelectric system. It depends on how much energy one envisages to produce and how much energy one plans to store and draw later.

The inverter will have a direct physical connection to the battery bank and the battery bank should be of sufficient capacity such that it is capable of coping with the current consumption of the inverter. Ideally a current of 1A a.c. on the demand (load) side translates into a requirement (a draw) of approximately 25 A on the DC side. When calculating how much battery bank capacity we should have, it's prudent to plan for a discharge of only half the battery bank so that it's not run down to the very bottom. In other words the depth of discharge (DoD) should be ideally 50%.

Table 4.2. - Typical battery bank sizes [42].

Inverter output	Typical Battery Bank size
1000 Watt h/Day	420 Ah
1500 Watt h/Day	540 Ah
2000 Watt h/Day	750 Ah
2500 Watt h/Day	1000 Ah

Lower temperatures cause batteries to be less efficient. Table 4.3 gives a multiplying factor depending on working temperature to arrive at the correct battery capacity needed.

Table 4.3. - Multiplying factor depending on working temperature.

Temp °F	Temp °C	Factor
80	26.7	1
70	21.1	1.04
60	15.6	1.11
50	10.0	1.19
40	4.4	1.3
30	-1.1	1.4
20	-6.7	1.59

A large spectrum of rechargeable solutions is available in the commercial market today, such as rechargeable batteries (Lead acid, NiCd, NiMH, Li ion, etc.), fuel cells, capacitors, and hybrids of these categories (e.g. ultra-capacitors).

In one's choice of a rechargeable energy storage system many factors must be taken into account. The main requirements to consider in selecting a rechargeable energy storage system, could be summarized as follows.

(i) The life span of the energy storage device, as well as the harvester, must match the estimated operational life for the system.

(ii) Having the ability to make available a continuous power supply through the longest expected period of inactivity, where energy harvesting will be unavailable. (e.g., bad weather that may last for several weeks).

(iii) The voltage of the energy storage must be consummate with both powering the load and also being charged by the power generated from the harvester.

(iv) The maximum level of current (or power) available from storage must outdo the peak current (or power) demand of the load.

(v) Appropriate design in meeting the challenges, demands and constraints of the application, including temperature, humidity, possible impact, etc.

(vi) The energy storage system must meet the environmental considerations with respect to safe disposal or recycling [106].

(vii) The possibility of providing a charging current of at least one tenth's of the battery's capacity or higher, throughout a majority time of operation [100].

Figure 78 shows a comparison between batteries and capacitors as far as energy density and power density is concerned.

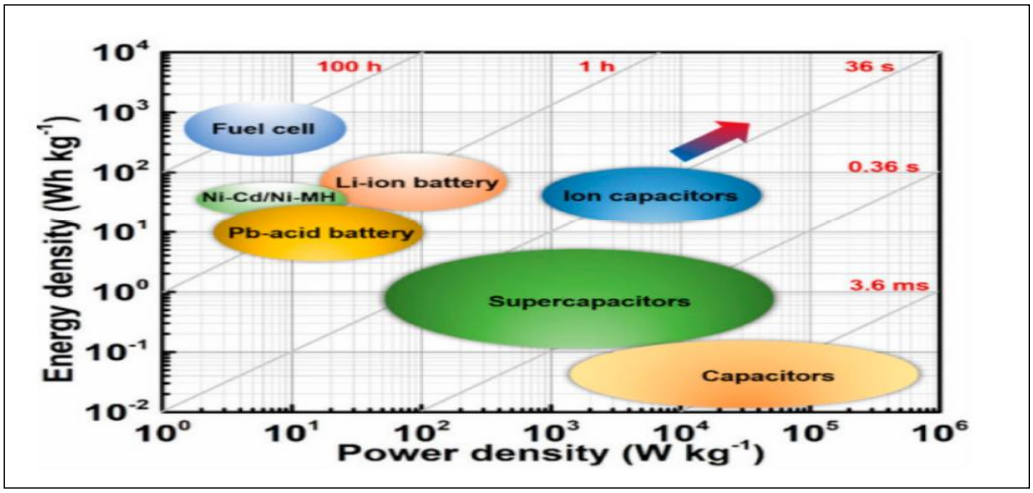

Figure 78. - Comparison of energy density against power density of popular charge storage devices [88].

The following table shows a detailed comparison of vital features between batteries and capacitors.

Table 4.4. - Comparison of major features between batteries and capacitors.

Feature being compared	Batteries	Capacitors
Charge storage methodology	The chemical reaction for storage	Electric field for storage
Type of interaction	Active component	Submissive component
Energy-density	High	low
Charging/discharging	Slow	fast
Output Voltage	constant	Relatively unstable
Operating temperature	25°C	3 °C to +125 °C
Composition	Contrive of metals, chemicals	Contrive of metal sheets
Charge/discharge Cycles	500	500,000
Cost	Low	Relatively high
Stress during peak demand	Stressed	Not stressed

Based on the above comparisons capacitors were selected as the charge storage device in this project, the main contribution features been charge/recharge cycles, high charge discharge rate and passivity of interaction.

3.9.9 The inverter stage

Inverters are required to convert Direct Current (DC) into alternating current (a.c.).

The input voltage could be 24, 36 or 48 V DC if it's for a home energy system and 200 to 400 V DC when the input power is from, for example, a photovoltaic solar panel.

If the inverter produces only a square wave output, it is suited only for applications that require low sensitivity such as lighting devices and heating devices. A circuit diagram of an inverter is shown in figure 79. When power inverters are used instead of a standard lines power supply the best effort should be made to create (produce) a sine wave output because most electrical/electronic appliances /devices are made to operate best with a sine wave power input. The aim when employing an inverter is to have an inverter that produces a pure sine wave. This is done with an intention of having a very low if not zero Total Harmonic Distortion (THD).

Total harmonic distortion

It is the ratio of the root of the sum of the mean squares of the harmonics to the root mean square of the fundamental.

$$\text{THD} = \frac{\sqrt{V_2^{\,2} + V_3^{\,2} + V_4^{\,2} + ...}}{V_1, rms} \qquad (4.21)$$

In square waveforms THD is found to be 48.3%. A pure sine wave would have a THD of zero. (Because it has no harmonics).

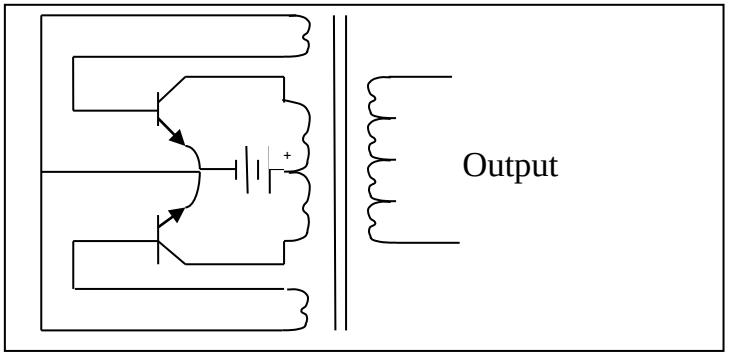

Figure 79. - A block diagram of a simple inverter.

3.10 Maximizing the net energy harvested

It is of paramount importance that the energy harvested be transferred to the load with the maximum possible efficiency. Power factor correction is as important as power management.

3.10.1 Power factor correction

Power factor correction plays an important role in power generation and distribution for a.c. loads. The ratio of consumed or delivered power to apparent power is defined as the power factor (PF).

The apparent power of an a.c. system would be equal to the multiple of voltage and current. i.e. VI. If power factor = Cos ϕ, where ϕ = phase difference between the alternating current and alternating voltage; then

$$Delivered\ power = VI\ Cos\ \phi \tag{4.22}$$

Therefore

$$Cos\phi = \frac{Power, Delivered}{Power, Apparent} \tag{4.23}$$

When the a.c. voltage and current supplied to the load is in phase the power factor is unity as Cos 0°= 1. The primary reason for wanting a PF close to unity in most large scale industrial applications is the increase in the electrical capacity of the distribution system (lower current requirements).

Consideration given to power factor correction offers immediate benefits at the micro level too, e.g. designing of energy-harvesting circuits. Power-conditioning circuits used in harvesting energy from ambient sources often result in harmonics in output current. This results in power losses. The use of either linear regulators or switched regulators could offer challenges; the first: reduced efficiency when operating outside an optimal operating envelope, the second: additional

design challenges required to address stability issues that can limit optimum power output. Power Factor Correction circuits are designed to address these challenges.

However, power factor correction consideration have been overlooked in this project as it is comprehended as being beyond the scope of this project and penalties for a low PF aren't viewed an issue as this project involves an experimental standalone installation.

3.11 Equivalent circuit of the basic piezoelectric sensor

A piezoelectric transducer can be modeled as a proportional voltage source and filter network because it has very high DC output impedance.

The applied force, pressure, or strain produces a voltage V at the source which is directly proportional to it. The output signal is therefore related to this mechanical force as if it had actually taken place (not physically though) within the equivalent circuit.

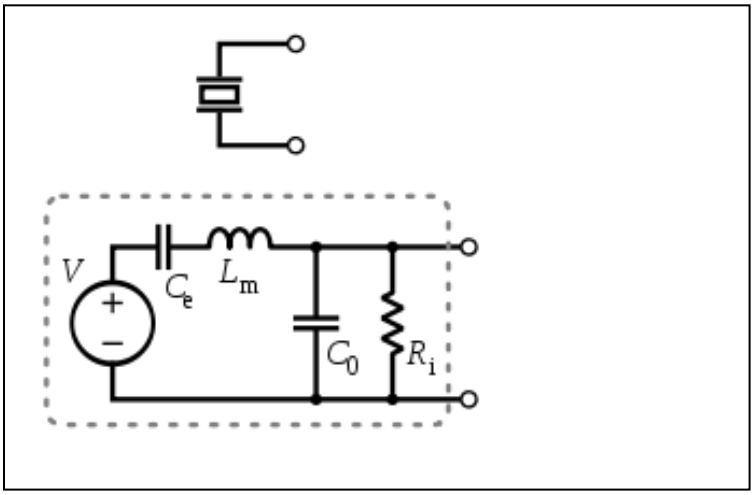

Figure 80. - Schematic symbol and detailed electronic model of a piezoelectric sensor [111].

An equivalent electronic model as indicated in figure 80 includes the effects of the piezoelectric sensor's mechanical and electrical characteristics. The inductance L_m is a representation of the seismic mass and inertia of the sensor. C_e is inversely proportional to the mechanical elasticity of

the sensor.C_0 is due to the static capacitance of the transducer. R_i is the insulation leakage resistance of the transducer element. If the load resistance is thought to act in parallel with the sensor insulation resistance, it contributes towards increasing the high-pass cutoff frequency (refer figure 47).

If the load and leakage resistance are large enough so that effects of low frequencies prevalent, are not lost, a more simplified equivalent circuit model can be used, in which C_s represents the capacitance of the sensor surface itself (determined by the standard formula for capacitance of parallel plates) as in figure 81 (a) or as a charge source (current source) in parallel with the source capacitance as in figure 81 (b), where the charge is directly proportional to the applied force.

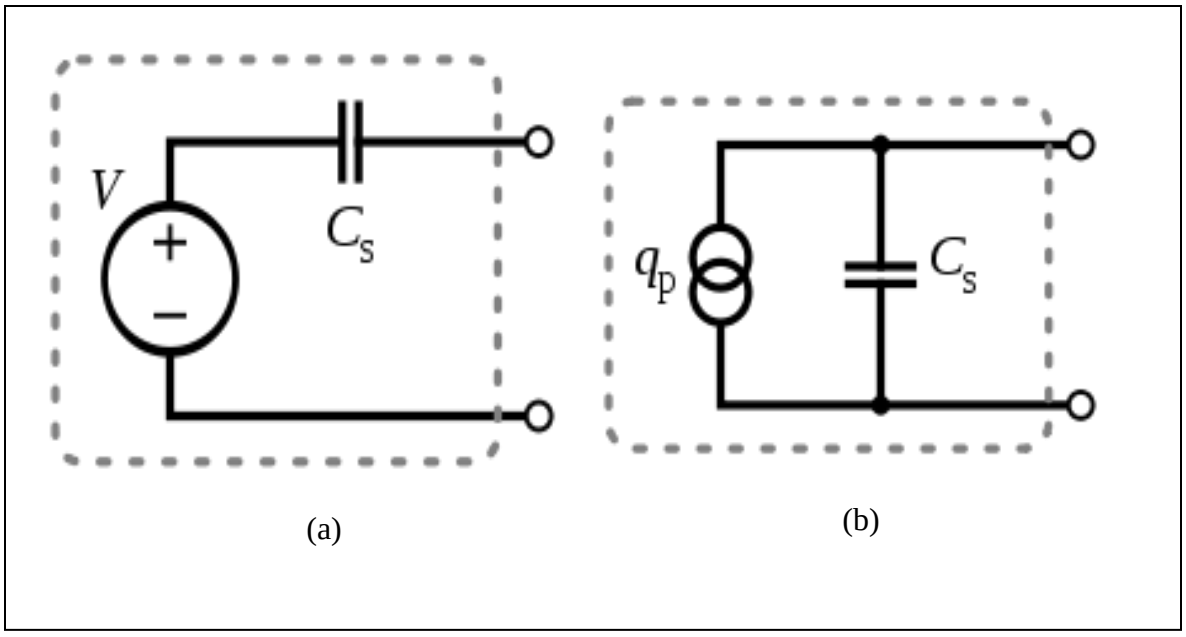

Figure 81. - Simplified equivalent circuit of a piezoelectric sensor [111].
(a) The piezoelectric sensor can be modeled as a voltage source in series with the sensor's capacitance or (b) A charge source in parallel with the capacitance.

3.12 Modelling and simulation of the composite energy harvester in MATLAB Simulink

3.12.1 Modeling of the basic piezoelectric unit (disc)

The equivalent circuit of the basic piezoelectric sensor implemented in SimscapeTM is as shown in figure 82. Blocks used for model execution are listed below.

(1) The Solver Configuration:

It is used to provide the specification of solver parameters for the start-up of the simulation, i.e. prior to the beginning of the actual simulation. All network blocks in Simscape^{TM} are required to have a separate solver configuration connected to that block.

(2) The PS-Simulink Converter:

This block is used to change a physical signal into a Simulink output signal. It also provides the related units of the signals that are traced at the output.

The Simulink-PS Converter

converts the unitless Simulink input signal into a physical signal.

(3) The Electrical Reference block:

The Electrical Reference block is used to provide an electrical ground. A model having electrical elements must include at least one Electrical Reference block.

(4) Voltage Sensor block:

This is to measure the voltage at the output.

(5) Current sensor block

The current sensor block is used to measure the current generated in the transducer.

If V_p is the output voltage of this basic piezoelectric sensor, C_p its piezoelectric capacitance, and Q, the charge applied, then $V_p = Q/(C_p)$

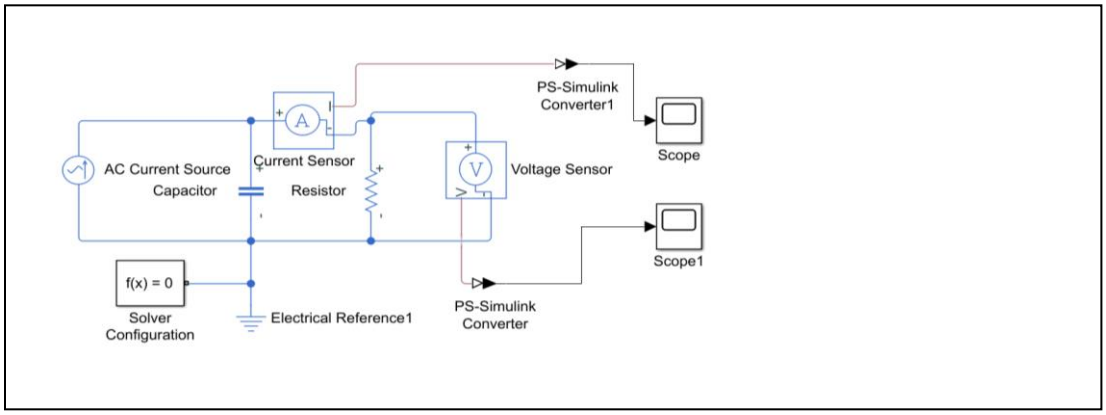

Figure 82. - Basic piezoelectric transducer unit (disc) modelled in MATLAB.

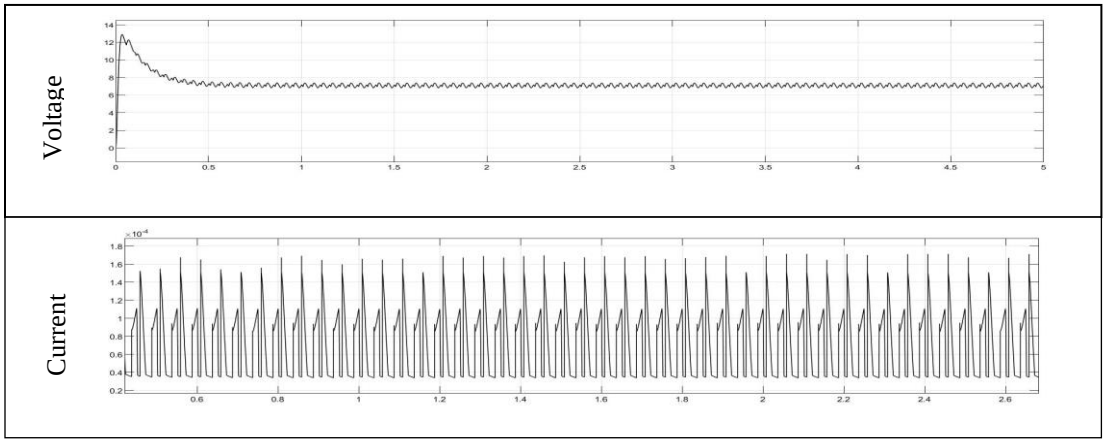

Figure 83. - Output voltage and output current of basic piezoelectric transducer unit (QP20W piezo disc) when modelled in MATLAB Simulink.

The output voltage and current waveforms which are shown in figure 83 (a) and (b) respectively are influenced directly by variations of the resistive load. The C_p and load resistance is taken as 12 nF and 10 Ω for simulation

Next the detailed piezoelectric electrical model was implemented, and the related results were recorded. As previously referred, the vibration energy harvesting system consists of two parts, the mechanical and electrical part.

3.12.2 Modeling of the mechanical input to the composite harvester unit

Figure 84 (a) shows the Simulation of the mechanical part of the piezoelectric transducer in MATLAB Simulink and Figure 84(b) shows the wave form of the input as observed in the scope, which has a 0.5 second period (frequency of 2 Hz) and 1 Newton of amplitude. A saw tooth waveform has been selected for the physical input because it very closely represents the pressure applied by physical footsteps i.e. a rising pressure and then release.

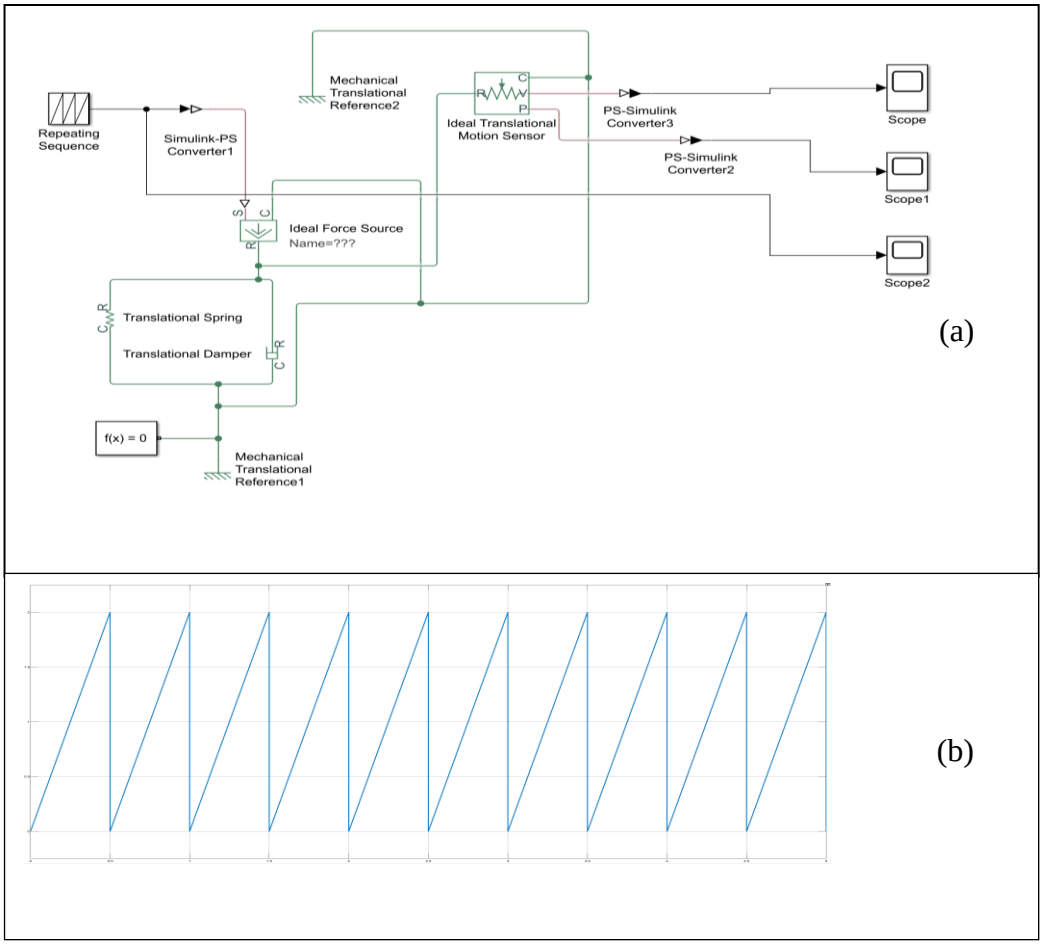

Figure 84. - Simulation of the mechanical input to the composite harvester unit.
(a) The Simulink model.
(b) The waveform of the input as observed in scope 2.

3.12.3 Modeling of the piezoelectric transducer sub-assembly

The Piezo Stack in figure 85 and figure 88 represents the piezoelectric transducer sub-assembly with parameters as shown in figure 85, 86 and 87. Only the 'all – parallel' PZ sub-assembly (Connections shown in figure 58) together with the EM sub-assembly is considered for modeling from section 4.12.3 up to section 4.12.9 with practical experimental results in 4.12.10, as that configuration proved to produce the best results.

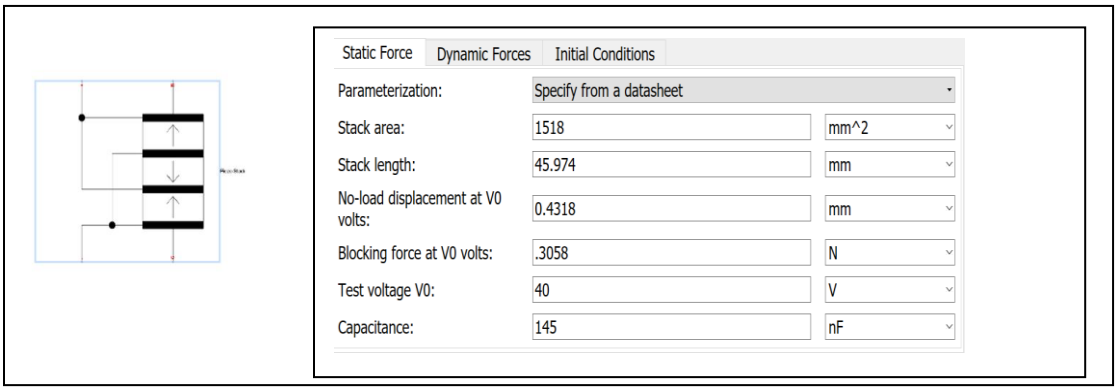

Figure 85. - Piezo stack parameters - Static Forces.

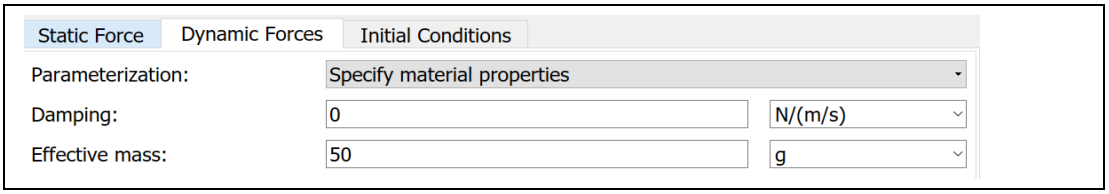

Figure 86. - Dynamic forces of the piezoelectric stack

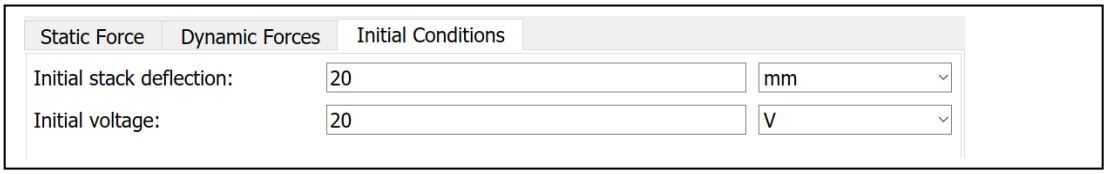

Figure 87.- Initial Conditions of the piezoelectric stack.

The piezo sensor is first tested without load, i.e, in open circuit, as shown in Figure 88.

The ideal force source represents a force proportional to the input physical signal. The 'mechanical translational reference' represents a mechanical translational reference point. The ideal translational motion sensor converts an across variable measured between two mechanical

translational nodes into a control signal proportional to velocity and position. The translational damper represents an ideal mechanical translational viscous damper with 12 N(m/s) and the Translational Spring is an ideal mechanical linear spring with 10 N/m value.

The simulation result of piezoelectric sensor output voltage and current with no load when a force of 1 Newton is applied is shown in figure 89 and 90.

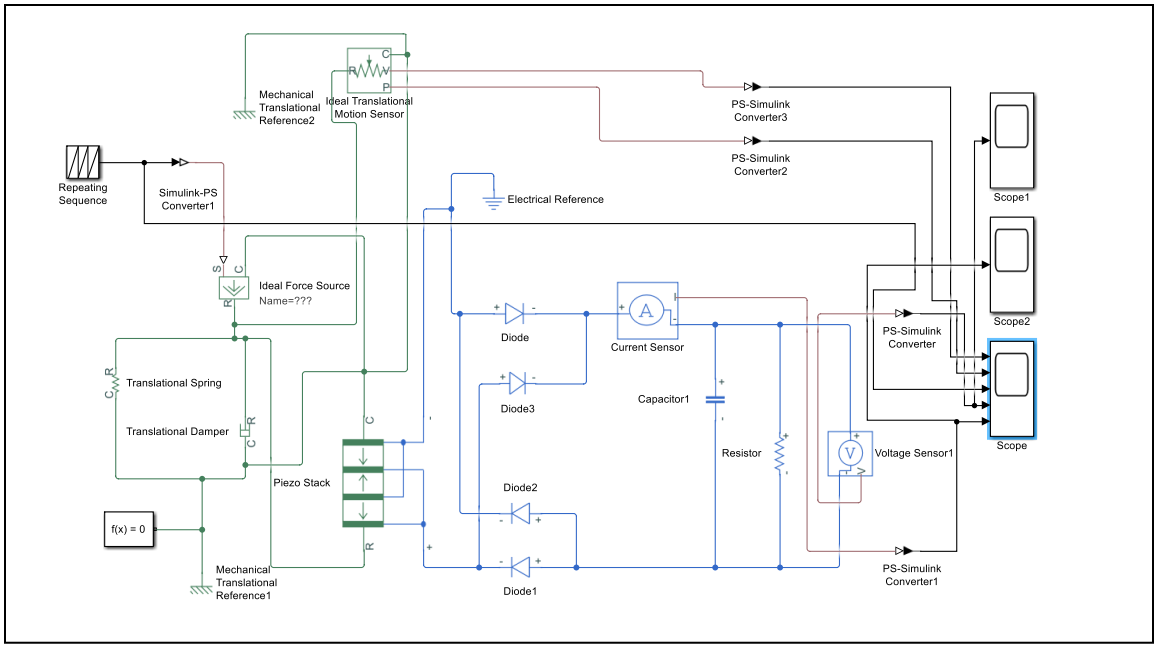

Figure 88. - Simulation of the piezoelectric transducer sub-assembly in MATLAB.

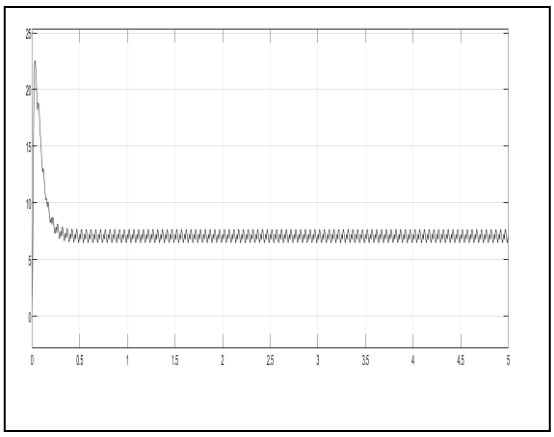

Figure 89. - Piezoelectric sub-assembly voltage output at 2 Hz frequency (scope 1).

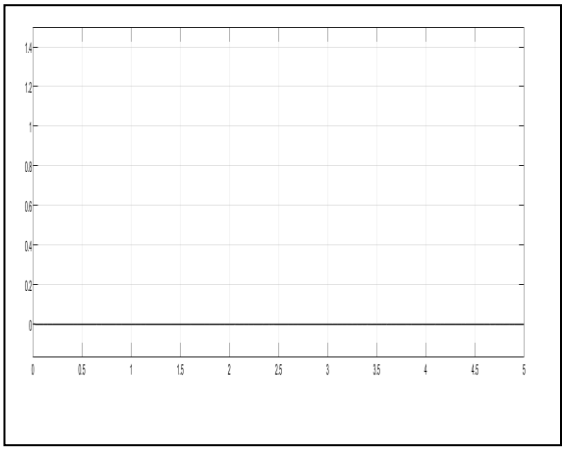

Figure 90. - Piezoelectric sub-assembly current output (scope 2).

3.12.4 Modeling of the piezoelectric transducer sub-assembly with buck converter added

Figure 91 shows the MATLAB Simulink model of the piezoelectric transducer sub-assembly coupled with the buck converter and figure 92 shows the output waveforms. All graphs from section 4.12.4 up to 4.12.9 show scope readings of probes taken top to bottom in the circuit diagrams and the corresponding graphs reading top to bottom first on the left and then right.

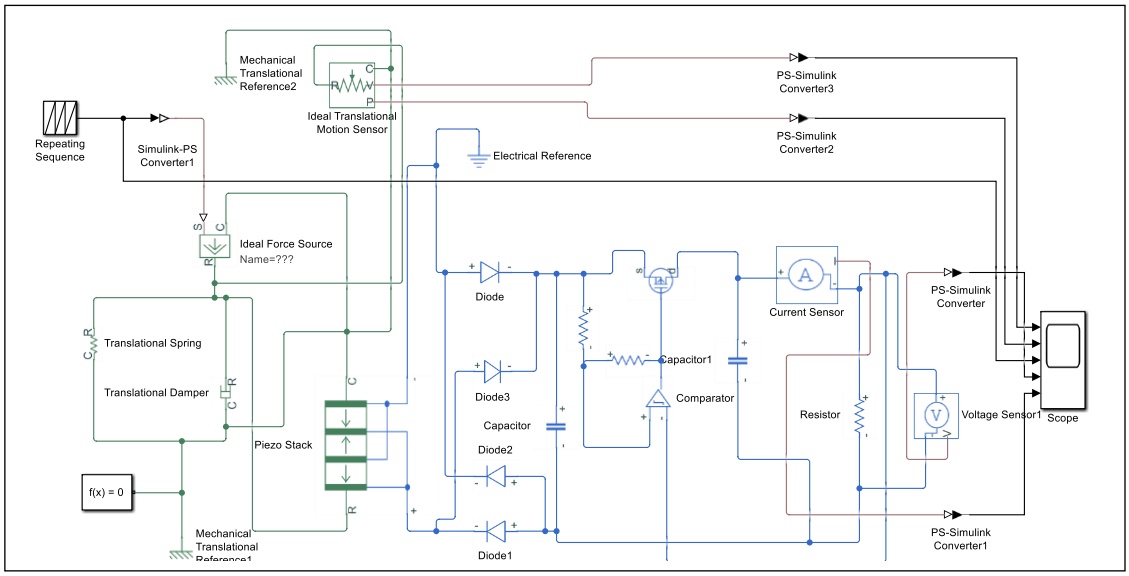

Figure 91. - MATLAB Simulink model of the piezoelectric transducer sub-assembly coupled with buck converter.

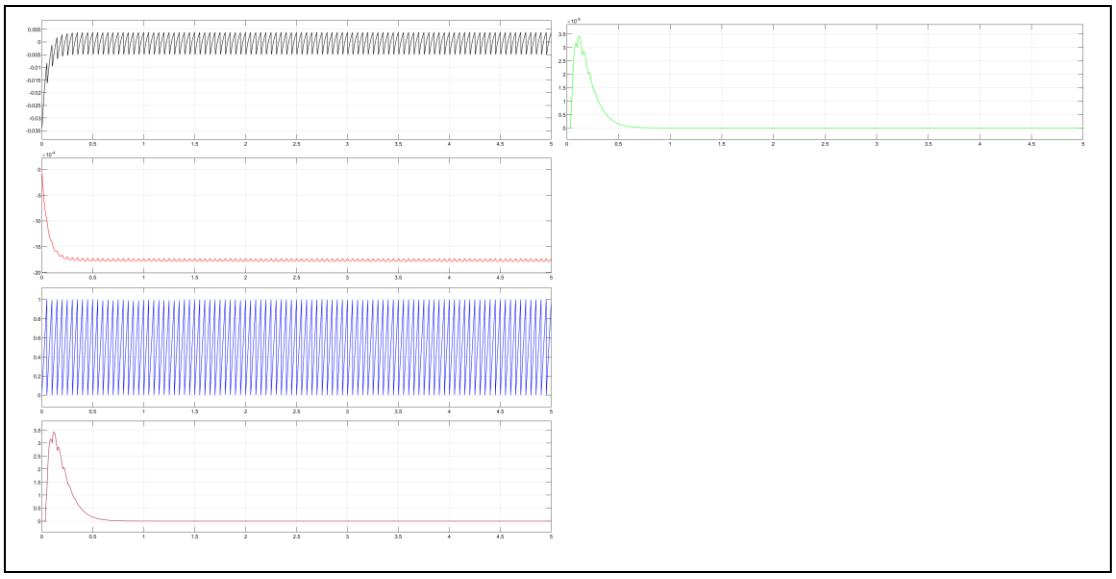

Figure 92. - Output wave forms of the piezoelectric transducer sub-assembly coupled with buck converter.

3.12.5 Modeling of the electro-magnetic sub-assembly

Figure 93 shows the MATLAB Simulink model of the electro-magnetic sub-assembly and the mechanical input, voltage and current output of the electro-magnetic sub-assembly are shown in that order in the first three graphs of figure 94.

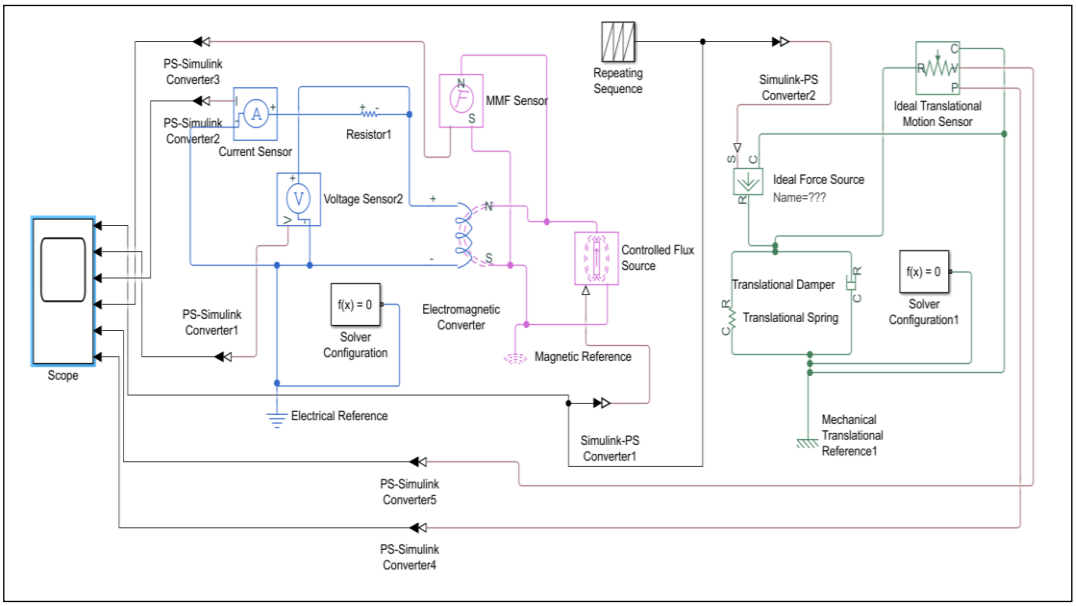

Figure 93. - The electro-magnetic sub-assembly modelled in MATLAB Simulink.

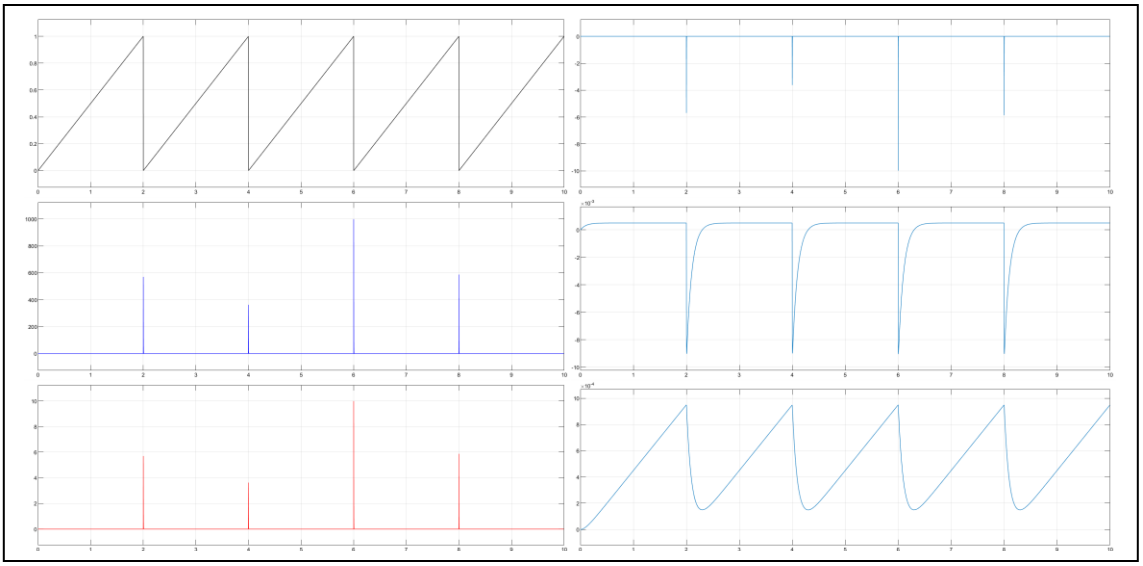

Figure 94. - The mechanical input waveform (in black), the voltage output (in blue) and the current output (in red) of the electro-magnetic sub-assembly.

3.12.6 Modeling of the piezoelectric sub-assembly and the electro-magnetic sub-assembly connected in parallel

Figure 95 shows the MATLAB Simulink model of the piezoelectric transducer sub-assembly coupled with the magnetic sub-assembly in parallel and figure 96 shows the output waveforms.

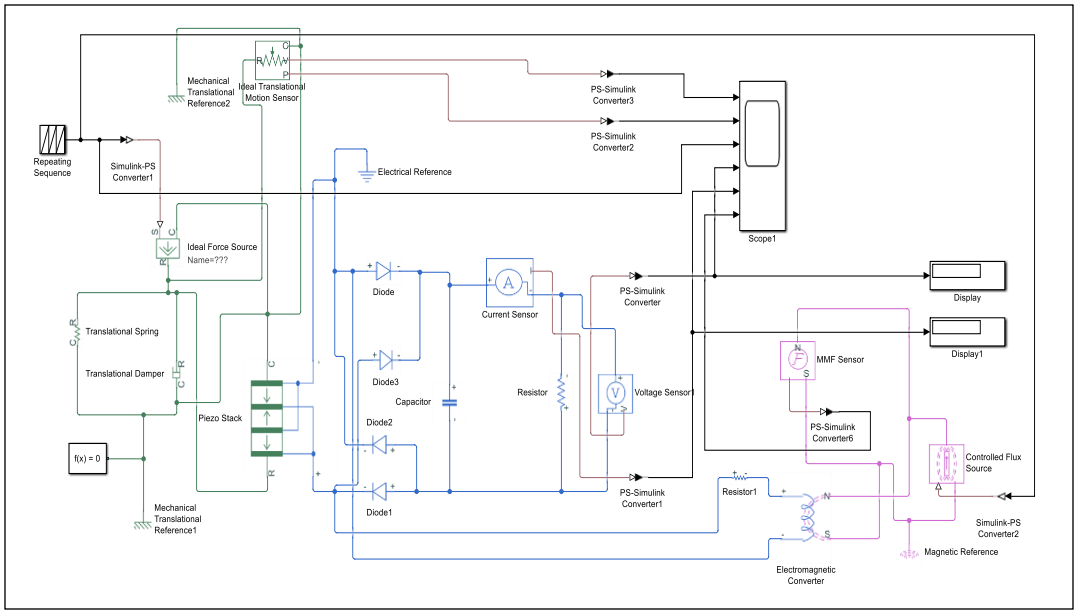

Figure 95. - Piezoelectric transducer sub-assembly coupled with the electro-magnetic sub-assembly (connected in parallel).

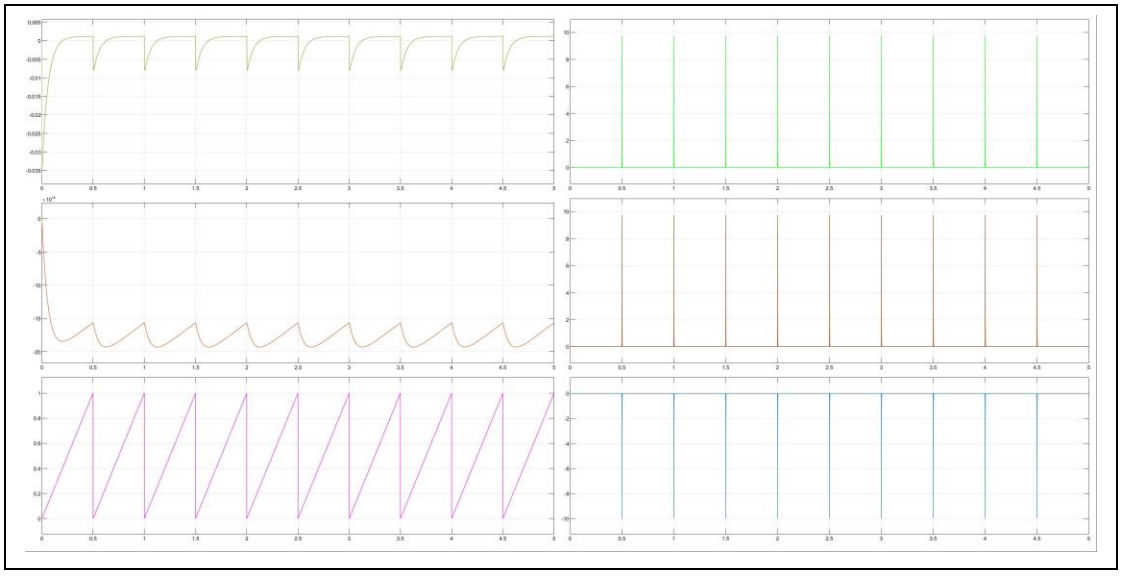

Figure 96. - Output waveforms of the piezoelectric transducer sub-assembly coupled with the electro-magnetic sub-assembly (connected in parallel).

3.12.7 Modeling of the piezoelectric sub-assembly and the electro-magnetic sub-assembly connected in series

Figure 97 shows the MATLAB Simulink model of the piezoelectric transducer sub-assembly coupled with the magnetic sub-assembly in series and figure 98 shows the output waveforms.

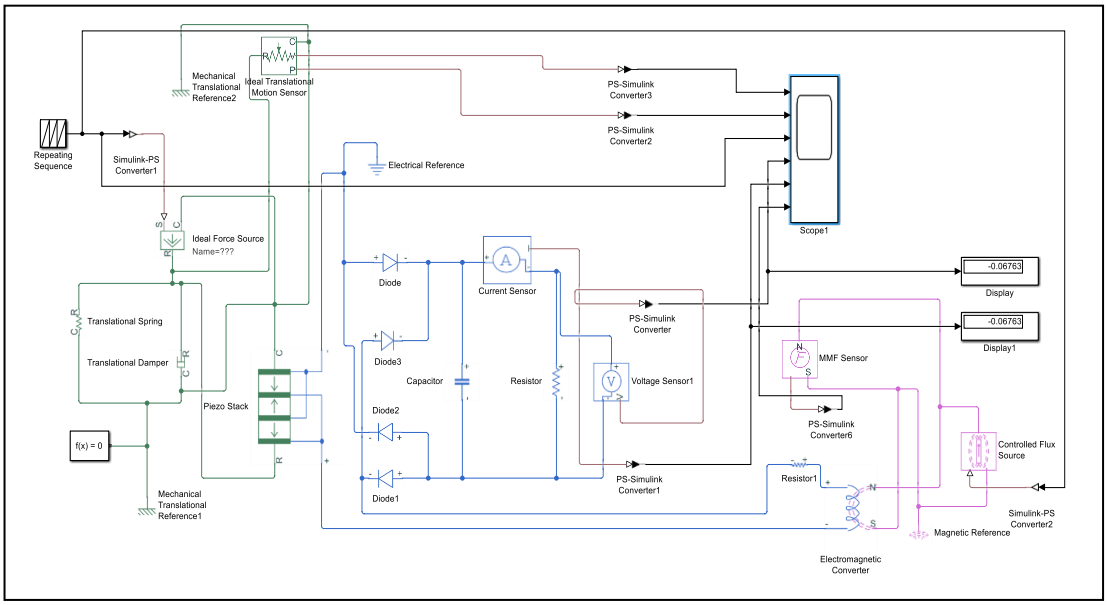

Figure 97. - Piezoelectric transducer sub-assembly coupled with the electro-magnetic.

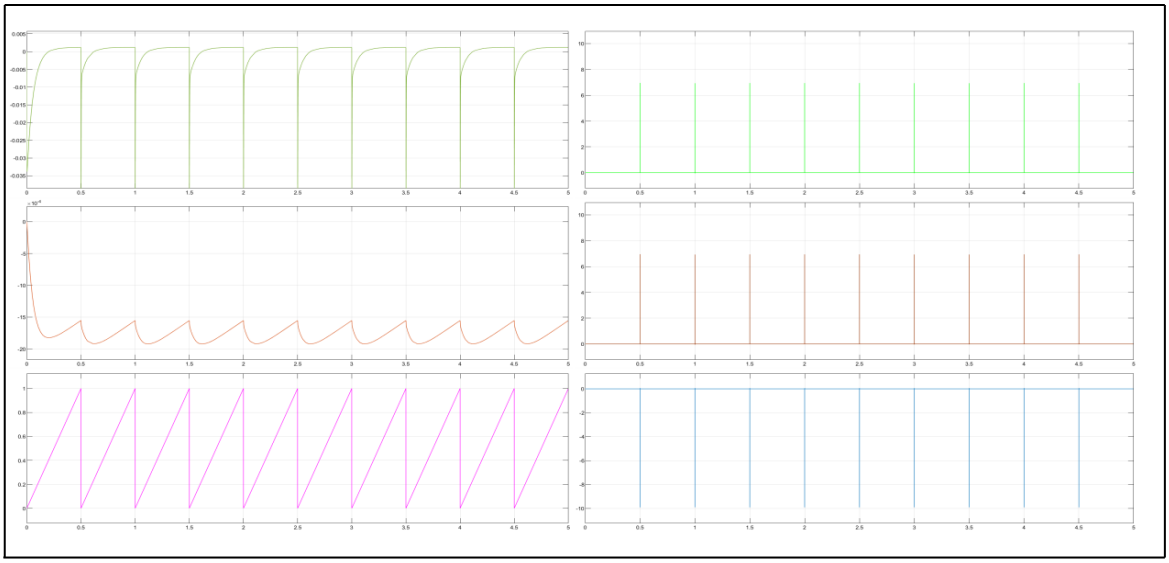

Figure 98. - Output waveforms of the piezoelectric transducer sub-assembly coupled with the electro-magnetic sub-assembly (connected in series).

3.12.8 Modeling of the piezoelectric sub-assembly and the electro-magnetic sub-assembly connected in parallel with buck converter added

Figure 99 shows the MATLAB Simulink model of the piezoelectric transducer sub-assembly with the electro-magnetic sub-assembly and buck converter and figure 100 shows the output waveforms

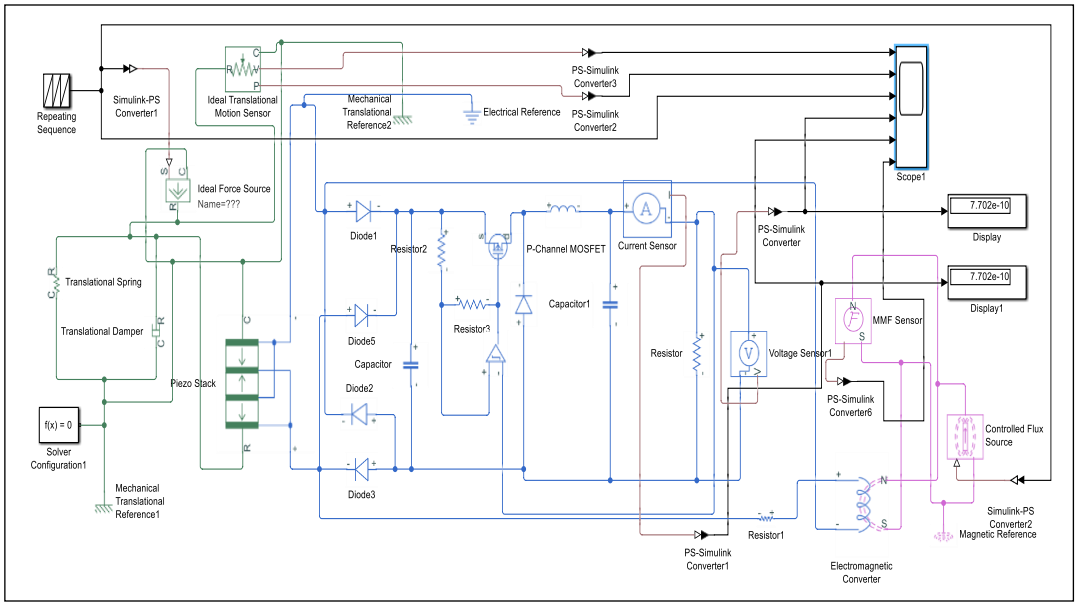

Figure 99. - MATLAB Simulink model of the piezoelectric transducer sub-assembly coupled with the electro-magnetic sub-assembly (connected in parallel) with buck converter.

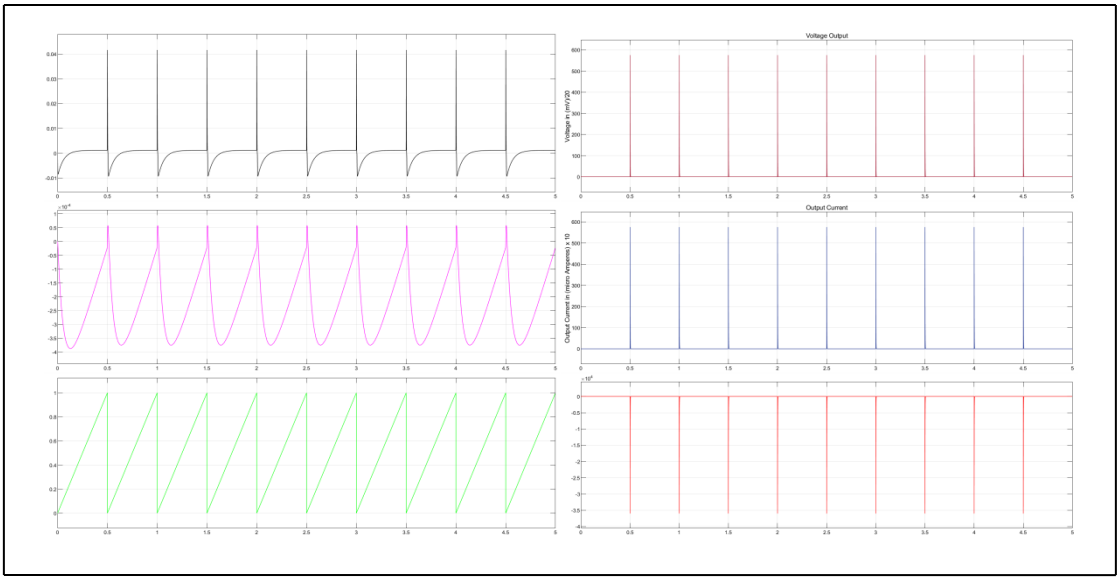

Figure 100. - Output waveforms of the piezoelectric transducer sub-assembly coupled with the electro-magnetic sub-assembly (connected in parallel) with buck converter.

3.12.9 Modeling of the piezoelectric sub-assembly and the electro-magnetic sub-assembly connected in series with buck converter added

Figure 101 shows the MATLAB Simulink model of the piezoelectric transducer sub-assembly with the electro-magnetic sub-assembly (connected in series) with buck converter and figure 102 shows the corresponding waveforms

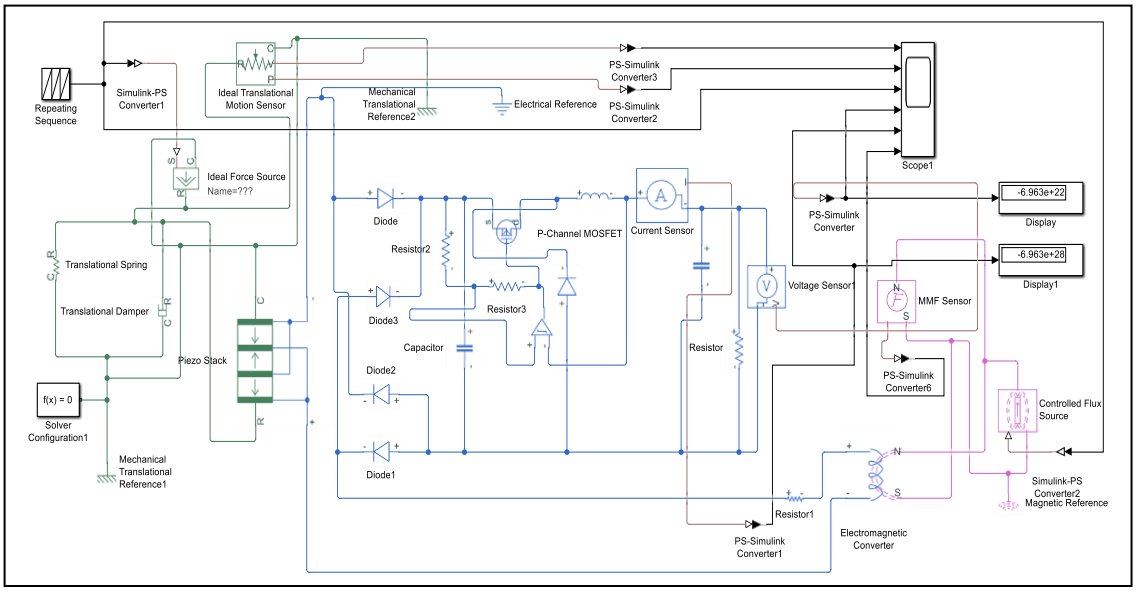

Figure 101. - MATLAB Simulink model of the piezoelectric transducer sub-assembly coupled with the electro-magnetic sub-assembly (connected in series) with buck converter.

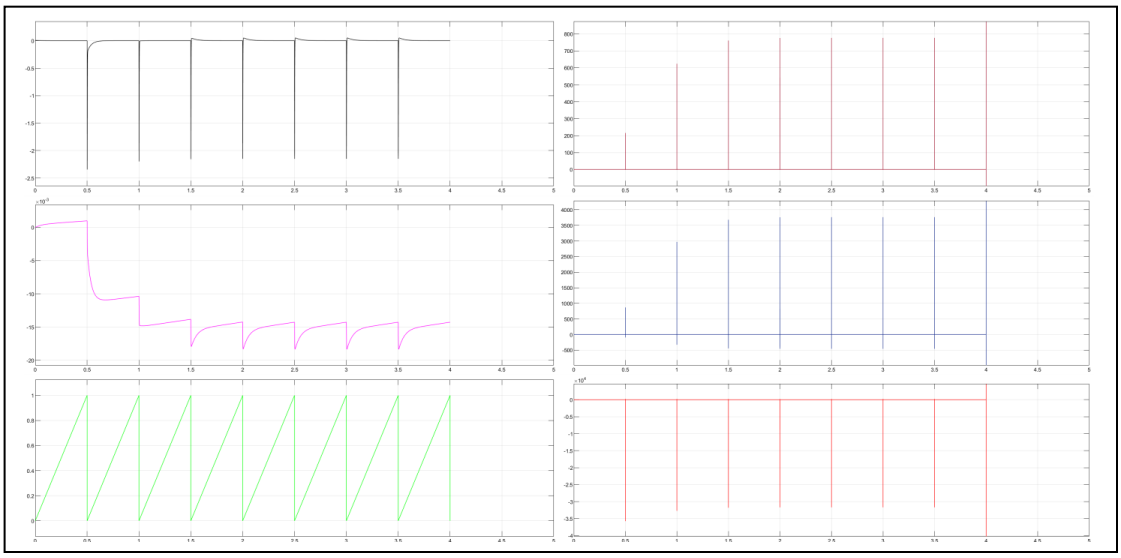

Figure 102. - Output waveforms of the piezoelectric transducer sub-assembly coupled with the electro-magnetic sub-assembly (connected in series) with buck converter.

3.12.10 Modeling of the piezoelectric sub-assembly and the electro-magnetic sub-assembly connected in series with buck converter and relay added

Figure 103 shows the MATLAB Simulink model of the piezoelectric transducer sub-assembly with the electro-magnetic sub-assembly (connected in series) with buck converter and figure 104 shows the corresponding waveforms

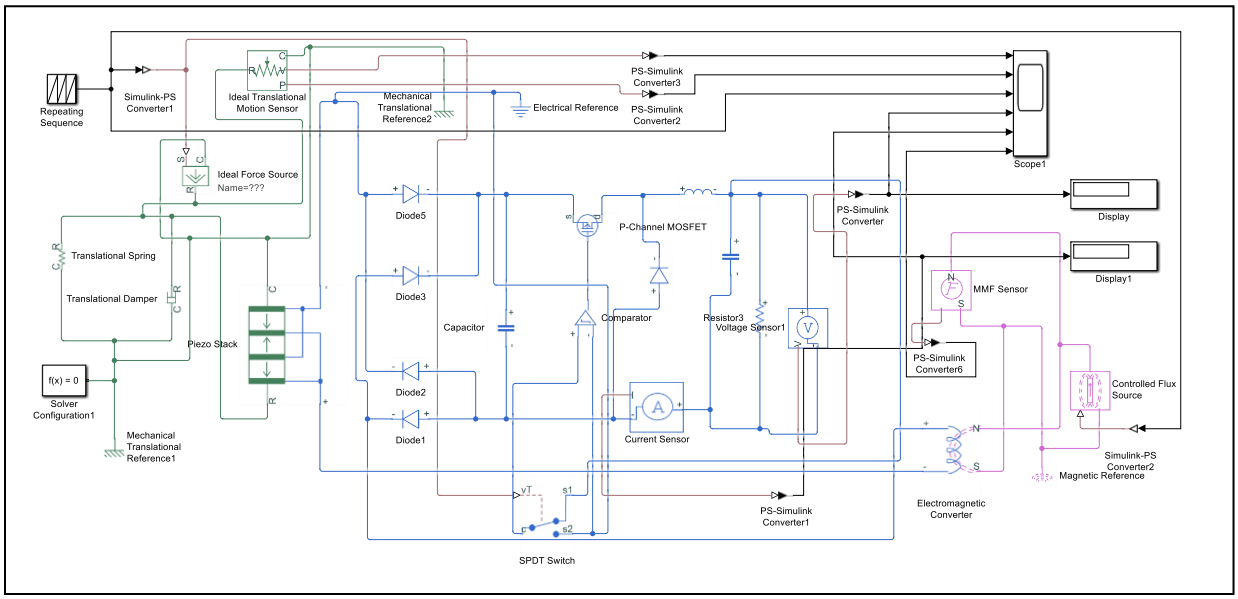

Figure 103. - MATLAB Simulink model of the piezoelectric transducer sub-assembly coupled with the electro-magnetic sub-assembly (connected in series) with buck converter and relay added.

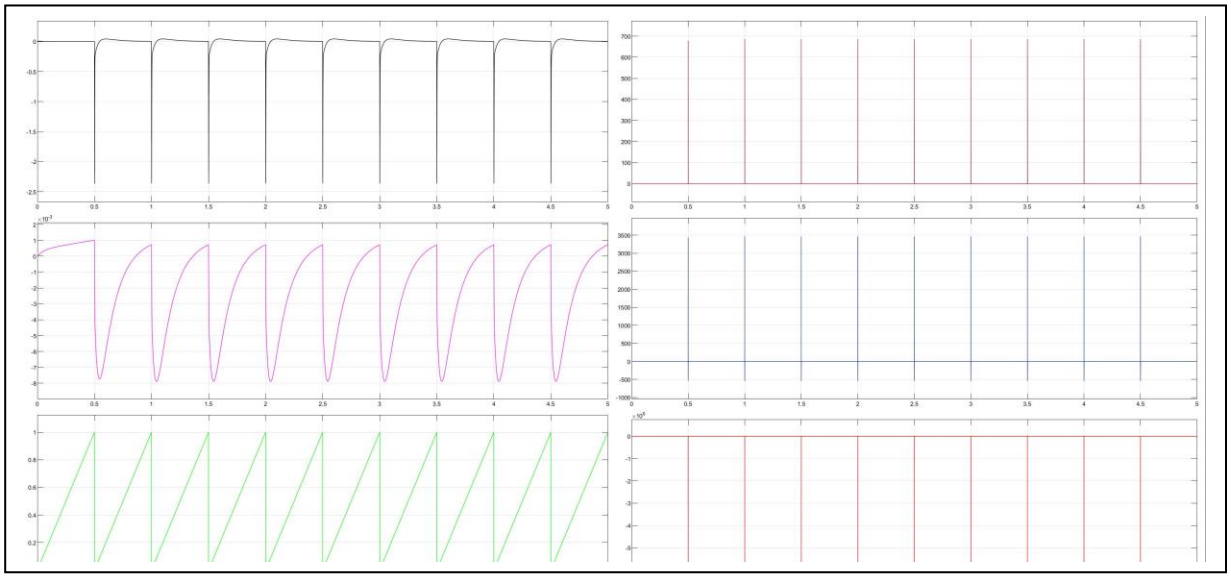

Figure 104. - Output waveforms of the piezoelectric transducer sub-assembly coupled with the electro-magnetic sub-assembly (connected in series) with buck converter and relay added.

3.12.11 Summary of output voltages and currents from practical experimentation of the various circuit connections

Table 4.5. - Summary of voltage outputs and currents for the various configurations of the 'serial-parallel' configuration for an applied force of 20 Newton.

	Configuration	Open Circuit Voltage (V) Peak value	Short Circuit Current (μA) Peak –Peak value
(1)	piezoelectric transducer sub-assembly	2.4	8.4 (Pk-Pk)
(2)	piezoelectric transducer sub-assembly coupled with boost converter	2.0	9.1 (Pk-Pk)
(3)	piezoelectric sub-assembly coupled with the electro-magnetic sub-assembly (connected in parallel)	15(mV)	19.6 (Pk-Pk)
(4)	piezoelectric sub-assembly coupled with the electro-magnetic sub-assembly (connected in series)	2.7	6.52 (Pk-Pk)
(5)	piezoelectric sub-assembly coupled with the electro-magnetic sub-assembly (connected in parallel) with boost converter	15(mV)	21.7(Pk-Pk)
(6)	piezoelectric sub-assembly coupled with the electro-magnetic sub-assembly (connected in series) with boost converter	2.9	5.2 (Pk-Pk)

Table 4.6. - Summary of voltage outputs and currents for the various configurations of the 'all-parallel' configuration for an applied force of 20 Newton.

	Configuration	Open Circuit Voltage (V) Peak Value	Short Circuit Current (μA) Peak-Peak value
(1)	piezoelectric transducer sub-assembly	3.0	60.4 (Pk-Pk)
(2)	piezoelectric transducer sub-assembly coupled with buck converter	3.8	40.1(Pk-Pk)
(3)	piezoelectric sub-assembly coupled with the electro-magnetic sub-assembly (connected in parallel)	12.0 (mV)	20.6 (Pk-Pk)
(4)	piezoelectric sub-assembly coupled with the electro-magnetic sub-assembly (connected in series)	3.9	76.5 (Pk-Pk)
(5)	piezoelectric sub-assembly coupled with the electro-magnetic sub-assembly (connected in parallel) with buck converter	10(mV)	23.7 (Pk-Pk)
(6)	piezoelectric sub-assembly coupled with the electro-magnetic sub-assembly (connected in series) with buck converter	3.3	80.2 (Pk-Pk)

3.13 Practical experimentation of composite energy harvester

The composite energy harvester is shown in figure 103. A galvanometer was used to determine the positive direction of current flow out of the piezoelectric sub-assembly and the electro-magnetic sub-assembly separately so that they could be joined accordingly to create the series or parallel configuration.

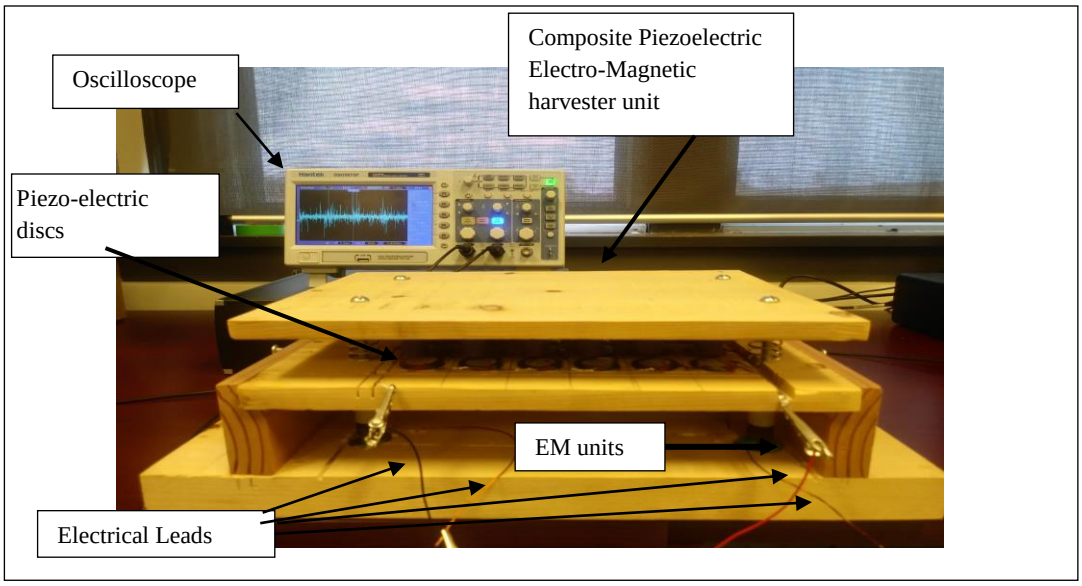

Figure 105. - Experimental layout of composite energy harvester.

Figure 104 shows the oscilloscope reading of the voltage output of only the PZ sub-assembly. The discontinuity and irregularity in amplitude is caused due to the unit being hand pumped.

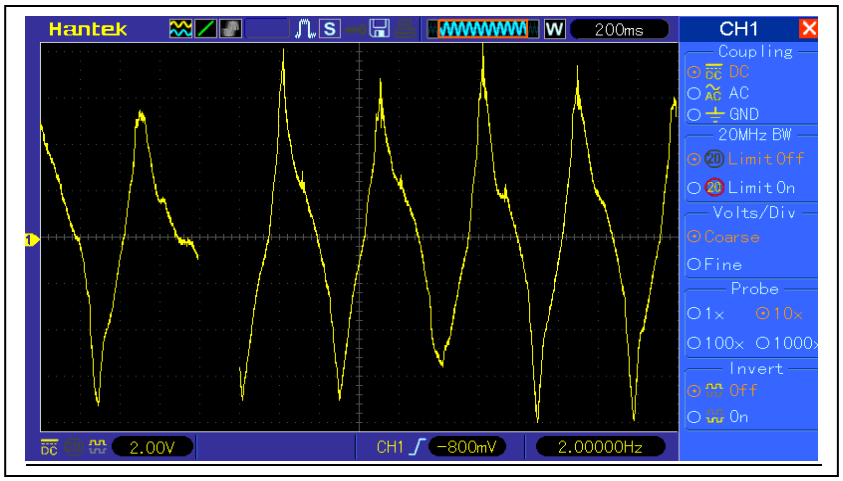

Figure 106. - Oscilloscope reading of the voltage output of the 'all-parallel' PZ sub-assembly (hand pumped, 20 Newton force).

Figure 105 shows the oscilloscope voltage reading of the PZ-EM composite energy harvester.

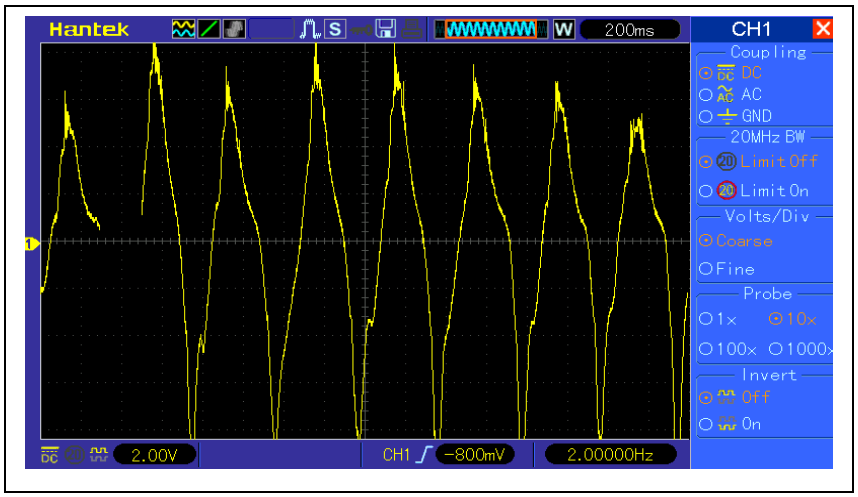

Figure 107. - Oscilloscope reading of the voltage output of the composite unit 'all-parallel' PZ sub-assembly and EM sub-assembly (hand pumped, 20 Newton force).

The discontinuity and irregularity in amplitude is caused due to the unit being hand pumped and not really subjected to a regular human weight. The difference between the theoretical output using Matlab Simulink and the real practical output is because the input used in the theoretical model is a continuously increasing ramp and abrupt release, but however practically the pressure applied by the physical step does not exactly bear resemblance to this shape.

4. RESULTS

The composite energy harvester would be referred to as a 'tile' and the following assumptions are made.

(1) Tiles are activated once per single footstep.

(2) A single pedestrian's two feet are upon two consecutive tiles within a second

(3) In a busy street a pedestrian behind would step onto a tile within 0.5 secs after the foot of the pedestrian before him is off it. (Giving a frequency of vibration of 2 Hz per tile). It follows that

the whole experimental area would be occupied by pedestrians with all tiles being activated at a frequency of 2 Hz.

With the above assumptions the current generated (I) can be calculated with the help of formula

$$I = f \, x \, m \, x \, M \, x \, q \qquad (5.1)$$

Where

I = current generated in Amperes (A)

f = frequency of vibration of each tile in Hertz (Hz)

m = total number of harvester units (tiles) operating at frequency f

M = force presented on a single tile by one footstep in Newton (N)

q = electricity generated by a single step per tile in coulombs (C)

'm' in the above equation is the number of tiles 's' stepped on by a pedestrian at any given time multiplied by the number of pedestrians over the experimental area.

In converting the body mass into Newton a figure of 1/5 of gravitational acceleration 'g' is to be used (2.5 m/s^2) which is typical of most low level vibrations [85]. 'q' in the above equation works out to be the 'charge generation constant' for the composite energy harvester.

Erika Butller of the 'Halifax Examiner' in their project 'Making room for pedestrians on Spring Garden Road' found out that there would be an average of 2600 pedestrians walking both ways down Spring Garden Road on a summer week day between 3.30 p.m. 5.30 p.m. and 2350 on a Saturday afternoon from 11.00 a.m. to 1.00 p.m. [39]. Assuming the average body mass of a person to be 70 Kg and the charge generation co-efficient per composite harvester unit to be an optimum figure of 5 µC/N, the current generated from *10* tiles placed on either side walk (total of 20), according to equation 5.1 would be 2 x (*2 x 5* x 2) x (70 x 2.5) x (5×10^{-6}) = 0.035 A. (Notice *2* x *5* = *10*). By increasing the total number of tiles to 2000 (1000 on each side of the

road) the generated current would be 3.5 A as it would be a scale up by a 100. i.e. 2 x (2 x 500 x 2) x (70 x 2.5) x (5 x 10^{-6}) = 3.5 A. To generate the above quantity of current we need 14,400 (=2 x 2 x 60 x 60) pedestrians during a period of 2 hours. The proportionate current generated with 1000 tiles on each sidewalk, for the given number of pedestrians during different periods of the day is given in table 5.1. Therefore, to charge a 40 AH battery it would take approximately 12 ½ days assuming 2 hours peak activity and 6 hours half peak activity and progressively reducing activity during the rest of the day.

Table 5.1. - Current generated during different times of the day.

Duration of the day	No. of hours	No. of pedestrians	Current generated
7.30 a.m.- 9.30 a.m.	2	1260	0.3062 A
9.30 a.m.- 11.30 p.m.	2	743	0.1805 A
11.30 p.m.- 3.30 p.m.	4	1260	0. 1531 A
3.30 p.m.- 5.30 p.m.	2	2600	0.63A
5.30 p.m.- 7.30 p.m.	2	371	0.09A
7.30 p.m - 9.30 p.m.	2	223	0.054 A
9.30 p.m.- 7.30 a.m.	10	74	0.0035 A

If X is the number of days, it would take to fully charge a 40 AH battery then value X could be obtained from the following equation.

$$[(0.63 \times 2) + (0.3062 \times 2) + (0.1805 \times 2) + (0.1531 \times 4) + (0.09 \times 2) + (0.054 \times 2) + (0.0035 \times 10)] X = 40$$

$$X = \underline{12.65 \text{ days}}$$

If the average output voltage is 2 V these results yield that 0.48 KWh/year can be harvested annually from pedestrian footstep vibration energy by considering only peak hours of weekdays. Calculations show that these composite energy harvesters can save Can $ 540 in the annual running costs and reduce 4 percent of greenhouse gas emissions by taking this amount of electricity off the power grid.

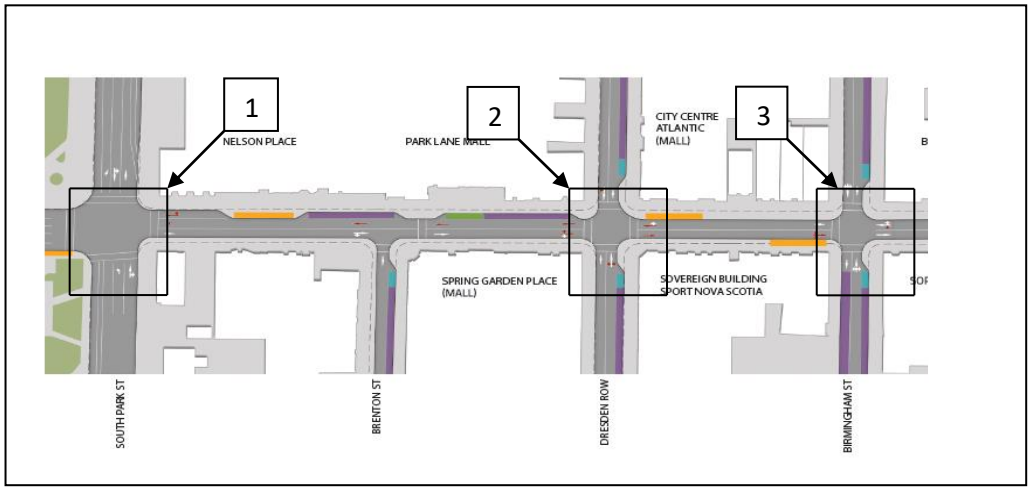

Figure 108. - Halifax city map with important intersections

The most populous intersections and crosswalks identified in Downtown Halifax area as shown in figure 106 are as follows.

(i) Spring garden- South Park Street Intersection

(ii) Spring Garden- Dresden Row Intersection

(iii) Spring Garden- Barrington Street Intersection

Visitors to the Halifax Public library are as appended in table 5.2 below.

Table 5.2. - Visitors to the Halifax public library.

Halifax Central Library - Visitor Counts			
	Visitors	Hours Open	Visitors per Hour
Aug-18	123122	309	398
Sep-18	121002	291	416
Oct-18	132467	315	421
Nov-18	107192	291	368
Dec-18	104072	275	378
Jan-19	128408	312	412
Feb-19	122467	264	464
Mar-19	142888	312	458
Apr-19	116842	284	411
May-19	115629	309	374
Jun-19	109682	303	362
Jul-19	122916	312	394
AVERAGE	120557	298	405

According to Darla Muzzerall, Manager, Research & Analytics Alderney Gate Public Library; visitors to the Halifax Public library on Spring Garden, number on average to about 400 per hour as shown in table 5.2. The figure doubles when both in and out movement is considered. Once again assuming 10 tiles are placed each way, the average body mass of a person to be 70 Kg and the composite charge co-efficient to be 5 μC/N, the current generated would be 2 x (2 x 0.12 x 2) x (75 x 2.5) x (5×10^{-6}) = 0.0009 A. The 0.12 in the above equation for the total number of commuters comes from the fact that there would be that number over the experimental area at any given time based on visitor statistics.

5. FUTURE EXPANSION: HARVESTING VIBRATION ENERGY FROM ROADS WITH MEDIUM/HIGH TRAFFIC

Each vibration event from one vehicle will not be independent of another, with only some dampening occurring before the next vehicle approaches. But for calculation purpose it has to be assumed that all vibration events are independent of each other. Therefore, the total energy harvested by all piezoelectric devices along a unit length of road is the multiplication of the 'number of cars that pass' by the 'sum vibrational energy' that one car transfers to the road along that unit length. The energy a car transfers as vibrations in asphalt would be, by common sense, less than the energy a car puts to mechanical work over a unit length of road. A close value for this amount of energy can be calculated by a multiplying the energy consumed from gasoline by thermal efficiency.

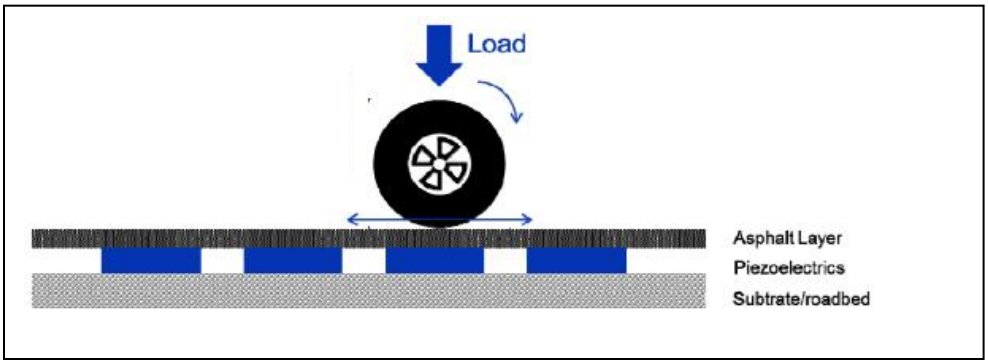

Figure 109. - Cross sectional schematic diagram for piezoelectric energy harvesting from motor traffic in roads/highways.
Source: DNV KEMA Energy and Sustainability, Oakland, California.

Factors to be considered in this calculation are

(i)Expended Energy (Gasoline Used) in terms of Joules

(ii)Energy Density of Gasoline in terms of Joules per Kilogram

(iii) Density of Gasoline in terms of Kilogram per Gallon

(iv)Thermal Efficiency (as a percentage)

(v) Number of vehicles passing by

(vi)Weight of vehicle

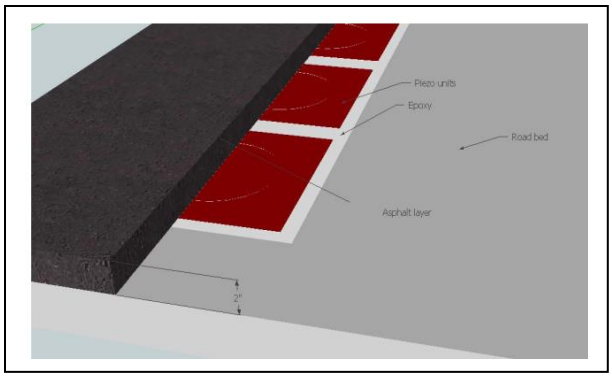

Figure 110. - 3D diagram of the roadway installation of piezoelectric energy harvesters
Source: DNV KEMA Energy and Sustainability, Oakland, Ca, U.S.A..

A modest figure of 0.1 or 10% has been assumed for thermal to vibrational energy transfer leaving a good 90% for other energy dissipations such as internal friction, friction between tires and asphalt, braking and air-conditioning/heating.

Transferred (or converted) energy per meter length of road

$$= \frac{\textit{(Density of Gasoline) x (Energy Density of Gasoline)} \times \textit{(Energy transfer factor)}}{\textit{(Gasoline consumption rate)}} \quad (6.1)$$

Using equation 6.1 figures could be calculated to be

$$\frac{[(1\ \text{km} \times 10^{-3}) \times (0.621\ \text{mi/km})] \times (2.8\ \text{kg/gal}) \times (4.43 \times 10^{7}\ \text{J/kg}) \times (0.1)}{(20\ \text{mi/gal})}$$

$$= \underline{0.385\ \text{KJ}}$$

Erika Butller of the 'Halifax Examiner' in their project 'Making room for pedestrians on Spring Garden Road' found out that there would be an average of 3400 motor vehicles plying down Spring Garden Road (both ways) on a summer week day between 3.30 p.m. 5.30 p.m. and an average of 2350 on a Saturday afternoon from 11.00 a.m. to 1.00 p.m. [39]. Eastward and Westward traffic on six consecutive days of a week in July 2018 is shown in figure 109.

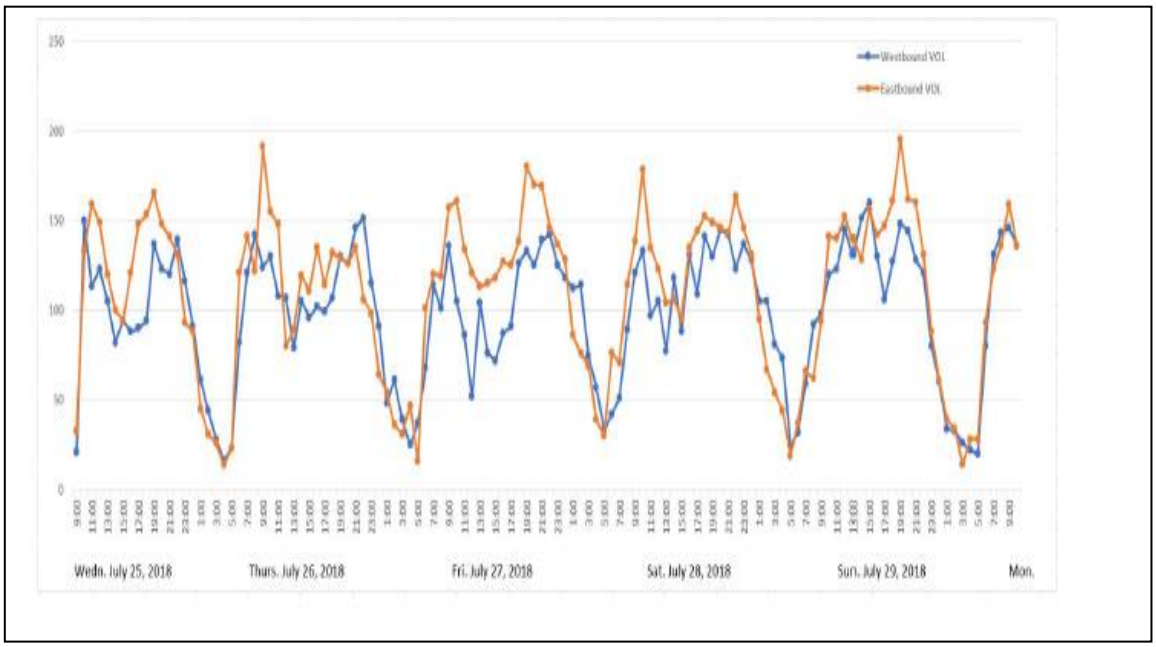

Figure 111. - Transportation patterns in Halifax, NS
Source: Halifax Regional Council, Transpotation standing commiittee March 2019.

Using these figures the energy converted by 1700 vehicles (plying both ways) per hour would be .385 x 1700 = 654.5 KJ per hour =181 W

The expectation of generating up to approximately 350 kilowatts of energy from a kilometer stretch of dual carriageway, assuming 450+ vehicles on average would ply through a road segment of this length in an hour, would not be too optimistic.

6. EVALUATION AND REFLECTION

Small-scale energy requirements powered by piezoelectric energy harvesters are picking up rapidly around the globe. In addition to small-scale applications, the manufacturing and construction industries are also finding applications for piezoelectric devices. The automotive industry is closely following on their heels. Applications in instruments in the medical field as well as powering devices in remote locations for information transmission in telecommunications are two distinct areas which offer piezoelectricity high prospects. Exploring and exploiting piezoelectricity in these areas will have high stakes. The piezo technique can also solve the problem of electricity to road lighting systems, obviating the need for kilometers of electrical wire running alongside roads. It is a more efficient operation technique with cost effectiveness. There exists piezoelectric materials that can carry high physical loads and also operate at very high frequencies. The correct choice of material will depend on the circumstances it is used. It requires little or no maintenance as there are no moving parts. However, protection of sensitive piezoelectric devices is required against harsh weather conditions, and strong electric fields (200-500V/mm) which can break down dipoles and depolarize piezoelectric material.

7.CONCLUSION

Piezoelectric materials have the unique ability of transforming mechanical stress or strain energy into electrical energy. Understanding and exploiting this phenomenon is quietly gaining momentum globally but the tangible outcome is still in its fledgling status though. The amount of energy produced solely depends on the volume of traffic (Human/Vehicular) and the number of piezoelectric elements placed under the surface. A vehicle that moves slowly and foot traffic that moves fast appears to generate slightly more energy. Further research is necessary to tap into the potential of piezoelectricity as a viable alternate power generation system. Research into materials that provide higher piezoelectric charge constants and possess lower resonance frequency has to be carried out. Different geometric structures have to be experimented with once again taking into account the material being used. This is important because different materials give different results for energy produced depending on the mode (33, 31, etc...) they are used. Hence the material used, the mode it's being used and the application for which it's used all have a bearing on the end result of the product.

Harvesting energy from ambient vibrations has tremendous scope for future energy/ power solutions and provides an impetus towards providing greener and more sustainable energy with creating a healthier environment as an equally valuable end result. It is really showing signs of being a viable alternative in proving power to wireless sensor nodes. The indirect piezoelectric effect which is used in actuators is already widely employed in the medical field.

In this project, the joint employment of piezoelectricity and electro-magnetism has been looked into. Further composition of technologies could be researched so that they could be combined to enhance the power generating potential. Considering seebeck effect is a worthwhile undertaking,

even though the amalgamation of a.c. and D.C. power could pose a challenge. But there is a way around it akin to the digital hierarchy in data systems.

The modest amount of energy produced by basic energy harvesting systems should not be a discouragement but rather an impetus to dig deeper in to this hitherto vastly latent area in the energy industry. Collaboration with other foreign universities in countries like Japan and Israel is recommended to get more exposure on how they have advanced in renewable energy technologies, especially vibration energy harvesting.

I really hope my research done in this project would help all future aspirants who have taken renewable energy technologies as a serious pre-occupation.

8. REFERENCES

[1] Ali B. and Mashaleh A. (2018) "Power generation using piezoelectric materials", no. pp. 0–4, December 2018.

[2] Ashraf K., Md Khir M. H., Dennis J. O. and Baharudin Z. (2013). "A wideband, frequency up-converting bounded vibration energy harvester for a low-frequency environment", *IOP Publishing Smart Materials and Structures* Smart Mater. Struct. 22 (2013) 049601 (1pp) doi:10.1088/0964-1726/22/4/049601 K 2013 *Smart Mater. Struct.* 22 025018

[3] Assaderaghi F., Sinitsky D., Parke S. A., Bokor J., Ko P. K. and Hu C. (1997). "Dynamic threshold-voltage MOSFET (DTMOS) for ultra-low voltage VLSI." *IEEETransactions on Electron Devices*, Vol. 44, No. 3, March 1997

[4] Bardaweel H., Hattamleh O. A., Richards R., Bahr D. and Richards C. (2006). A comparison of piezoelectric materials for MEMS power generation. *The Sixth International Workshop on Micro and Nanotechnology for Power Generation and Energy Conversion Applications*, Nov. 29 - Dec. 1, 2006, Berkeley, U.S.A.

[5] Başak E.M. and Kaçar F. (2017). **"**Ultra-low voltage VDBA design by using PMOS DTMOS transistors". *IU-JEEE Vol*. 17(2), (2017), 3463-3469

[6] Batra A. K., Alomari A., Chilvery A. K., Bandyopadhyay A. and Grover K. (2016). "Piezoelectric power harvesting devices: An overview", *Advanced Science, Engineering and Medicine* Vol. 8, 1–12, 2016 www.aspbs.com/asem

[7] Bera B. and Sarkar M. D. (2017). "Piezoelectricity in PVDF and PVDF based piezoelectric nano-generator: A concept ", *IOSR Journal of Applied Physics* (IOSR-JAP) e-ISSN: 2278-4861.Volume 9, Issue 3 Ver. I (May – June 2017), PP 95-99 www.iosrjournals.org , doi: 10.9790/4861-0903019599 www.iosrjournals.org

[8] Brown L. F. (1992). "Ferro-electric polymers: current and future ultrasound applications," *IEEE 1992 Ultrasonics Symposium Proceedings 1-2*, 1992, pp. 539-550 vol.1, https://doi: 10.1109/ULTSYM.1992.275948. https://doi.org/10.1109/ULTSYM.1992.275948

[9] Brown L. F. (2000). "The effects of material selection for backing and wear protection/quarter-wave matching of piezoelectric polymer ultrasound transducers," *2000 IEEE Ultrasonics Symposium. Proceedings. An International Symposium (Cat. No.00CH37121)*, 2000, pp. 1029-1032 vol.2, doi: 10.1109/ULTSYM.2000.921500.

[10] Buck-Boost Converters (learnabout-electronics.org)

[11] Caliò R., Rongala U. B., Camboni D., Milazzo M., Stefanini C., Petris G. de and Oddo C. M. (2014). "Piezoelectric energy harvesting solutions", *Sensors* 2014, 14, 4755-4790; doi:10.3390/s140304755 ISSN 1424-8220 www.mdpi.com/journal/sensors

[12] Cha Y., Shen L. and Porfiri M. (2013). "Energy harvesting from underwater torsional vibrations of a patterned ionic polymer metal composite", *IOP Publishing Smart Materials and Structures*, 22 (2013) 055027 (13pp) doi:10.1088/0964-1726/22/5/055027

[13] Cook-Chennault K. A., Thambi N. and Sastry A. M. (2008). "Powering mems portable devices- a review of non-regenerative and regenerative power supply systems with special emphasis on piezoelectric energy harvesting system." *Smart materials and structures17,*4 (2008) (33pp) .

[14] Covaci C. and Gontean A. (2020). "Piezoelectric energy harvesting solutions: A review *Sensors*; 21 June 2020

[15] Curry A. (2009). "Ecology. Deadly flights". *Science*, 325(5939):386±7

[16] Dahiya R.S., Ravinder S. and Valle M. (2013). "Robotic tactile sensing", *Technologies and System* (2013), ISBN 978-94-007-0579-1

[17] Dahiya R.S. and Valle M. (2013). "Robotic tactile sensing", *Springer Science+Business Media Dordrecht* (2013), doi 10.1007/978-94-007-0579-1

[18] Dannier A., Brando G. and Ruggiero F. N. (2019). "The piezoelectric phenomenon in energy harvesting scenarios: A theoretical study of viable applications in unbalanced rotor systems", *Energies 12*, 708 (2019), doi:10.3390/en12040708 www.mdpi.com/journal/energies

[19] Datta S. (2014). *COMSOL Blog*, *https://www.comsol.com/blogs/piezoelectric-materials-crystal-orientation-poling-direction*/Feb 2014

[20] Edery-Azulay L. (2010). "Harvesting energy and data, a stand-alone technology", *Innowattech: The CEO's report* (2010)

[21] Elahi, H., Eugeni M. and Gaudenzi P. A. (2018). **"**Review on mechanisms for piezoelectric-based energy harvesters." *Energies* Volume 11 -Issue 7, 2018, *11*, 1850; https://doi:10.3390/en11071850 www.mdpi.com/journal/energie

[22] Energy / Climate Change. (2008). "Power generating floor tested at JR Tokyo train station", May 9, 2008, *Japan for Sustainability*, Referenced 28th Dec 2020, https://www.japanfs.org/en/news/archives/news_id027023.html (Last visited Jan 2021.)

[23] Engadget, "Power generating dance-floor". (2008). *Engadget Company*. https://www.engadget.com/2008/07/17/power-generating-dance-floor-hits-uk-club.html (Last viewed Referenced 20th July 2020).

[24] Garimella R. C., Dr. Sastry V. R. and Mohiuddin M. (2015). "PiezoGen, an approach to generate electricity from vibrations", *Proceedia Earth and planetary Science* 11(2015)445-456

[25] Gupta A., Imran M., Agarwal R., Yadav R., Jangir P. and Poonia R. (2016). **"**Energy Harvesting through Dance Floor using Piezoelectric Device", *International Journal of*

Engineering and Management Research, Volume-6, Issue-2, March-April 2016 SSN (ONLINE): 2250-0758, Pages: 36-39, ISSN (PRINT): 2394-6962

[26] Gupta M. N., Suman S.Y. and Yadav S.K. (2014). "Electricity generation due to vibration of moving vehicles using piezoelectric effect", *Advance in Electronic and Electric Engineering*, ISSN 2231-1297, Volume 4, Number 3 (2014), pp. 313-318 © Research India Publications http://www.ripublication.com/aeee.htm

[27] Gururaja T. R., Schulze W. A., Cross L. E., Newnham R. E., Auld B. A.

and Wang Y. J. (1985). "Piezoelectric composite materials for ultrasonic transducer applications. Part I: Resonant modes of vibration of PZT rod-polymer composites" , *IEEE Trans. Sonics Ultrasonics*. 32(4), 481–498 (1985). https://doi.org/10.1109/TSU.1985.31623,

[28] Hadhazy A. (2009). "Power plants: Artificial trees that harvest sun and wind to generate electricity". *Scientific American*. https://www.scientificamerican.com/article/artificial-trees-harvest-sun-and-wind-energy/

[29] Hill D., Agarwal A. and Tong N. (2014). "Assessment of piezoelectric materials for roadway energy harvesting cost of energy and demonstration roadmap", *DNV KEMA Inc Energy & Sustainability* January 2014, CEC-500-2013-007

[30] Hillenbrand J. and Sessler G. M. (2004). "High-sensitivity piezoelectric microphones based on stacked cellular polymer films (L)", *The Journal of the Acoustical Society of America* 116, 3267 (2004); https://doi.org/10.1121/1.1810272 2021

[31] https://www.ceramtec.comstandard-shapes-and-sizesdiscs# (Last viewed Dec 2019)

[32] https://en.wikipedia.org/wiki/Buck_converter

[33] https://inhabitat.com/kinetic-energy-floors-convert-sweet-dance-moves–into-power/

[34] https://mvsa-architects.com › projects-new-stadium-superkuip-sports. (Last viewed Jan 2021)

[35] http://www.com/piezobasics/version1604 (Last viewed Sep 2019)

[36] https://www.comsol.com/blogs/piezoelectric-materials-crystal-orientation-poling-direction/

[37] https://www.engineering.com/ElectronicsDesign/ElectronicsDesignArticles/ ArticleID/5879/Power-Walking-with-Energy-Floors.aspx (Last viewed Jan 2021)

[38] https://www.fierceelectronics.com/sensors/underwater-communication-system-uses battery-free-sensors. (Last viewed Jan 2021.)

[39] https://www.halifaxexaminer.ca/ (Last viewed Jan 2020)

[40] https://www.instructables.com/id/Piezo-Tiles-Generate-Electricity-by-Walking/ (Last viewed Jan 2021.)

[41] https://www.intemag.com/magnet-design-guide

[42] https://www.leadingedgepower.com/support/contact-us.html (Last visited Jan 2020.)

[43] http://www.noliac.com/news/item/show/piezo-products-in-underwater-applications/ (Last viewed Jan 2021.)

[44] https://www.supermagnete.de/eng/faq/How-do-you-calculate-the-magnetic-flux-density (Last refereed on 24th Aug 2021)

[45] http://www.sayedsaad.com/fundmental/10_power%20loss%20in%20an%20inductor .htm

[46] http://www.sayedsaad.com/fundmental/12_capacitor%20losses.htm#:~:text =The%20power%20loss%20of%20a,a%20power%20loss%20of%20zero.

[47] Jones C.A., Reynolds P. and Pavic A. (2011). "Vibration serviceability of stadia structures subjected to dynamic crowd loads: A literature review", *Journal of Sound and Vibration* 330(8):1531-1566 March 2011, doi: 10.1016/j.jsv.2010.10.032

[48] Johnson T. J., Charnegie D., Clark W. W., Buric M. and Kusic G. (2006). "Energy harvesting from mechanical vibrations using piezoelectric cantilever beams", *Smart structures and materials* (pp. 61690D-61690D). International Society for Optics and Photonics. (2006, March).

[49] Jingmin W., Zheng Y., Zhangming Z. and Yintang Y. (2016). **"**An ultra-low voltage rectifier for PE energy harvesting applications". *Journal of Semiconductors Vol.* 37, No. 2 February 2016.

[50] Katzir S. (2007). "The Beginning of piezoelectricity – A study in mundane physics" Springer; 2006th edition (April 8 2007)

[51] Keane B. (2013). "Electrical equipment in cold weather applications.-white paper" WP083007EN IEEE October 2013

[52] Khandy S. A. and Gupta D. C. (2020). "Magneto-electronic, mechanical, thermoelectric and thermodynamic properties of ductile perovskite Ba_2SmNbO_6", *Materials Chemistry and Physics* 239 (2020) 121983 journal homepage: www.elsevier.com/locate/matchemphys

[53] Kim H. W., Batra A., Priya S., Uchino K. Markley D., Newnham R.E.and Hofmann H.F. (2006). "Modeling of piezoelectric energy harvesting using cymbal transducers". *Japanese journal of applied physics 45*, 7 (2006), 5836–5840.

[54] Kim Y.I., Kim G., Bae Y.M., Ryu Y.H., Jeong K.J., Oh C.H. and Kim K.B. (2015). "Comparison of PMN-PT and PZN-PT single crystal based ultrasonic transducers for nondestructive evaluation applications". *Sensors and Materials*, Vol.

27, No. 1 (2015) 107–114, MYU Tokyo S & M 1051

[55] Kingatua A. (2016). “The how and why of energy harvesting for low-power applications. Retrieved from all about circuits”. https://www.allaboutcircuits.com/technical-articles/how-whyof-energy-harvesting-for-low-power-applications/, 2016.

[56] Kong N., Deyerle T.S. and Ha D.S. (2011). “Universal power management IC for small-scale energy harvesting with adaptive impedance matching”, Department of Electrical and Computer Engineering Virginia Tech Blacksburg, VA 24061 USA, 2011

[57] Kulah H. and Najafi K. (2008). “Energy scavenging from low-frequency vibrations by using frequency up-conversion for wireless sensor applications”. *IEEE Sensors Journal* 8, 3 (2008), 261–268.

[58] Leinonen M., Palosaari J., Sobocinski M., Juuti J. and Jantunen H. (2011). “Energy harvesting from vibration and walking with piezoelectric materials”. In *MATINE* (2011), University of Oulu.

[59] Li H., Tian C. and Deng D. (2014). “Energy harvesting from low frequency applications using piezoelectric materials”, *Applied Physics Reviews 1*, 041301(2014) https://doi.org/10.1063/1.4900845, https://aip.scitation.org/doi/10.1063/1.4900845

[60] Li X. and Strezov V. (2014). “Modeling piezoelectric energy harvesting potential in an educational building”. *Energy Conversion and Management 85* (2014), 435–442. doi:10.1016/j.enconman.2014.05.096.

[61] Li Z., Wang Y. and Cheng Z.Y. (2006). "Electro-mechanical properties of poly (vinylidenefluoride- chlorotrifluoroethylene) copolymer", *Applied physics letters*, vol. 88, p. 062904, 2006. https://doi.org/10.1063/1.2170425

[62] Li Z., Zhou G., Zhu Z. and Li W. (2016). "A study on the power generation capacity of piezoelectric energy harvesters with different fixation modes and adjustment methods", *Energies* 9(2):98 February 2016, doi: 10.3390/en9020098

[63] Lindner M., Hoislbauer H., Schwodiauer R., Bauer-Gogonea S.and Bauer S. (2004). "Charged cellular polymers with Ferro-electretic behavior", *IEEE Transactions on Dielectrics and Electrical Insulation*, vol. 11, no. 2, pp. 255-263, April 2004, doi: 10.1109/TDEI.2004.1285895.

[64] Liu Y.C., Aoyagi Y. and Chung D. (2008). "Development of epoxy-based electrets", *State University of New York. Journal of Materials Science* 43(5):1650-1663 · March 2008, doi: 10.1007/s10853-007-2391-2

[65] Luo J. and Zhang S. (2014). "Advances in the growth and characterization of relaxor PT-based Ferro-electric single crystals". *Crystals* 2014, 4, 306-330;-doi:10.3390/cryst4030306, ISSN 2073-4352, www.mdpi.com/journal/crystals

[66] Makki N. and Pop-Iliev R. (2011). "Pneumatic tire-based piezoelectric power generation", February 2011, *Proceedings of SPIE, The International Society for Optical Engineering*, DOI: 10.1117/12.880636

[67] Makki N. and Pop-Iliev R. (2012). "Battery- and wire-less tire pressure measurement systems (TPMS) sensor". *Microsyst. Technol.* 2012, *18*, 1201–1212

[68] Mallick A., Guin P. and Roy A. (2020). "Micropower Harvesting From Vibration Of Cantilever Type Piezofilm Sensor", *International Journal Of Scientific & Technology Research*, Volume 9, Issue 01, January 2020 ISSN 2277-8616 2100 IJSTR©2020 www.ijstr.org

[69] Manla G., White N. and Tudor J.(2009). “Harvesting energy from vehicle wheels”. *Proceeding of Transducers 2009* (Denver, CO, USA, June 2009). DOI: 10.1109/SENSOR.2009.5285831

[70] Mason W.P. (1950) “Piezoelectric crystals and their application to ultrasonics”, D. Van Nostrand Company Inc.

[71] McCloskey M. A., Mosher C. L. and Henderson E. R. (2017). “Wind energy conversion by plant-Inspired designs”. *PLOS ONE*, 12 (1): e0170022

[72] Neese B., Wang Y., Chu B., Ren K., Liu S. and Zhang Q. (2007). "Piezoelectric responses in poly (vinylidene fluoride/hexafluoropropylene) copolymers", *Applied physics letters*, vol. 90, p. 242917, 2007. https://www.researchgate.net/publication/234874200, DOI:10.1063/1.2748076

[73] Ottman G.K., Hofmann H.F., Bhatt A.C. and Lesieutre G.A. (2002). “Adaptive piezoelectric energy harvesting circuit for wireless remote power supply”, *IEEE transactions on power electronics, Vol 17*, No 5 September 2002

[74] Paajanen M., Lekkala J. and Kirjavainen K. (2000). "Electro-Mechanical film (EMFi)—a new multipurpose electret material", *Sensors and Actuators* A: Physical, vol. 84, pp. 95-102, 2000.

[75] Paajanen M., Wegener M. and Gerhard-Multhaupt R. (2001). “Understanding the role of the gas in the voids during corona charging of cellular electret films - a way to enhance their piezoelectricity”, *Journal of Physics D: Applied Physics*, Volume 34, Number 16 , August 2001.

[76] Pan W. Y., Sun S. and Tuttle B. A. (1992). “Electro-mechanical and dielectric instability induced by electric field cycling in Ferro-electric ceramic actuators”,

Journal of Smart Materials and Structures, Vol. 1, pp. 286{293, 1992.

[77] Parali L. & Sari A. (2017). “Vibration modelling of piezoelectric actuator (PEA) using simulink software”, 4th International Conference on Electrical and Electronics Engineering, DOI: 10.1109/ICEEE2.2017.7935811

[78] Parry M.L., Canziani O.F., Palutikof J.P., Van der Linden P.J. and Hanson C.E. (Eds.). (2007). “Climate change 2007: Impacts, adaptation and vulnerability”. Contribution of Working Group II to the Fourth Assessment Report of the Intergovernmental Panel on Climate Change (IPCC). Cambridge University Press, Cambridge, UK.

[79] Patro T. U., Mhalgi., M. V., Khakhar D. V. and Misra A. (2008). "Studies on poly(vinylidene fluoride)–clay nanocomposites: Effect of different clay modifiers", *Polymer*, vol. 49, pp. 3486-3499, 7/28/ 2008.

[80] Paul D. and Roy A. (2015). “Piezoelectric effect: smart roads in green energy harvesting”, *International Journal of Engineering and Technical Research (IJETR)* ISSN: 2321-0869, Volume-3, Issue-2, February 2015

[81] Piezo Kinetics Incorporated, “Piezoelectric Elements”, Referenced 23 Feb 2020, http://www.channeltechgroup.com

[82] Piezo Systems Inc, Introduction to Piezo transducers, Transducer elements, catalog 8 2011

[83] Piezo-Systems, Piezoelectric Motor/Actuator Kit Manual, Piezoelectric Products, Inc, Advanced Technology Group, Cambridge, Maryland, 456, 1987

[84] Prechtl E. F. http://hdl.handle.net/1721.1/35912, 1994-04-24

[85] Priya L. and Jog J. (2002). “Poly (vinylidene fluoride)/clay nanocomposites prepared by melt intercalation: crystallization and dynamic mechanical behavior studies”, August 2002 *Journal of Polymer Science Part B Polymer Physics* 40(15):1682 – 1689, doi: 10.1002/polb.10223

[86] Priya L. and Jog J. (2003). "Polymorphism in intercalated poly (vinylidene fluoride)/clay nanocomposites", *Journal of Appl. Polym. Sci.,* vol. 89, pp. 2036-2040, 2003.

[87] Rastegar J., Pereira C. and Nguyen H.L. (2006). "Piezoelectric based power sources for harvesting energy from platforms with low frequency vibration". *Proceding of Industrial and Commercial Applications of Smart Structures Technologies* (2006), vol. 6171, SPIE.

[88] Riaz A., Sarker M. R.., Saad M. H. M. and Mohamed R. (2021). "Review on comparison of different energy storage technologies used in micro-energy harvesting, WSNs, low-cost microelectronic devices: challenges and recommendations". *Sensors* 2021, 21, 5041. https://doi.org/10.3390/s21155041 https://www.mdpi.com/journal/sensors

[89] Roundy S., Leland E.S., Baker J., Carleton E., Reilly E., Lai E., Otis B., Rabaey J.M., Wright P. K. and Sundararajan V. (2005). "Improving power output for vibration-based energy scavengers", *PERVASIVE computing* published by the IEEE CS and IEEE ComSoc 1536-1268/05/$20.00 © 2005 IEEE

[90] Roundy S., Wright P. K. and Rabaey J. (2003). "A study of low level vibrations as a power source for wireless sensor nodes", *Computer Communications*. 26(11), 1131–1144 (2003). https://doi.org/10.1016/S0140-3664 (02)00248-7

[91] Saadon S. and Sidek O. (2015). "Micro Electro – Mechanical system (MEMS) based piezoelectric energy harvester for ambient vibrations", *Proceedia Earth and planetary Science*, 195(2015) 2353-2362

[92] Salimi A. and Yousefi A. A. (2003). "Analysis method: FTIR studies of β-phase crystal formation in stretched PVDF films", *Polymer Testing*, vol. 22, pp. 699-704, 9// 2003.

[93] Sarker M. R., Ali S. H M., Othman M. and Islam S. (2013). "Designing a battery-less piezoelectric based energy harvesting interface circuit with 300 mV

startup voltage", 2013, *Journal of Physics Conference Series* 431 (2013) 012025, doi:10.1088/1742-6596/431/1/012025

[94] Sarker M. R., Mohmed A. and Mohmed R. (2016). "A new method for a piezoelectric energy harvesting system using a backtracking search algorithm-based PI voltage controller", *Micromachines* 23 September2016, 7, 171; doi:10.3390/mi7100171 www.mdpi.com/journal/micromachines

[95] Sarker M. R., and Mohmed R. (2014). Battery-less low input voltage micro-scale thermoelectric based energy harvesting interface circuit with 100mv start-up voltage. (2014). *Przeglad Elektrotechniczny* 2014, 90, 49–52.

[96] Sensor Technology Limited, https://www.sensortechcanada.com

(Last accessed December 30, 2019).

[97] Sharma J. and Ravindranath N. H. (2019). "Applying IPCC 2014 framework for hazard-specific vulnerability assessment under climate change". *Environmental Research Communication* 1 (2019) 051004 https://doi.org/10.1088/2515-7620/ab24ed

[98] Sharma V. and Singh M.P. (2016). AKGEC, *International Journal of technology*, 7, 16, (2016)

[99] Smith W. A. (1992). "New opportunities in ultrasonic transducers emerging from innovations in piezoelectric materials", Proc. SPIE 1733, 3–26 (1992), https://doi.org/10.1117/12.130585,

[100] Sodano H.A., Inman D.J. and Park G. (2005). "Comparison of piezoelectric energy harvesting devices for recharging batteries". *J Intell Mater Syst Struct* 2005; 16(10):799–807

[101] Thorat B. S. and Raut S. M. (2019). "A generator of electricity in future", VOL. IX, Issue XXIX, April 2019 Multilogic in Science ISSN 2277-7601

[102] Toyabur R.M., Salauddin M., Cho H. and Park J.Y. (2018). "A multimodal hybrid energy harvester based on piezoelectric electro-magnetic mechanisms for low-frequency ambient vibrations, energy conversion and management", 168 (2018) 454–466, journal homepage: www.elsevier.com/locate/enconman https://doi.org/10.1016/j.enconman.2018.05.018, 4 May 2018

[103] Triono A. D., Limantara A. D., Gardjito E., Purnomo Y. C. S., Ridwan A. , Sudarmanto H. L., Setiono G. C., Windradi F. and Mudjanarko S. W. (2018). "Utilization of pedestrian movement on the sidewalk as a source of electric power for lighting using piezoelectric censors". IEEE Proceedings, 3rd International Conference on Intelligent Transportation Engineering, ICITE 2018 September 3-5, 2018 Singapore

[104] Wang J., Hsu T.H., Yeh C.N., Tsai J.W. and Su Y.C. (2011). "Piezoelectric polydimethylsiloxane films for MEMS transducers", *Journal of Micromechanics and Microengineering*, vol. 22, p. 015013, 2011.

[105] Wang J., Wu J. Xiao D., Wu W., Chen Q., Zhu J. and Yang Z. (2012). "Composition and poling condition-induced electrical behavior of $(Ba_{0.85}Ca_{0.15})(Ti_{1-x}Zr_x)O_3$ lead-free piezoelectric ceramics". *Journal of the European Ceramic Society* Volume 32, Issue 4, April 2012, Pages 891-898

[106] Weaver J. M., Wood K. L., Crawford R. H. & Jensen D. (2010). "Design of energy harvesting technology: Feasibility for low power wireless sensor networks". Proceedings of the ASME 2010 International Design Engineering Technical Conferences & Computers and Information in Engineering Conference IDETC/CIE 2010 August 15 – 18, 2010, Montreal, Quebec, Canada

[107] Wegener M. and Bauer S. (2005). "Microstorms in cellular polymers: A route to soft piezoelectric transducer materials with engineered macroscopic dipoles"

First published: 08 June 2005, https://doi.org/10.1002/cphc.200400517

[108] Wegener M., Tuncer E., Wirges W., Dietrich J. and Gerhard-Multhaupt R. (2005). "Polyethylene terephthalate (PETP) foams as Ferro-electrets", ISE-12. 2005 *12th International Symposium on Electrets*, pp 28–30. (2005)

DOI: 10.1109/ISE.2005.1612310

[109] Wegener M., Wirges W. and Raukola J. (2004). "Controlled inflation of voids in cellular polymer Ferro-electrets: optimizing electro-mechanical transducer properties", *Applied Physics Letters*, vol. 84, pp. 392-394, 2004. doi:10.1063/1.1641171

[110] Wei C. F. and Jing X. (2017). "A comprehensive review on vibration energy harvesting: modelling and realization". *Renewable and Sustainable Energy Reviews*, Vol. 74, 2017, p. 1-18.

[111] Wikipedia Commons, https://en.wikipedia.org/wiki/Piezoelectric_sensor#mw-head

[112] Piezoelectricity - Wikipedia Perovskite – https://en.wikipedia.org/wiki/Piezoelectricity (Last viewed Sep 2019)

[113] Wu L., Kuang J., You Z., Liu P. and Cai S. (2016). "A parallel SSHI rectifier for ultra-low voltage piezoelectric vibration energy harvesting". *IEICE Electronics Express*, Volume 13, No. 17, 1-8

[114] Xu X., Cao D., Yang H. and He M. (2018). "Application of piezoelectric transducer in energy harvesting in pavement", *International Journal of Pavement Research and Technology* 11 (2018) 388–395, https://doi.org/10.1016/j.ijprt.2017.09.011

[115] Yang H., Wang L., Zhou B., Wei Y. and Zhao Q. (2018). "A preliminary study on the highway piezoelectric power supply system", *International Journal of Pavement Research and Technology* 11 (2018) 168–175

[116] Yang L., Ji H., Zhu K., Wang J. and Qiu J. (2016). "Dramatically improved piezoelectric properties of poly (vinylidene fluoride) composites by incorporating aligned TiO_2", *MWCNTs Composites Science and Technology Volume* 123, 8 February 2016, Pages 259-267, https://doi.org/10.1016/j.compscitech.2015.11.032

[117] Zhang S., Li F., Jiang X., Kim J., Luo J. and Geng X. (2014). "Advantages and challenges of Relaxor-PbTiO3 Ferro-electric crystals for electro-acoustic transducers", *Prog Mater Sci*. 2015 March 1; 68: 1–66. doi:10.1016/j.pmatsci.2014.10.002.

[118] Zylka P. (2015). "Current progress in ambient energy harvesting using piezoelectric materials and electro-active polymers", *Research Gate*, Wroclaw University of Technology, Institute of Electrical Engineering Fundamentals, Wroclaw, Poland

GLOSSARY OF TERMS

A

B

C